AD NUMBER

**ADB004735**

LIMITATION CHANGES

TO:

**Approved for public release; distribution is unlimited.**

FROM:

**Distribution authorized to U.S. Gov't. agencies only; Critical Technology; MAR 1975. Other requests shall be referred to Federal Aviation Administration, Supersonic Transport Office, 800 Independence Avenue, SW, Washington, DC 20590. This document contains export-controlled technical data.**

AUTHORITY

**FAA ltr, 26 Apr 1977**

Report No. FAA-SS-73-11-8

# SST Technology
# Follow-On Program—Phase II
# NOISE SUPPRESSOR/NOZZLE DEVELOPMENT
# VOLUME VIII

## PERFORMANCE TECHNOLOGY
## MULTITUBE SUPPRESSOR/EJECTOR INTERACTION EFFECTS
## ON STATIC PERFORMANCE (AMBIENT AND 1150° F JET TEMPERATURE)

D. B. Morden, R. S. Armstrong

Boeing Commercial Airplane Company
P.O. Box 3707
Seattle, Washington 98124



D6-42318

March 1975

FINAL REPORT

Task III





Prepared for
FEDERAL AVIATION ADMINISTRATION
Supersonic Transport Office
800 Independence Avenue, S.W.
Washington, D.C. 20590

The contents of this report reflect the views of the Boeing Commercial Airplane Company, which is responsible for the facts and the accuracy of the data presented herein. The contents do not necessarily reflect the official views or policy of the Department of Transportation. This report does not constitute a standard, specification, or regulation.

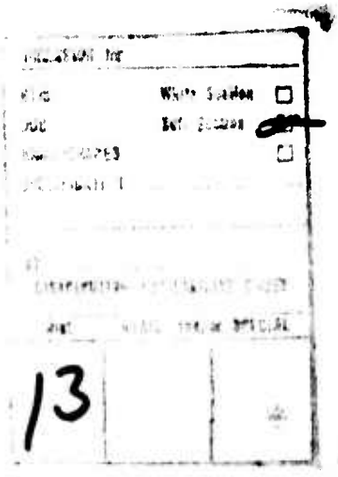

TECHNICAL REPORT STANDARD TITLE PAGE

| 1. Report No. | 2. Government Accession No | 3. Recipient's Catalog No. |
|---|---|---|
| FAA-SS-73-11-8 | | |

4. Title and Subtitle: SST Technology Follow-On Program—Phase II Noise Suppressor/Nozzle Development Vol. VIII—Performance Technology Multitube Suppressor/Ejector Interaction Effects on Static Performance (Ambient and 1150° F Jet Temperature)

5. Report Date: Mar[illegible]75

6. Performing Organization Code:

7. Author(s): D. B. Morden, R. S. Armstrong

8. Performing Organization Report No.: D6-42318

9. Performing Organization Name and Address:
Boeing Commercial Airplane Company
P. O. Box 3707
Seattle, Washington 98124

10. Work Unit No.:

11. Contract or Grant No.: DOT-FA-72WA-2893

12. Sponsoring Agency Name and Address:
Federal Aviation Administration
Supersonic Transport Office
800 Independence Avenue S.W.
Washington, D.C. 20590

13. Type of Report and Period Covered: Final Report, Task III

14. Sponsoring Agency Code:

15. Supplementary Notes

S. Blatt, DOT/SST Technical Monitor

16. Abstract

The effects of geometric variables and temperature on the static performance of multitube suppressor/ejector exhaust nozzles are described and quantified. Six suppressor and four ejector parameters are investigated to establish the criteria for maximum performance. Results are presented for a model scale test of 102 related suppressor/ejector configurations operated at pressure ratios from 2 to 4 and at ambient and 1500° F jet temperatures. Performance trends as a function of geometry are presented in a manner which allows the selection of the best geometry for any desired set of suppression and installation constraints.

SST Technology Follow-On Program-Phase II. Noise Suppresser/Nozzle Development. Volume VIII. Performance Technology Multitube Suppressor/Ejector Interaction Effects on Static Performance (Ambient and 1150° F Jet Temperature).

| 17. Key Words | | 18. Distribution Statement |
|---|---|---|
| Suppressor nozzle | Jet noise | Approved for U.S. Government only. This document is exempted from public availability because of restrictions imposed by the Export Control Act. Transmittal of this document outside the U.S. Government must have prior approval of the Supersonic Transport Office. |
| Multitube suppressor/ejector | Aircraft propulsion | |
| Nozzle performance | | |
| Base ventilation | | |
| Supersonic transport (SST) | | |
| Ejector performance | | |

| 19. Security Classif. (of this report) | 20. Security Classif. (of this page) | 21. No. of Pages | 22. Price |
|---|---|---|---|
| Unclassified | Unclassified | 111 | |

Form DOT F 1700.7 (8-69)

390 145 ✓ mt.

## PREFACE

This is one of a series of final reports on noise and propulsion technology submitted by the Boeing Commercial Airplane Company, Seattle, Washington, 98124, in fulfillment of Task III of Department of Transportation Contract DOT-FA-72WA-2893, dated 1 February 1972.

To benefit utilization of technical data developed by the noise suppressor and nozzle development program, the final report is divided into 10 volumes covering key technology areas and a summary of total program results. The 10 volumes are issued under the master title, "Noise Suppressor/Nozzle Development." Detailed volume breakdown is as follows:

| | | | Report No. |
|---|---|---|---|
| Volume I | – | Program Summary | FAA-SS-73-11-1 |
| Volume II | – | Noise Technology | FAA-SS-73-11-2 |
| Volume III | – | Noise Technology–Backup Data Report | FAA-SS-73-11-3 |
| Volume IV | – | Performance Technology Summary | FAA-SS-73-11-4 |
| Volume V | – | Performance Technology–The Effect of Initial Jet Conditions on a 2-D Constant Area Ejector | FAA-SS-73-11-5 |
| Volume VI | – | Performance Technology–Thrust and Flow Characteristics of a Reference Multitube Nozzle With Ejector | FAA-SS-73-11-6 |
| Volume VII | – | Performance Technology–A Guide to Multitube Suppressor Nozzle Static Performance: Trends and Trades | FAA-SS-73-11-7 |
| Volume VIII | – | Performance Technology–Multitube Suppressor/Ejector Interaction Effects on Static Performance (Ambient and 1150° F Jet Temperature) | FAA-SS-73-11-8 |
| Volume IX | – | Performance Technology–Analysis of the Low-Speed Performance of Multitube Suppressor/Ejector Nozzles (0-167 kn) | FAA-SS-73-11-9 |
| Volume X | – | Advanced Suppressor Concepts and Full-Scale Tests | FAA-SS-73-11-10 |

This report is volume VIII of the series and was prepared by the Propulsion Research Staff of the Boeing Commercial Airplane Company.

# FOREWORD

This document extends the investigation of bare multitube suppressor performance (ref. 1) and studies the suppressor/ejector interaction effects on the performance of these exhaust systems. Noise suppression characteristics of the same hardware are presented in reference 2. Reference 3 extends this study to include the effects of low forward velocity on suppressor/ejector performance. The work was accomplished under Task III of the DOT/SST Follow-On Technology Phase II contract, number DOT-FA-72WA-2893.

# CONTENTS

## CONTENTS (Concluded)

# FIGURES

## FIGURES (Continued)

## FIGURES (Concluded)

# SYMBOLS AND ABBREVIATIONS

| | |
|---|---|
| $A_A$ | Minimum annular area between the ejector lip and the exits of the outer row tubes |
| $A_B$ | Suppressor base area in square inches: $A_P$ (NAR −1) |
| $A_{eff}$ | Effective suppressor exit area: $C_D \cdot A_P$ |
| $A_P$ | Geometric flow area (in square inches) of primary nozzle measured at 70° F |
| $A_{PH}$ | Geometric flow area of the nozzle including temperature-induced area growth |
| $A_S$ | Measured area, in square inches, between the tubes in the outer row of a suppressor |
| $A_V$ | Total ventilation area: $A_S$ + the calculated area between plumes of the jets in the outer row of a suppressor |
| $C_D$ | Discharge coefficient, accounting for temperature-induced nozzle area growth, calculated as follows: |

$$\frac{WP}{\frac{A_{PH} \cdot PR \cdot P_{amb}}{\sqrt{T_{TP}}} \left[\frac{2g\gamma}{R(\gamma-1)} \left(PR^{-2/\gamma} - PR^{-(\gamma+1/\gamma)}\right)\right]^{1/2}}$$

For this equation, if

$$PR \geq \left(\frac{\gamma+1}{2}\right)^{\frac{\gamma}{\gamma-1}} \text{ let } PR = \left(\frac{\gamma+1}{2}\right)^{\frac{\gamma}{\gamma-1}}$$

| | |
|---|---|
| $C_f$ | Skin friction coefficient |
| $C_{f_g}$ | Gross thrust coefficient (measured suppressor and ejector thrust-drag)/($\dot{m}$ V$IP_0$) |
| C.P. | Close-packed—an arrangement of tubes with approximately the same distance between any two adjacent tubes |
| $C_{V\ int}$ | Nozzle internal velocity coefficient |

| | |
|---|---|
| $D_{aft}$ | Afterbody drag: Sum of the baseplate and ramp drags |
| $D_B$ | Baseplate drag in pounds, calculated from static pressure measurements taken at area-weighted taps on the baseplate |
| $D_B$/FID | Baseplate drag expressed as a percentage of ideal thrust |
| D/d | Upstream to exit diameter ratio |
| $D_{eq}$ | The exit diameter, in inches, of a single round convergent nozzle area equal to the total effective flow area of a multitube nozzle |
| $D_{ramp}$ | Drag in pounds calculated on the nozzle ramp using static pressure measured at area-weighted taps |
| EAR | Ejector area ratio: geometric area at ejector throat divided by $A_P$ |
| Effective EAR | Geometric area of the ejector divided by ($C_D \cdot A_P$) |
| FID | Ideal thrust in pounds; measured primary mass flow rate multiplied by the ideal, fully expanded velocity (VIP) |
| $L_A$ | Axial distance in inches between ejector throat and exit |
| $L_B$ | Axial distance in inches from ejector hilite to ejector throat |
| $L_E$ | Ejector length: distance in inches from the flightlip hilite to the ejector exit measured with zero setback |
| $L_E$/d | Ejector length divided by individual tube diameter |
| LIP | The absolute value of the lip suction force calculated from area-weighted static pressure on the lip |
| LIP/FID | The absolute value of the lip force expressed as a percentage of ideal thrust (FID) |
| $L_T$ | Tube length measured on the outside of the tube: distance in inches from the tube exit to the baseplate |
| $\dot{m}$ | Measured mass flow rate: WP/g |
| N | Total number of tubes in a suppressor |
| NAR | Nozzle area ratio: area inside a circle circumscribed around the outside of the outermost tubes (where they meet baseplate), divided by $A_P$ |

| | |
|---|---|
| $P_{amb}$ | Ambient pressure |
| $P_B$ | The average static pressure in PSIA obtained at area-weighted taps on the nozzle baseplate |
| PR | Nozzle pressure ratio: $P_{T_o}/P_{amb}$ |
| PSIG | Gauge pressure: pounds per square inch of pressure above atmospheric |
| $P_{T_o}$ or $P_{T_P}$ | The charging total pressure, i.e., total pressure PSIA at a station upstream of the tube entrances |
| q | Dynamic pressure = $1/2\rho V^2$ |
| R | Radius in inches of the inlet to a tube (also gas constant) |
| Radial Array | An arrangement of tubes in radial lines to maximize ventilation |
| R/C | Round convergent reference nozzle with 10° internal half-angle |
| Re | Reynolds number |
| $R_{ej}$ | Radius from the ejector centerline to the throat, in inches |
| $R_H$ | Radius from ejector centerline to the flightlip hilite, in inches |
| $R_{in}$ | Radius in inches from the nozzle centerline to the outside of a $C_D = 1$ jet issuing from the suppressor measured at the nozzle exit plane |
| $R_o$ | Radius in inches from the centerline to the outermost portion of ejector |
| $R_P$ | Radius from the nozzle centerline to the outside of the outer tubes, in inches |
| $SB/D_{eq}$ | The amount of setback nondimensionalized by the equivalent diameter of a jet having the same effective flow area as the total flow of the given configuration |
| Setback | A method of altering the secondary air inlet area of a fixed ejector suppressor geometry by repositioning the ejector along the centerline of the suppressor/ejector system. Positive setback is measured as the axial distance from the suppressor exit plane to the flightlip hilite of the ejector. The setback for bellmouth lips is defined as having the same throat location as the flightlip throat with that setback. |
| $T_T$, $T_{T_P}$ | Average total temperature of the primary flow (Fahrenheit unless otherwise noted) |

| | |
|---|---|
| $VIP, VIP_0$ | Ideal primary jet velocity expanded to ambient pressure, $\left\{2gR\left(\frac{\gamma}{\gamma-1}\right)T_{TP}\left[1-(PR)^{-((\gamma-1)/\gamma)}\right]\right\}^{1/2}$ |
| WA | Measured weight flow rate of air in pounds/second |
| WP | Measured weight flow rate of fuel and air in pounds/second |
| $\alpha$ | Internal half-angle of the round convergent portion of the tube in degrees |
| $\gamma$ | Ratio of specific heats |

# 1.0 SUMMARY

## 1.1 INTRODUCTION

Jet noise has been recognized as a major problem for supersonic transport aircraft. A critical factor in the development of exhaust systems that reduce jet noise to satisfactory levels is the maintenance of acceptable thrust performance over the flight regime. Application to advanced supersonic aircraft demands that the suppressor cause little or no performance loss at cruise conditions. This constraint generally means that the suppressor must be retracted out of the jet stream except during takeoff and approach flight modes, and this, in turn, severely limits the range of suppressor hardware parameters that can be considered for practical configurations.

This document presents a portion of the DOT-sponsored program to advance technology and establish a performance design capability within mechanical constraints and acoustic criteria for low-noise multitube suppressor exhaust systems. The investigation extends the study of bare multitube suppressor nozzles (ref. 1) to include the interactions between ejectors and suppressors and to maximize the static performance of the nozzle system. Results are presented from a systematic, model-scale experimental program which investigated the effects of six suppressor and four ejector geometric parameters over a range of pressure ratios from 2 to 4 at ambient and 1150°F jet temperatures. Suppressor variables were tube length, shape, number, and placement as well as nozzle area ratio and ramp shape. The ejector variables were setback, ejector area ratio, length, and lip shape. Ejector length and maximum area ratios were constrained by SST installation requirements for most configurations. Where previous testing or analysis suggested that large performance benefits might be derived through the relaxation of constraints, sample configurations were tested to provide a quantitative measure of the performance penalties associated with the various restrictions. The noise suppression characteristics of the same hardware are presented in reference 2.

## 1.2 RESULTS

An analysis of the experimental results presents the various performance effects that are pressure ratio sensitive. Performance changes as a function of each suppressor and ejector geometric parameter and temperature are discussed. The effective ejector inlet area is shown to be the mechanism allowing the optimum trade between the lip suction and suppressor afterbody drag. A qualitative inlet flow model is presented describing the effective inlet area.

Performance trends as a function of geometry, for a fixed pressure ratio, are presented in a manner which allows the selection of the best geometry and gives the appropriate level of static performance as a consequence of any desired constraints for suppressor/ejector nozzles similar in nature to those investigated.

## 1.3 SUMMARY OF FINDINGS

The performance of multitube suppressor/ejector nozzles is shown to be primarily a function of the ejector inlet area and ejector area ratio and length. Ejector lengths of 12 to 15 individual jet diameters are shown to provide adequate mixing lengths from a peak thrust standpoint for EAR/NAR ratios $< 1.3$. If additional ejector length is provided, the static performance of the system continues to increase with increasing ejector area ratio.

Over the range of pressure ratios investigated (2-4), the maximum static performance of suppressor/ejectors occurs at or near pressure ratio = 2. Figure 1 shows an example of the experimental results. The performance and surface forces are shown as a function of pressure ratio and inlet geometry for a constant ejector and suppressor. Similar curves are presented for all experimental results.

Ejector inlet area plays a major role in determining the tradeoff between lip suction and base drag. For each operating condition (jet temperature, pressure ratio, and freestream velocity), there exists an optimum ejector inlet area. This can be seen in figure 2. As the area is decreased from the optimum, large performance losses are observed. In the limit, the secondary air chokes at the ejector, producing shock-induced flow instabilities and ejector vibration. Increases in ejector inlet areas beyond the optimum cause relatively small performance losses.

The majority of the secondary air passes through the annular area between the ejector lip and the exit of the outer row tubes. The annular area (and hence the majority of the effective inlet area) is established by the EAR/NAR ratio and the ejector setback. The level of performance, on the other hand, is governed largely by suppressor afterbody drag for tube lengths compatible with the stowable tube concept. The ejector geometry, particularly the ventilation area, and the paths between the tubes regulate the distribution of pressure on the base. Static pressure reduction caused by secondary air entering the ejector increases drag by shifting the entire base pressure distribution to a higher value. Increasing tube length, while not contributing substantially to an increase in secondary air, results in an increase in base ventilation.

It is recommended that base drag be minimized by placing tubes on radial lines and by using the fewest number of tubes that will satisfy the suppression requirements while providing 12 to 15 jet diameters of ejector length within the installation requirement. Within the presently understood airplane constraints, an EAR = 3.0 or 3.1 and an EAR/NAR = 1.2 are recommended. For this configuration, nearly zero setback should be required and setback can be used to "fine tune" the configuration.

A chart format of data presentation is developed which shows general performance trends over a broad range of suppressor and ejector geometries. Each summary chart considers a particular suppressor array and identifies performance trends as a function of nozzle tube length, ejector area ratio, and setback. A sample summary performance chart is shown in figure 3. The example is based on the 37-tube, NAR = 2.75, close-packed array suppressor. The numbers within the boxes at the left of the chart are measured static gross thrust coefficients for the bare suppressor (primary alone) with various tube lengths.

The effect of adding ejectors of increasing size is shown in the boxes to the right. Performance with ejector setback of $SB/D_{eq} = 0.25$ is depicted in the dashed-line boxes. The arrows on lines connecting the boxes show the direction of increasing performance; the amount in percent is also shown. The summary charts provide a guide to the design of suppressor/ejector nozzles.

# 2.0 INTRODUCTION

Aircraft designed for supersonic cruise require engines with a high thrust to frontal area ratio and high exhaust jet velocities. Noise suppression is essential during takeoff, initial climb-out, and landing. The noise associated with the high velocity jet can be substantially reduced by placing hardware into the primary exhaust flow to break the jet into small elements. However, the extreme sensitivity of the supersonic aircraft mission to nozzle performance during supersonic cruise dictates that the suppressor hardware, with its inherent thrust loss, be retracted from the jet during cruise. SST technology (ref. 4) demonstrated high suppression values for multitube suppressor nozzles that could be stowed into the divergent portion of a high-performance con-di nozzle during transonic acceleration and supersonic cruise (fig. 4). At low speeds the divergent portion of the cruise nozzle could be moved outward to form nearly constant area ejector.

By providing an inlet for ambient (secondary) air to be accelerated into the ejector by the entrainment of the high-velocity primary jets, a static pressure reduction is created which produces a thrust force on the ejector lip. The amount of air entrained by the primary is a function of, among other things, the ejector area and length. On the order of 12 individual jet diameters are required to provide sufficient mixing lengths to entrain the maximum amount of secondary air and obtain maximum ejector lip suction. The use of a multitube suppressor makes the required ejector length feasible from an installation and weight point of view.

The static pressure reduction at the ejector inlet also produces an increase in the afterbody drag on the suppressor nozzle. Reference 1 demonstrated that the overall nozzle performance is strongly influenced by the lower-than-ambient pressure acting on the base area between the tubes. The amount of base drag is a function of both the ventilation provided by the suppressor geometry and the static pressure reduction due to the secondary air inlet velocity.

Provided the inlet area is large enough, the net effect of the partially counteracting ejector lip suction and suppressor afterbody drag is a static performance augmentation due to the secondary air handled by the ejector. Given sufficient ejector length, the amount of secondary air handled (and hence the static performance) continues to increase with increasing ejector area ratio.

Performance data are presented from a model-scale investigation of families of multitube suppressor/ejector systems. Six geometric variables for the suppressor and four for the ejector are studied to determine the effect on the internal and external performance of nozzles including stowable configurations compatible with supersonic transport requirements. Performance data and acoustic near- and far-field measurements were acquired simultaneously during the test. The acoustic characteristics are reported in reference 2.

The testing was conducted on families of suppressors with 19 to 61 equal-sized tubes and a matrix of tube lengths, shapes, nozzle area ratios and arrays (tube placement). The nozzle area ratios, NAR = 2.75 to 3.3, were partially dictated by airplane installation requirements and partially by the optimums suggested in reference 1. The total effective flow area was

13.2 $in^2$ for each model. Bellmouth and flightlip ejectors were tested with area ratios from 2.6 to 3.7. The ejectors were mounted on balance but independent of the suppressors to avoid configuration-oriented inlet strut losses. Ejector setback and length were also investigated. The investigation included pressure ratios from 2 to 4 at ambient and 1150°F temperatures. Figure 5 shows a typical installation.

This report will summarize the experimental results for the configurations tested on plots of gross thrust coefficient, suppressor afterbody drag, and ejector lip suction as functions of geometry, temperature, and pressure ratio. An analysis will treat each of the suppressor and ejector parameters individually. For any fixed ejector geometry, the effective ejector inlet area will be shown to regulate the system performance through the tradeoff between afterbody drag and lip suction. The behavior of restricted inlets and the importance of setback as a mechanism to optimize the suppressor drag/lip suction interaction will be presented along with an inlet flow model. Finally, performance trends as a function of geometry, for a fixed pressure ratio, will be presented in a manner which allows the selection of the best geometry and gives the appropriate level of static performance as a consequence of any desired geometric constraints for suppressor/ejector nozzles similar to those investigated.

# 3.0 VARIABLES, CONSTANTS, AND DEFINITIONS

## 3.1 RANGE OF VARIABLES

- Primary jet pressure ratio: 2-4
- Primary jet temperature: ambient and 1150° F

Figure 6 shows suppressor and ejector variables.

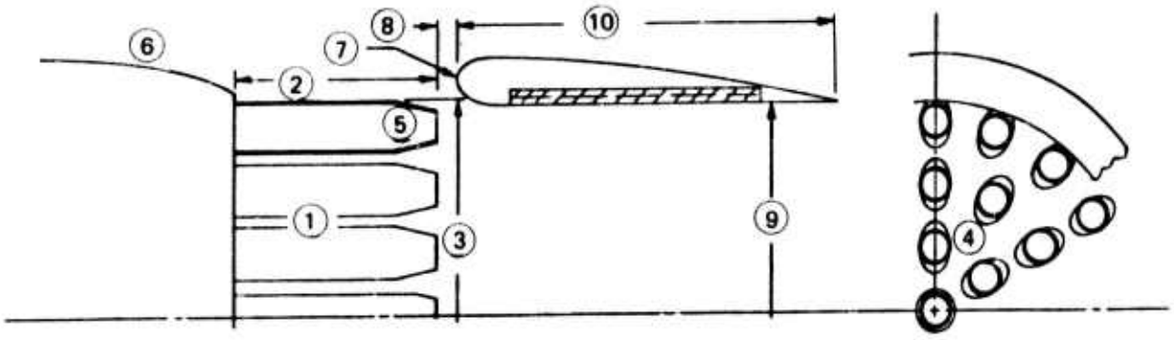


**Suppressor Variables**

(1) Tube number: 19 to 61

(2) Tube length: 1 to 4 in. ($L_T/D_{eq}$ = 0.25 to 1.0)

(3) Area ratio: 2.75 and 3.3 ($\pi R_b^2$/geometric flow exit area)

(4) Base array: close-packed and radial

(5) Tube shape: round convergent, round nonconvergent, elliptical convergent (round exit)

(6) Ramp shape: elliptical, circular arc, and contoured

**Ejector Variables**

(7) Lip shape: bellmouth and flightlip

(8) Setback: 0 to 1 in. ($SB/D_{eq}$ = 0 to 0.25)

(9) Ejector area ratio: 2.6 to 3.7

(10) Ejector length: 8 to 24 in. ($L_E/D_{eq}$ = 2 to 6)

*Figure 6.–Suppressor/Ejector Schematic*

## 3.2 CONSTRAINTS

The suppressor variables and constraints for this investigation are the same as those discussed in detail in reference 1. The suppressor area ratios were limited to 2.75 and 3.3 as a result of both a performance optimum discussed in reference 1 and a supersonic transport nacelle size constraint.

For most configurations, the ejector length was fixed at the maximum allowed on the SST at the termination of the aircraft project (8-in. model scale). To better understand the degree of mixing that was occurring in the fixed length, the constraint was relaxed for a few configurations.

The area ratio 3.7 ejector, which is too large to meet SST constraints, was tested to demonstrate the acoustic and static performance benefits of relaxing the area ratio constraint.

### 3.2.1 SUPPRESSOR CONSTRAINTS

- Total effective exit area 13.2 $in^2$ (geometric exit area $\approx$ 13.6 $in^2$ for convergent tubes; approximately 1/10 scale SST)
- Approximately 0.5 internal Mach number for convergent tubes
- Coplanar tube exits
- Flat baseplate (except R/37)
- Each tube within an array is the same (e.g., a 37-tube array has 37 tubes each with 0.36 $in^2$ of effective flow area)
- Outside nacelle diameter held constant (8.89 in. to be representative of an actual scale SST nacelle)

### 3.2.2 EJECTOR CONSTRAINTS

- 8 in. long (unless otherwise stated)
- Flightlip profile constant (2:1 ellipse)
- No suppressor/ejector mounting struts (i.e., no inlet losses due to installation)
- Constant internal area
- For a given setback, the axial distance from the tube exit plane to the ejector throat is the same for all configurations; i.e., for setback the hilite of the ejector is set even with the tube exit plane while the bellmouth ejector is set with the throat at the same location as the flightlip throat. (A bellmouth ejector with zero setback does not have its hilite coincident with the tube exit.)

## 3.3 NOZZLE AREA RATIO AND EJECTOR AREA RATIO DEFINITIONS

The various area ratios used within this investigation are defined with the aid of figure 7.

### 3.3.1 SUPPRESSOR (OR NOZZLE) AREA RATIO (NAR)

Throughout this study the suppressor area ratio or nozzle area ratio (NAR) refers to the total area within a circle tangent to the outermost portion of the outside tubes divided by the geometric primary flow area. This definition is chosen to be representative of the physical area required to install the suppressor. Notice that configurations with convergent tubes can have nozzle area ratios larger than ejector area ratios without implying jet scrubbing on the ejectors.

### 3.3.2 EFFECTIVE NOZZLE AREA RATIO

The effective nozzle area ratio is defined as the area within a circle tangent to the outside of the outer jets, at the nozzle exit plane, divided by the effective primary flow area ($C_D \cdot A_P$). This area ratio is representative of the jet that must be contained by the ejector.

### 3.3.3 EJECTOR AREA RATIO (EAR)

Throughout the present investigation constant mixing area ejectors are used. The ejector area ratio is defined as the geometric ejector area divided by the nozzle flow geometric area.

### 3.3.4 EFFECTIVE EJECTOR AREA RATIO

The effective ejector area ratio is defined as the geometric flow area within the ejector divided by the effective primary flow area ($C_D \cdot A_P$).

# 4.0 TEST AND HARDWARE DESCRIPTION

## 4.1 FACILITY AND TEST PROCEDURE

The testing was conducted on the Boeing Hot Nozzle Test facility (fig. 8), a 2000-lb single-axis thrust rig located at North Boeing Field, Seattle. The rig was equipped with an "on-balance" overhead ejector support beam. By rigidly suspending the ejectors from the beam (figs. 8 and 9), the ejector body forces were measured without any installation losses due to struts between the suppressor and ejector.

As shown in figure 10, a variable slot inlet burner provided acceptable temperature profiles for testing at 1150°F. The airflow rate was obtained using a critical flow venturi. Ambient and hot-jet testing was conducted for pressure ratios from 2 to 4. Thrust measurements were the average of five 1-second integrated samples for each test condition.

Results were demonstrated to be repeatable to ±0.25% for performance values obtained at ambient jet temperature and ±0.5% for those acquired at 1150°F. The level of performance agrees with previous testing (refs. 1 and 5).

As pressure ratio was increased, some configurations experienced local supersonic conditions within the ejector. The fluctuating forces, probably produced by transient, shock-induced separations, were large and low enough in frequency (<200 Hz) to cause severe vibration of the ejector and overhead beam assembly. For these configurations, data were acquired up to the highest pressure ratio at which the system would remain steady.

## 4.2 DESCRIPTION OF NOZZLES

### 4.2.1 ROUND CONVERGENT REFERENCE NOZZLE (R/C)

The R/C, a 10° half-angle round convergent nozzle (fig. 11), was used as a noise and performance referee throughout the program. The nozzle has an upstream to exit diameter ratio (D/d) of 1.44 and a geometric exit area of 13.825 $in^2$. The external contour consists of a 12° half-angle boattail tangent to a 35.5-in.-radius arc which, in turn, is tangent to the 8.89-in. nacelle diameter upstream.

### 4.2.2 SUPPRESSOR RAMP SHAPES

#### 4.2.2.1 Elliptical Ramp

The elliptical ramp was used in the majority of configurations (fig. 12) and consisted of a segment of an ellipse with foci on the nozzle centerline. The segment is tangent to the nacelle and extends to the center of the outer tube row.

#### 4.2.2.2 Circular Arc Ramp

The circular arc ramp (fig. 13) consists of a 35.5-in.-radius circular arc tangent to the nacelle and intersecting the baseplate just outside of the outer tubes.

Because of the large base area and possible restriction to the effective ejector inlet with forward velocity the circular arc ramp was tested only on the 37-tube, area ratio = 3.3, close-packed suppressor.

#### 4.2.2.3 Contoured Ramp

The contoured ramp shown in figure 11 consists of a 40-in. boattail radius tangent to the 8.89 nacelle diameter and terminating in a central hole coplanar with the tube exits. Though incompatible with the stowable tube concept, the contoured ramp/base allows maximum ventilation and ejector inlet area and minimizes the separation region on the base.

The contoured base was tested only on the 37-tube, area ratio = 3.3, close-packed suppressor with round convergent tubes (R/37).

### 4.2.3 TUBE LENGTH

Tube length, defined as the distance from the baseplate to the nozzle exit plane, was incremented from stowable tube lengths to those sufficient to produce nearly the maximum $C_{fg}$. The stowable tube concept, as shown in figure 4, requires that the tubes be short enough to fold into the void left as the internal ejector wall moves inward to form the divergent portion of the con-di transonic acceleration and supersonic cruise nozzle. Present installation constraints require that the tube length nondimensionalized by the equivalent round convergent jet diameter ($L_T/D_{eq}$) be equal to or less than 0.4 for stowable tubes.

To assess the performance gradients due to tube length, values of $L_T/D_{eq}$ equal to 0.25, 0.50, 0.75, and 1.0 were tested. The total effective exit areas of the tubes were held constant at approximately 13.2 $in^2$; thus the tube lengths tested were 1, 2, 3, and 4 in.

### 4.2.4 FOUR CLOSE-PACKED ARRAYS WITH ELLIPTICAL TUBES AND ELLIPTICAL RAMPS

One 19-, two 37-, and one 61-tube, 13.6 $in^2$ area ratio = 3.3 suppressors were tested to investigate the natural progression of nozzles with approximately equal spacing between all tubes in the array. Figures 14 and 15 show key dimensions for each nozzle. All tubes are elliptical converging to round coplanar exits, have a tube internal area to exit area ratio of 1.34 (M = 0.5), and have tube inlet radius to tube diameter ratios greater than 0.1 to minimize inlet losses. Tube lengths were varied from 0.25 to 1.0 $D_{eq}$. A 37-tube, area ratio = 2.75 nozzle was built similar to the 37-tube, area ratio = 3.3 nozzle in all other respects as shown in figure 15. Variations in tube shape and ramp shape for 37-tube, area ratio = 3.3 nozzles are shown in figures 16 and 17.

### 4.2.5 R/37: 37-TUBE, NAR = 3.3 SUPPRESSOR WITH CONTOURED RAMP

The R/37 configuration (fig. 11) is a 13.695-$in^2$, area ratio = 3.3, close-packed suppressor using 37 equal-diameter round convergent tubes of varying length. The nozzle was tested repeatedly throughout the program as a performance and noise referee.

To maximize the ventilation and minimize separation, a contoured baseplate was used. All tube entrances have bellmouth radius to tube diameter ratios greater than 0.1 to minimize inlet ($\Delta P_T/q$) losses. All tube exits are coplanar and the average length of the internal constant area portion of the tubes is 4.4 in. The tube internal upstream area to exit area ratio is maintained at 1.34 to produce a maximum Mach number of 0.5. The performance of the R/37 with contoured ramp is described in detail in reference 6.

### 4.2.6 37-TUBE, NAR = 3.3, CLOSE-PACKED ARRAY WITH ELLIPTICAL RAMP AND R/C TUBES

To establish the effect of varying only tube shape, the R/37 nozzle was fitted with an elliptical ramp to produce a 37-tube, NAR = 3.3, close-packed array with round convergent tubes as shown in figures 16 and 18. To provide the same ventilation parameter (ref. 1) range as the 37-tube, NAR = 3.3 array with elliptical convergent tubes, nondimensional tube lengths ($L_T/D_{eq}$) of 0.5 and 0.75 were used. A correction for excessive internal losses was applied using the technique of reference 1.

### 4.2.7 RADIAL ARRAY SUPPRESSORS (TWO)

A 37-tube, area ratio = 3.3 radial array was constructed using nonconvergent tubes (fig. 19). To account for the inherently low discharge coefficient of nonconvergent tubes ($C_D \approx 0.91$), the total geometric flow area was 14.93 $in^2$ to produce an effective mass flow rate similar to that of the other nozzles tested. The tube inlet radius to tube diameter ratio was greater than 0.1.

Removal of the central row of six tubes results in a radial array with a more evenly distributed flow that could also be constructed at a significantly smaller area ratio. The resulting 31-tube nozzle was constructed with an area ratio of 2.75 (fig. 19). The difference in ventilation paths between the 37-tube, close-packed nozzle and the 31-tube radial array (both with NAR = 2.75) is apparent in figure 20.

### 4.2.8 SUMMARY OF SUPPRESSOR SPECIFICATIONS

| Number of Tubes | Area Ratio | Effective Area Ratio[1] | Array Type | $A_j$ ($in^2$) | $A_s$ ($in^2$) | Type of Tube[a] | $C_D$[b] | Mean Diam (In.) to Outerside of Outer Jet |
|---|---|---|---|---|---|---|---|---|
| 1 (R/C) | — | — | — | 13.825 | — | — | 0.980 | 4.186 |
| 19 | 3.3 | 3.1 | C.P. | 13.610 | 5.979 | EC | 0.983 | 7.262 |
| 37 | 3.3 | 3.1 | C.P. | 13.543 | 6.197 | EC | 0.968 | 7.243 |
| 37 | 3.3 | 3.1 | C.P. | 13.695 | 5.269 | RC | 0.956 | 7.432 |
| 61 | 3.3 | 3.1 | C.P. | 13.616 | 6.064 | EC | 0.969 | 7.257 |
| 37 | 2.75 | 2.7 | C.P. | 13.432 | 4.369 | CC | 0.983 | 6.703 |
| 31 | 2.75 | 2.7 | Rad. | 13.610 | | EC (M = 0.65) | 0.970 | 6.703 |
| 37 | 3.3 | 3.1 | Rad. | 14.931 | 11.995 | R nonC | 0.925 | 7.440 |

| | |
|---|---|
| % of total flow exiting from outer row: | 63%, 48%, and 38% for the 19-, 37-, and 61-tube, close-packed arrays, respectively; 38% and 32%, respectively, for the 31- and 37-tube radial arrays |

[a]EC Elliptical converging to round exit (M = 0.5)
RC Round converging to round exit (M = 0.5)
R nonC Round nonconverging

[b]Using $C_D$ from reference 1

Detailed dimensions available for all configurations on Boeing drawing number 5457-0 through -8 and -10, -11, and -27

## 4.3 EJECTORS

### 4.3.1 GENERAL DESCRIPTION

Each ejector in the present investigation had a constant internal area. A range of effective ejector area ratios divided by effective nozzle area ratios from 1.0 to 1.4 was tested ($R_{ej}^2/R_{in}^2$ = 1.0 to 1.4). Ejector area ratios were varied from 2.6 to 3.7. Most configurations were designed with the tightest ejector permitting the wall of the ejector to coincide with the outermost boundary of the overexpanded plume of a jet issuing from the outer tube row at the highest pressure ratio (4.0). The largest area ratio (3.7) is substantially larger than practical for SST application but is used to demonstrate the importance of area ratio on static performance and suppression.

The ejector length is defined as the distance from the suppressor exit plane to the ejector exit (measured with setback = 0). This definition describes the distance in which the mixing process occurs. The ejector length, constrained by SST installation requirements, was held at $L_E/D_{eq}$ = 2 (i.e., 8-in. model scale) for most configurations. This constraint results in ejector length to individual jet exit diameter ratios of 8.5, 12, and 15.4 for the 19-, 37-, and 61-tube nozzles, respectively. Reference 7 shows that the ejector length to jet diameter ratios of the 37- and 61-tube nozzles are sufficient to produce complete mixing from a peak thrust standpoint.

To provide sufficient mixing length for the 19-tube nozzle and to establish the effect of the SST length constraint, the requirement was relaxed for a few configurations. Because the required mixing length increases with area ratio, the largest area ratio ejector (3.7) was also built in $L_E/D_{eq}$ = 3.6 and 6.0 (14.3- and 24-in.) lengths. The resulting ejector length to individual jet diameter (d) ratios are presented below.

| Number of Tubes | $\frac{L_E}{d}$ for $\frac{L_E}{D_{eq}} = 2$ | $\frac{L_E}{d}$ for $\frac{L_E}{D_{eq}} = 3.6$ | $\frac{L_E}{d}$ for $\frac{L_E}{D_{eq}} = 6$ |
|---|---|---|---|
| 19 | 8.5 | 15.2 | 25.6 |
| 37 | 12.0 | 21.5 | 36.1 |
| 61 | 15.4 | N/A | N/A |

The ejectors were designed with 2:1 elliptical flightlips to minimize losses both statically and in the low-speed tunnel tests to follow (ref. 3). The configuration-oriented inlet losses due to ejector mounting struts were avoided by mounting the ejectors independently (but on the same balance) from an overhead support as shown in figure 9. Ejector area ratios were chosen to ensure that suppressor and ejector area ratios could be varied while the radial distance between the outer jets and ejector wall was held constant. This condition prevails when the EAR = 2.6 ejector on a 2.75 area ratio nozzle is compared with an EAR = 3.1 ejector on a 3.3 nozzle area ratio suppressor.

To establish the static performance penalty due to the flightlips, identical area ratio ejectors were built with bellmouths. As shown in figure 21, the distance from the throat to the ejector exit (at zero setback) was held constant for both bellmouth and flightlip configurations. Ejector setback is defined as zero when the flightlip hilite is coplanar with the nozzle exit plane. Thus, for zero setback, the bellmouth extends upstream of the nozzle exit plane.

All ejectors were instrumented with area-weighted lip static pressure taps (in line with and between representative jets) and internal static pressure taps. Flightlip configurations included external pressure taps and internal thermocouples.

### 4.3.2 AREA RATIO (EAR) = 2.6 EJECTORS

Bellmouths and flightlip versions of the 8-in. ($L_E/D_{eq}$ = 2) ejector were tested. As shown in figure 21, both versions have 6.83 in. between the throat and the ejector exit plane. The ejector area at the hilite of the flightlip is 140% of the ejector throat area, and a 2:1 single ellipse segment is used for both the internal and external lip shape. The effective ejector area ratio is 2.7, and the ejector length-to-diameter ratio ($L_E/2R_e$ at zero setback) is 1.2.

### 4.3.3 AREA RATIO (EAR) = 3.1 EJECTORS

The bellmouth and flightlip versions of the area ratio = 3.1 ejectors are also dimensioned in figure 21. The lip shapes, ejector lengths, and throat-to-exit distances are identical to those of the area ratio = 2.6 ejectors. The effective ejector area ratio is 3.2, and the ejector length-to-diameter ratio is 1.09.

The outer nacelle diameter of the flightlip configuration is the same as the suppressor nacelle diameter, and thus the 3.1 ejector is representative of the scaled dimensions for SST configuration requirements for both ejector length and diameter. When these ejectors were used in conjunction with area ratio (NAR) = 3.3 suppressors, the radial distance between the outer jets and the ejector wall was nominally the same as for EAR = 2.6 ejectors paired with area ratio (NAR) = 2.75 nozzles.

### 4.3.4 AREA RATIO (EAR) = 3.7 EJECTORS

To build an area ratio = 3.7 ejector while maintaining the constraint on nacelle diameter would result in an ejector only 58% as thick as the EAR = 3.1 configurations. Such an ejector would suffer larger static inlet losses and be impractical for the stowable tube concept. To evaluate the effects of area ratio on performance without simultaneously introducing changes due to lip shape, the outer nacelle diameter constraint was relaxed, resulting in the

flightlip ejectors shown in figure 22. One of these ejectors meets the $L_E/D_{eq} = 2$ constraint, while the other is an $L_E/D_{eq} = 6$ ejector for use with the 19-tube nozzle to ensure full mixing. The longer ejector was also used on some 37-tube nozzles. The 2:1 ellipse used as the flightlip shape produces an axial distance from hilite to throat of 1.33 in. The various $L_E/D_{eq} = 2.0$ flightlip ejectors are shown in figure 23. Bellmouth versions of the above ejectors were tested to evaluate the inlet losses due to the flightlip (see fig. 24). In this case the minimum distance between the NAR = 3.3 suppressor outer tube exits and the lip was held constant at setback equals zero. The result is a slight variation (0.16 in.) in the throat location between the flightlip and bellmouth configurations. An intermediate length bellmouth ejector (fig. 25) was constructed with $L_E/D_{eq} = 3.6$ (14.3 in.) and a distance of 1.17 in. between the throat and nozzle exit plane when the setback was defined as zero.

### 4.3.5 SUMMARY OF EJECTOR SPECIFICATIONS

| EAR | Effective EAR | Type of Lip | Lip Shape | $L_E$,[a] in. | $L_A$,[b] in. | $L_B$,[c] in. | Ejector Area, $in^2$ |
|---|---|---|---|---|---|---|---|
| 2.6 | 2.7 | Flightlip | 2:1 Ellipse | 8 | 6.83 | 1.17 | 34.9 |
| 2.6 | 2.7 | Bellmouth | 2 in. Radius | 8 | 6.83 | 1.17 | 34.9 |
| 3.1 | 3.2 | Flightlip | 2:1 Ellipse | 8 | 6.83 | 1.17 | 42.5 |
| 3.1 | 3.2 | Bellmouth | 2 in. Radius | 8 | 6.83 | 1.17 | 42.5 |
| 3.7 | 3.8 | Flightlip | 2:1 Ellipse | 8 | 6.67 | 1.33 | 50.1 |
| 3.7 | 3.8 | Bellmouth | 4 in. Radius | 8 | 6.43 | 1 57 | 50.0 |
| 3.7 | 3.8 | Bellmouth | 2 in. Radius | 14.3 | 13.14 | 1.17 | 50.0 |
| 3.7 | 3.8 | Flightlip | 2:1 Ellipse | 24 | 22.67 | 1.33 | 50.0 |
| 3.7 | 3.8 | Bellmouth | 4 in. Radius | 24 | 22.43 | 1.57 | 50.0 |

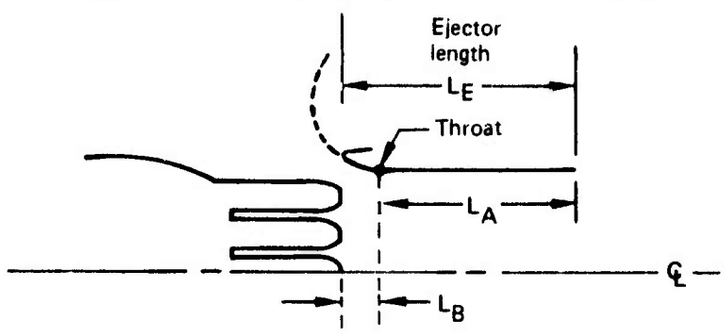


[a]Length of ejector measured from the suppressor exit plane to the ejector exit plane when setback = 0.

[b]$L_A$ = Distance from ejector throat (T.P. from lip) to exit

[c]$L_B$ = Axial distance from suppressor exit plane to ejector throat when setback = 0. Also axial distance from ejector throat to hilite for flightlip configurations

## 4.4 MODEL INSTRUMENTATION

### 4.4.1 CHARGING STATION INSTRUMENTATION

Four coplanar rakes, located in the 6-in. internal diameter instrumentation section (fig. 8), were used to measure the primary flow temperature and total pressure profiles. A horizontal pair of rakes contained 14 thermocouples spaced across the entire duct to sample regions of equal area (i.e., they were "area-weighted"). Fourteen total-pressure probes, on two vertical rakes, were also area-weighted.

### 4.4.2 SUPPRESSOR STATIC PRESSURE INSTRUMENTATION

Each nozzle included area-weighted static pressure taps on the baseplate and ramps. The pressure lines were routed inside the baseplate/ramp assemblies, resulting in "clean" baseplates (i.e., devoid of extraneous protrusions).

### 4.4.3 EJECTOR INSTRUMENTATION

#### 4.4.3.1 Static Pressures

All ejectors were instrumented with area-weighted (flush) lip static pressure taps and internal static pressure taps. To allow proper calculation of lip suction, rows of taps were mounted in line with and between representative suppressor jets. Flightlip configurations also have external static pressure taps.

#### 4.4.3.2 Thermocouples

Three thermocouples were located 15° away from vertical at the top of each ejector on the area ratio = 2.6 and 3.1 ejectors (fig. 26). This results in wall temperature monitoring between jets for radial configurations and for the 19-tube suppressor. The maximum ejector wall temperature is monitored with the 61-tube nozzle where the thermocouples are in line with the center of a jet. A near average temperature is monitored for 37-tube, close-packed configurations where the thermocouples are halfway between being in line with and between the jets (i.e., jet centerlines 20 apart and thermocouples 5 from one centerline). The area ratio = 3.7 ejectors have the thermocouples 22 from vertical. The axial locations of the three thermocouples for each ejector are: at the throat, at 0.57 $L_E$ (halfway between ejector throat and exit), and at 0.99 $L_E$ (as close to the exit as physically possible).

## 4.5 DATA ACQUISITION AND REDUCTION

The data presented in this document have a repeatability of ±0.25% for ambient test conditions and ±0.5% for data acquired at a primary jet temperature of 1150° F. The R/C nozzle was used repeatedly to ensure that the level of performance continued to agree with previous data (refs. 1 and 5).

# 5.0 ANALYSIS OF RESULTS

## 5.1 INTRODUCTION

This chapter analyzes the experimental results, establishes the relative importance of each of the parameters, and presents performance trends and tradeoffs. The various performance effects that are pressure-ratio-sensitive are investigated. Then, with the pressure ratio held constant, the performance changes due to each of the suppressor and ejector parameters are discussed separately. Performance trends as a function of geometry at a constant pressure ratio are summarized, and the section displays the optimum geometry and performance of suppressor/ejector nozzles within any desired set of geometric constraints. Interspersed throughout the chapter as applicable, the effects of jet temperature are discussed.

## 5.2 PRESSURE RATIO EFFECTS

The experimental results as a function of pressure ratio and geometry show the following general characteristics.

### 5.2.1 BARE SUPPRESSOR (WITHOUT EJECTOR)

Peak performance and minimum afterbody drag as a percentage of ideal thrust occur between pressure ratio 2.5 and 3.0. Reference 1 presents a detailed description of bare nozzle performance. The complete set of curves showing these effects is presented in the appendix.

### 5.2.2 SUPPRESSOR/EJECTORS

- The addition of an ejector results in an increase in the amount of afterbody drag compared to a similar bare nozzle configuration.
- The location of the peak performance and maximum lip suction and afterbody drag as percentages of ideal thrust shifts to a lower pressure ratio (relative to bare nozzle). Most of the recorded peaks occurred at pressure ratio 2 (the lowest pressure ratio investigated).
- Typically, both lip suction and afterbody drag become decreasing percentages of ideal thrust as pressure ratio increases.
- Lip suction decreases more than base drag with increasing pressure ratio.
- Afterbody drag and lip suction (as percentages of FID) are decreasingly dependent on the geometry as pressure ratio increases.
- The pressure ratio at which peak performance occurs shifts to slightly higher values as setback is increased.

- Ejector vibration (due to supersonic flow near the ejector wall at the throat) shifts to a higher pressure ratio as the effective ejector inlet area increases.

- Setback is a more effective way to increase the inlet area than increased tube length.

A complete set of curves for performance and surface forces as functions of pressure ratio are presented in the appendix.

## 5.3 NOZZLE GEOMETRY EFFECTS

### 5.3.1 TUBE LENGTH

The stowable tube concept allows the noise suppressor to be stowed into the divergent portion of a con-di nozzle during transonic acceleration and supersonic cruise. The installation requirements place severe limitations on tube length, requiring tube length/$D_{eq}$ ratios of about 0.35 to 0.4.* The present study concentrated on tube lengths in this range. Other lengths were also investigated in order to establish the performance trends associated with changes in the length constraints.

The effect of tube length on the static performance of bare suppressors is detailed in reference 1. Figure 27 presents the performance as a function of tube number and length for otherwise similar close-packed arrays. Increasing tube length results in a tradeoff between decreasing base drag and increasing internal losses. The base drag decreases asymptotically as tube length increases. The amount of decrease is a function of the ventilation area between the tubes in the outer row and the flow paths provided to allow ventilation to the center of the array (ref. 1). The internal losses of the convergent tubes are small enough that, for the close-packed arrays shown in figure 27, the decrease in base drag outweighs the increase in internal losses for nonlinear tube length up to 0.75. For comparison, a 37-tube radial array with nonconvergent tubes is also shown in figure 27. The high internal losses and good ventilation of this array result in peak performance at a tube length of 0.5 $D_{eq}$.

The introduction of an ejector to the suppressor configuration results in large changes in performance with tube length as shown in figure 28 for suppressors fitted with a "tight" (EAR/NAR = 0.94)** ejector. The base drag is much more sensitive to changes in tube length than is lip suction because of gradients in static pressure caused by the secondary air accelerating into the ejector. The 61-tube nozzle with 0.25 $D_{eq}$ tube length, for example, has 33% of FID afterbody drag with the zero setback EAR = 3.1 ejector, compared to 5% for the same suppressor without ejector. Above the choke pressure ratio the internal performance is not affected by the presence of an ejector. The afterbody drag again approaches a constant with increasing tube length as it did for the no-ejector case, only now the rates of change are much more dramatic. Because of the ejector augmentation, some of the configurations shown in figure 28 produce a static performance better than the R/C nozzle even with stowable tube

---

* The $D_{eq}$ used to nondimensionalize all experimental testing was 4 in. For substantially different flow areas, Reynolds number effects may have to be considered.

** EAR/NAR<1 does not imply jet scrubbing. (See sec. 3.3.)

lengths. Figure 29 shows that static performance of all the suppressors discussed above is better than that of the R/C nozzle if EAR = 3.7 ejector is used. The high performance values and low rates of change of performance with tube length are a result of the large ejector inlet area which provides large augmentation without high inlet velocities.

Figures 30 and 31 show the effect of tube length on performance of the various ejectors discussed above the 37-tube and 61-tube, NAR = 3.3, close-packed arrays.

For each configuration investigated, base drag decreased slightly with increasing suppressor jet temperature. The internal nozzle performance as a function of tube length and temperature is presented in reference 1.

### 5.3.2 NOZZLE AREA RATIO

A parameter which strongly influences the performance of a suppressor/ejector system is the inlet area of the ejector. For given primary gas conditions and a fixed EAR (and length) an ejector has a natural capacity for air handling. The ejector inlet area determines the velocity of the secondary air and, in turn, affects the tradeoff between the lip suction and afterbody drag. In the limit it also governs the secondary air handling capacity. Figure 32 illustrates the contributions to performance of nozzle area ratio, tube length, and ejector setback. The example uses 37-tube, close-packed array nozzles and an EAR = 3.1, $L_E/D_{eq} = 2$ ejector. Since the given ejector tends to require a fixed amount of secondary air (at the fixed gas conditions), the performance variations shown in the figure are a result of changes in the ejector inlet area. For a fixed tube length the NAR = 2.75 ("loose") configurations allow a larger inlet area and have higher performance than the "tight" EAR = 3.3 ejector.*

The effective ejector inlet area increases with tube length so that setback and NAR become slightly less important. As tube length continues to increase, a point is reached where the reduction in inlet velocity due to increased setback results in a larger decrease in lip suction than gain in base drag and overall performance begins to suffer. The $L_T/D_{eq} = 1.0$ and NAR = 2.75 is such a configuration. The data trends of the plots and the need for a constant effective inlet area suggest the possibility of a locus of points as shown by a-a on figure 32. This line demonstrates that the nozzle area ratio at which the zero setback and 0.25 setback configurations produce the same performance increases with increasing tube length.

Ejector and suppressor pressure distributions are studied in order to establish the loss mechanisms within the nozzle system. Baseplate drag and lip suction derived from integrated static pressures are representative of the major body forces applied to the system when no excessive scrubbing occurs.

Figure 33 shows the effect on baseplate drag coefficient of the primary nozzle area ratio, tube length, and ejector setback for the same configurations used in figure 32. With a tight ejector (i.e., large area ratio nozzle) the baseplate drag is quite large as a result of insufficient

---

*In figure 32, straight lines are used to connect configurations. Intermediate NAR points were not obtained; therefore, the actual effects are probably nonlinear.

base ventilation due to the limited secondary flow area. As the nozzle area ratio is decreased, the drag decreases and becomes less sensitive to the above parameters due to the increase in inlet area. The loss in performance due to baseplate drag (shown in fig. 33) closely reflects in the parametric variations in the general changes in $\Delta C_{f_g}$ (gross thrust of the multi-tube nozzle versus R/C nozzle $C_{f_g}$), described in figure 32.

Figure 34 compares ejector lip suction calculated from integrated pressure measurements as a function of primary nozzle area for either ejector setback indicated. Lip suction is higher for a large area ratio nozzle, the restricted secondary flow being felt as a high-velocity flow by the lip. Setback opens up the secondary flow area, thus reducing local velocities and lip suction. The lip suction is a very weak function of tube length. The lack of sensitivity of the lip thrust to tube length suggests that the velocity of the flow entering the ejector near the lip is independent of tube length. This would occur if the majority of the flow enters the ejector through the annular area, $A_A$, between the lip and outer row tube exits. The distance along the tubes appears to act primarily as a "buffer zone" to provide pressure gradients which allow base pressure relief as tube length increases.

### 5.3.3 NOZZLE ARRAY

The arrangement of the tubes was shown in reference 1 to be the best method of providing good ventilation to nozzles using stowable tube length.

The radial array incorporating tubes in radial lines produces good ventilation and good flow penetration paths to the center of the array. The close-packed array, with its approximately equal spacing between all tubes, allows less ventilation and more restricted flow paths than the radial array but produces superior suppression characteristics in the region where postmerged jet noise is the dominant noise source (ref. 2). Thus, for gas conditions above pressure ratio 3.0 and 1150°F, the suppression requirements must be considered coincident with the performance. From a performance standpoint, the radial array is always superior to the close-packed array with other geometric parameters held constant. At or below pressure ratio 3.0, the radial array produces large gains in performance without suppression loss.

Figure 35 demonstrates the performance benefit of the radial array over a similar close-packed array* when both are fitted with the same "tight" ejector. The static pressure reduction at the ejector inlet and the difference in ventilation result in nearly twice as much afterbody drag on the close-packed array as for the configuration with tube length $L_T/D_{eq} = 0.5$. For this tube length the difference in afterbody drag and a change in lip suction result in 7.2% better performance for the radial array using zero setback. For the zero setback case of the tight ejector to produce the same performance as the radial array with the shortest tubes, the tube length of the close-packed array must be two and one-half times as long. The afterbody drag for both configurations improves as the inlet area increases with setback, resulting in 6% better performance for the radial array with tube length and setback equal to 0.50 and 0.25 $D_{eq}$ respectively.

---

*The difference in tube number is due to the difference in the natural progression of tube numbers for the two arrays (i.e., close-packed: 7, 19, 37; radial: 7, 13, 31.)

Figure 36 shows the same pair of NAR = 2.75 suppressors now fitted with an EAR = 3.1 ejector. The performance of the radial array is again better than the close-packed array, but the increase in inlet area reduces the inlet velocity to the point where setback results in a performance penalty for tube lengths greater than 0.5 $D_{eq}$. The tradeoff between base drag, lip suction, and internal losses for these configurations is such that the performance of the radial array, even with the shortest tubes, is better than with any combination of tube lengths and setback for the close-packed array.

While pure radial arrays may not be compatible with postmerge suppression requirements for some gas conditions, actual designs for airplane installation must emphasize a maximum distance between tubes in the outer rows and must provide for as many radial ventilation paths to the nozzle center as possible. The ventilation should be such that the ratio of the area between the tubes in any row, $r_j$, to the total base area within $r_j$ increases slightly for successive rows from the array center.

### 5.3.4 NUMBER OF TUBES

Figure 37 shows the difference in performance between several NAR = 3.3 arrays with an EAR = 3.1 ejector and the bare R/C nozzle operating at the same gas conditions. The number of tubes varies from 19 to 61 but, because the arrays are all close-packed, the ventilation parameter per unit tube length ($A_S/A_B \cdot L_T$) is the same for all configurations, i.e., ± 2%. The effect of tube number is shown for various tube lengths and for ejector setback. Tube number is shown to produce a relatively small effect (with the exception of the 19-tube nozzle, which has a ventilation benefit due to having only two rows of close-packed tubes). The 61-tube nozzle is operating at the pressure ratio limit just before the inlet flow becomes supersonic at the throat.* The 37-tube, zero-setback data are extrapolated from pressure ratio 2.8** where supersonic flow at the ejector throat was monitored. The difference in jet plume size for the two nozzles may have been responsible for the difference. The 19-tube suppressor/ejector probably performed to a higher pressure ratio before the onset of supersonic flow because of an insufficient ejector length (to individual tube diameter ratio) to entrain the same amount of secondary air as the other nozzles.

As setback is increased to allow sufficient ejector inlet area the performance trends are more clear-cut. Increased internal losses and decreased ventilation result in decreasing performance as the number of tubes increases. While the number of tubes used should be held at the minimum consistent with suppression requirements, the number of tubes is of secondary importance when compared to the use of radial arrays, optimum ejector inlet area, and maximum possible tube length for configurations incorporating stowable tube lengths and 30 to 70 tubes.

### 5.3.5 TUBE SHAPE

The effects of tube shape are discussed in reference 1. Convergent tubes are recommended to minimize internal losses. A tube entry radius to tube internal diameter ratio greater than 0.1

---

*Pressure ratio information obtained from figure 73

**From figure 68

should be used to avoid large inlet losses. Elliptical tubes converging to round exits provide low internal losses while maintaining good base ventilation and providing structural hoop strength at the tube exit. The difference in ventilation area between the round convergent and elliptical convergent tubes does not significantly alter the effective ejector inlet area but does produce a substantially larger afterbody drag for round convergent tubes of stowable length.

## 5.4 EJECTOR EFFECTS

### 5.4.1 INLET FLOW CHARACTERISTICS

#### 5.4.1.1 Inlet Flow Model

Secondary air entering the ejector to mix with the primary flow must pass through either the area between the outer tubes, $A_S$, or the annular area, $A_A$ (fig. 38).

An effective inlet area can be determined by assigning discharge coefficients to the two geometric flow areas

$$A_{eff} = C_{D_S} A_S + C_{D_A} A_A$$

where $A_{eff}$ is the effective ejector inlet area

$C_{D_S}$ is the discharge coefficient of the flow passing between the outer row tubes

$C_{D_A}$ is the discharge coefficient of the minimum annular area between the outer row tubes and the ejector lip

The present investigation did not measure secondary mass flow rate and thus does not quantify the values of $C_{D_S}$ and $C_{D_A}$. On the other hand, the results and analysis presented in this chapter give a qualitative understanding of the relative importance of $C_{D_S}$ and $C_{D_A}$.

For a fixed primary geometry, constant primary gas conditions, and constant ejector area ratio and length, a given primary nozzle tends to entrain a constant amount of secondary air, and thus any changes in the secondary air handling must be due to ejector inlet losses. The ejector inlet area can be altered by using setback to increase the annulus area $A_A$. Experimental results suggest a flow field as shown in figure 39.

A large recirculation region exists aft of the baseplate. The jets exiting the central tubes entrain air from the recirculation region which must be replaced by air having a radial component crossing $A_S$. The remainder of the secondary air goes directly into the ejector through $A_A$ and a small portion of $A_S$. Statically, as the annulus area $A_A$ is reduced by decreasing setback (with constant suppressor and ejector geometry and gas conditions) the velocity of the secondary mass flow must increase, resulting in a static pressure depression at the outside of the recirculating region. The demand for mass flow into the recirculating region remains similar because the suppressor jets tend to entrain a quantity of mixing air that is independent of the inlet size. The pressure near the outside of the baseplate, produced by the velocity of the air entering the ejector, causes large changes in the base

pressure and hence the level of drag. Using setback as a technique to increase the annular inlet to the ejector and lower the velocity of the inlet air results in a substantial reduction in base drag.

Reference 3 shows that changes in inlet geometry produce large changes in the surface pressure forces while creating relatively small variations in the rate of change in performance with forward velocity. This suggests that any given ejector has a reasonably fixed capacity for handling secondary air (provided the ejector length/individual tube diameter is sufficient). Over a large range of inlet areas, the size and shape of the inlet regulate the inlet velocity and hence the static pressure and gradients in static pressure from the base to the lip. The base drag is shown to be strongly dependent on ejector inlet area for short tube. As the inlet area is increased through setback or increased EAR/NAR ratio, the base drag decreases asymptotically. This method of changing base drag produces simultaneous changes in lip suction, suggesting a change in the pressure due to decreased inlet velocity. Increased tube length, on the other hand, produces larger changes in base drag than lip suction, implying a reasonably constant flow velocity through $A_A$ but a decrease in base drag due to a larger pressure gradient along the "buffer zone" between the baseplate and tube exits. The ventilation parameter and paths regulate the pressure distribution on the base. The pressure on the outside of the recirculation region, produced by the velocity of the air entering the ejector and the pressure gradient along the tube, regulates the level of the entire baseplate pressure distribution.

#### 5.4.1.2 Oil-Flow Example

To provide a qualitative picture of the ejector inlet flows, an oil-flow plate was obtained using the 37-tube, NAR = 3.3, close-packed array with an EAR = 3.1 ejector and zero setback (PR = 3.0, $T_T$ = ambient). The plate bisected the ejector and "cut" the center of a radial ray of seven tubes (line A-A in fig. 19). The resulting oil flow for this "tight" ejector is shown in figure 40.

Traditionally, it has been thought that the radial component of secondary air combined with the low static pressures between the plumes would cause the jet centerlines to move toward the ejector centerline as they progressed along the ejector. Instead, the oil flow suggests that, at least for EAR/NAR $\approx$ 1 ejectors, the outer jet moves out and attaches to the ejector wall. The exit profile for this configuration, figure 41, shows the high velocity peak near the ejector wall. Similar velocity peaks at the outside of the profile are shown for other tight ejectors in references 2 and 8.

The high-velocity flow on the wall will produce some additional skin friction losses in performance, but these appear to be small. The main cognizance of the high-velocity, high-temperature flow near the ejector wall should be in ejector lining technology and structural design.

### 5.4.2 INLET GEOMETRY

#### 5.4.2.1 Setback

For any given set of primary gas conditions, size of tubes, and ejector area ratio and lengths, the capacity of the ejector to entrain secondary air tends to be constant. This air must enter the ejector through the areas $A_S$ and $A_A$ shown in figure 38. The size of $A_S$ is determined entirely by suppressor geometry, while the size of $A_A$ is a function of the ejector area, the EAR/NAR ratio, and the setback. For any fixed suppressor/ejector geometry, ejector setback provides a useful mechanism for optimizing performance through the tradeoff between lip suction and base drag.

The static pressure reduction resulting from the velocity of secondary air affects both the base drag and lip suction. As setback increases, the available inlet area increases and the base drag decreases as shown in figure 42.

The natural air-handling capacity of the ejector is a function of the jet pressure ratio and temperature. The increase in primary jet velocity with pressure ratio increases the amount of secondary air entrained into a given ejector to the limit where choked ejector flow occurs.

If the EAR/NAR is $\approx 1$, the zero setback cases will produce supersonic flow at the ejector inlet at some pressure ratio. For the configurations tested, the supersonic flow was monitored at pressure ratios near 3.0. The condition always occurred at the ejector throat (tangent point between the ejector lip and constant internal area). At this pressure ratio, severe ejector vibration occurred, presumably as a result of shock-induced flow instabilities. For any fixed pressure ratio, the lip suction is a maximum at the minimum inlet area that allows the ejector to handle its natural capacity of secondary air. The general trend for lip suction as a function of setback is shown in figure 43.

If the systems are operating at pressure ratios above suppressor nozzle choke, the primary nozzle internal performance is independent of changes in ejector geometry.

Thus, the base drag and lip suction are partially counteracting forces that determine the setback at which the optimum static performance will occur. The general trend of performance versus setback is shown in figure 44 using the surface forces presented in figures 42 and 43.

Since setback is only a mechanism used to optimize the inlet area to match the ejector capacity, the amount of setback required for peak performance is also a function of the variables held constant on figures 42, 43, and 44. The capacity of the ejector increases with ejector area ratio if sufficient mixing length is provided. The required length, discussed in section 5.4.3.1, is a function of the size of tube, EAR, and EAR/NAR ratio.

For fixed ejector area ratios and sufficient mixing length, the peak setback is a function of $A_A$, or EAR/NAR, and, to a lesser extent, $A_S$. All "tight" ejectors (i.e., EAR/NAR $\approx$ 1) tested produced higher performance at setback = 0.25 $D_{eq}$ than at zero setback. As the inlet area is increased by decreasing NAR to produce EAR/NAR $\approx$ 1.13, the optimum performance for configurations tested requires a setback between zero and 0.25 $D_{eq}$. If the NAR is

reduced until the EAR/NAR is greater than 1.3 for the configurations tested, the inlet velocity is low enough that setback produces a larger decrease in lip suction than the relief of base drag and, hence, for all setbacks, the performance is always less than the peak value obtained with the EAR/NAR = 1.13 configuration.

Figure 45 summarizes the typical behavior of the suppressor/ejector performance as a function of EAR/NAR and setback for constant gas conditions and ejector.

Figure 46 shows the performance of a radial and close-packed array with EAR/NAR = 1.13 as a function of tube length and setback. The 10% gain in performance for an increase in tube length from 0.25 to 0.75 $D_{eq}$ for the 37-tube, close-packed array without setback was due to a 3% decrease in lip suction and a 13% decrease in base drag. The lip suction for the setback case of the same suppressor is completely independent of tube length and was 2% lower than the value for any tube length without setback. The example again suggested that the majority of the mass flow and hence the velocity near the lip is more dependent on $A_A$ than $A_S$. Figure 46 demonstrates that as the tube length increases, providing better base ventilation, less setback is needed to provide peak performance. The "a" shown in figure 46, where the performance is the same with zero and 0.25 $D_{eq}$ setback, is not the peak performance; rather, the peak performance occurs at an intermediate setback as shown in figure 45. The comparison of the radial with the close-packed configuration points out the difficulty in quantifying the setback required for optimum inlet area. The close-packed array with tube length 0.57 $D_{eq}$ (a on fig. 46) and the radial array with tube length 0.42 $D_{eq}$ (b) should both require about 0.125 $D_{eq}$ setback to produce peak performance. For these configurations $A_A$ is the same but $A_S$ is different. The close-packed configuration a has 37% more tube length than the radial array b, but the $A_S/L_T$ is almost twice as large for the radial array. Thus, even though the setback, EAR and EAR/NAR, and $A_A$ required to produce optimum static performance are the same for the two configurations the $A_S$ required by the radial array is 42% larger than for the closed-packed array. As temperature increases the amount of secondary air handled by a given ejector decreases* suggesting that less setback is required to produce optimum performance. Reference 3 demonstrates that setback, unlike ejector area ratio and length, provides a method of simultaneously optimizing static performance and minimizing lapse rate. The reference also suggests that a configuration designed to optimize takeoff performance requires a slightly larger setback than required to produce the peak static performance.

#### 5.4.2.2 Lip Shape

The ejectors were designed with 2:1 ellipse-shaped flightlips to minimize losses statically and in the low-speed forward velocity investigation. To establish the static performance penalty due to flow separation on the flightlip, if any, bellmouth configurations were also tested. Experimental results indicate that separation did not occur on the flightlip for any of the configurations tested. Instead, the flightlip performed as well as or better than the

*Though the secondary mass flow rate was not measured during the present configuration, the decrease in air handling with increasing primary jet temperature is implied by the decrease in lip suction and the decrease in lapse rate with increasing temperature shown in reference 6.

bellmouth for all conditions. The reason for a slightly lower performance for some bellmouth cases appears to be redistribution of the pressure gradient between the lip and baseplate caused by a greater axial momentum of the secondary air near the baseplate due to the forward extension of the bellmouth lip.

#### 5.4.2.3 Effect of Suppressor Ramp Shape

Reference 4 indicated a performance gain due to the use of a ramp rather than allowing a separated region to exist between the outer tubes and the nacelle o.d. Ramps were always used in the present investigation to minimize the separated base region. Two ramp shapes were used: a circular arc ramp terminating at the outside of the outer tubes and an elliptical ramp extending to the center of the outer row tubes. The total projected area of the sum of the ramp and base is the same for the two configurations. It was assumed at the outset that the increase in minimum dimensions from the baseplate to the ejector, provided by the elliptical ramp, would result in improved mass flow into the ejector, therefore, the radial location of the separated flow should be less.

Over the range of tube lengths tested, the performance of the elliptical ramp configuration had a $C_{f_g}$ no more than 1/2% higher than that of the circular arc ramp. Reference 3 concludes that even with forward velocity the lip suction does not "know" which ramp is used and that the overall performance is improved with the use of a ramp, but that the shape of the ramp is relatively unimportant. The gentle contoured ramp/base used on the R/37 reference model demonstrated that the extremely long tubes in the outer row ($\approx 1.75\ D_{eq}$) improved the pressure ratio at which choking occurred for the "tight" EAR = 3.1 ejector but did not improve the performance over that of the similar suppressor with elliptical converging tubes, elliptical ramp, and a tube length of $0.75\ D_{eq}$.

### 5.4.3 EJECTOR GEOMETRY

#### 5.4.3.1 Area Ratio and Length

The ejector length required to produce peak static thrust is a function of suppressor element size and the ratio of the ejector to suppressor area ratios (EAR/NAR). One-dimensional ejector flow analysis (ref. 9) demonstrates that, for constant primary gas conditions, the secondary mass flow rate increases as ejector area ratio increases. (The analysis assumes that sufficient ejector length is available for mixing and does not treat the effect of length.) The peak performance of any suppressor ejector system occurs when the ejector length is sufficient to provide optimal mixing of the primary jets with the secondary flow, provided the inlet area is also optimized. Large local peaks in the velocity profile can still be present, but their values must be slightly less than the primary core velocity. If the length increases substantially beyond this, the reduction in effective area due to boundary layer growth and drag due to increased wetted area reduces the system performance. The individual element size affects the length required to mix out the primary core. As the number of primary nozzle tubes is increased, the amount of primary jet perimeter available to induce mixing increases and the ejector length required for maximum secondary air handling decreases. For the multitube suppressor, the required length is conveniently nondimensionalized by the individual tube diameter. The jet core mixes out in approximately 12 length-to-individual-jet diameters (ref. 7). Aircraft constraints required an ejector of $L_E/D_{eq} = 2.0$. This ejector

length requires 37 equal-area tubes to provide 12 individual jet diameters within the $L_E/D_{eq}$ = 2 ejector. As the distance between the outer jets and the ejector wall (i.e., EAR/NAR) increases, the required ejector length increases to provide enough distance for the mixing to extend across the ejector. When the ejector length is less than that required for optimum entrainment, the secondary air decreases, resulting in lower lip suction and hence lower static performance. Figure 47 demonstrates the above effects on the lip suction as a percentage of ideal thrust for various area ratio ejectors fitted to the 31-tube, NAR = 2.75 radial array suppressor. Since the lip suction increases with increased secondary air handling, the behavior of the EAR = 2.6 and 3.1 ejectors is straightforward. The failure of the 3.7 area ratio ejector to produce more lip suction than the EAR = 3.1 ejector is due to insufficient ejector length to individual jet diameter for EAR/NAR = 1.35. The performance produced by these ejectors is shown in figure 48 to directly reflect the lip suction. The performance of the EAR = 3.7 ejector is shown to produce more thrust than the EAR = 3.1 ejector when sufficient mixing length is provided.

An ejector length of 12 individual jet diameters is sufficient to produce nearly maximum static performance for EAR/NAR = 1.12, as shown in figure 49 for the 37-tube, NAR = 3.3 radial array fitted with EAR = 3.7 ejectors of various lengths.

At pressure ratio 3.0, the actual ejector length to individual tube diameter required to produce peak performance is between 12 and 22. The severity of the performance penalty when the ejector is too short greatly exceeds that of an excessively long ejector. Thus, it is estimated that the tube length required to produce peak performance for the EAR/NAR = 1.12 ratio is 14 to 15 when EAR = 3.7.

#### 5.4.3.2 Ejector Wall Temperature

Wall temperatures were measured at three locations inside the ejectors: at the ejector throat, midway, and as close as possible to the ejector exit. The wall total temperatures are plotted in figure 50 for various configurations at nozzle pressure ratio 3.0 and suppressor jet total temperature of 1150°F.

## 5.5 SUMMARY OF PERFORMANCE AS A FUNCTION OF GEOMETRY (CONSTANT PRESSURE RATIO)

### 5.5.1 FORMAT

The performance results for variations in ejector area ratio, setback, and tube length are presented on a single plot for each suppressor configuration at pressure ratio = 3.0. Section 5.5.2 lists the summary plots for the various suppressor configurations. The general formats of these plots are shown in figure 51.

Any geometric constraints can be placed on the suppressor/ejector system, and the summary plot will display the optimum geometry and performance within the desired constraints. Similar plots can be constructed at other pressure ratios using data from the figures listed in the appendix.

### 5.5.2 MATRIX CURVES

| Figure Number | Configuration* |
|---|---|
| 52 | 19-tube, NAR = 3.3, C.P. |
| 53 | 37-tube, NAR = 2.75, C.P. |
| 54 | 37-tube, NAR = 3.3, C.P. |
| 55 | 37-tube, NAR = 3.3, C.P. (circular arc ramp) |
| 56 | 37-tube, NAR = 3.3, C.P. (contoured ramp, R/C tubes) |
| 57 | 61-tube, NAR = 3.3, C.P. |
| 58 | 31-tube, NAR = 2.75, radial array |
| 59 | 37-tube, NAR = 3.3, radial (round nonconvergent tubes) |

*Configurations use elliptical convergent tubes and elliptical ramps unless otherwise noted.

## 5.6 THRUST LOSS VERSUS SUPPRESSION

The suppression characteristics of the hardware used in this investigation are presented in reference 2. Figure 60 presents the small thrust loss and suppression characteristics of the 31-tube, NAR = 2.75 radial array with various ejectors.

# 6.0 CONCLUSIONS AND RECOMMENDATIONS

The performance of multitube suppressor/ejector nozzles has been shown to be primarily a function of the ejector inlet area and ejector area ratio and length. Ejector lengths of 12 to 15 individual jet diameters have been shown to provide adequate mixing lengths from a peak thrust standpoint for EAR/NAR ratios $< 1.3$. If additional ejector length is provided, the static performance of the system continues to increase with increasing ejector area ratio.

For each fixed ejector area ratio, pressure ratio, and primary jet temperature, the performance is a function of the effective ejector inlet area. For small inlets the base drag is dominant over the lip suction. As inlet area increases, the base drag decreases asymptotically while the lip suction increases until the inlet is passing the amount of air required to satisfy the natural capacity of the ejector. If the inlet area is increased beyond this value, the velocity of the nearly constant amount of secondary air decreases and hence the lip suction decreases and the decrease in base drag approaches zero. Hence, for each suppressor/ejector there is an optimum inlet area, and setback provides a mechanism for obtaining the optimum performance provided the EAR/NAR ratio is not too large. For configurations investigated, a setback of 0.25 is required for EAR/NAR = 1. For EAR = 3.7 and EAR/NAR = 1.3, the inlet is so large that peak performance cannot be obtained by using setback. Within the presently understood airplane constraints, an EAR = 3.0 or 3.1 and an EAR/NAR = 1.2 are recommended. For this configuration nearly zero setback should be required and setback can be used to "fine tune" the configuration. The majority of the secondary air was shown to pass through the annular area between the ejector lip and the exit of the outer row tubes. Thus, lip suction is reasonably insensitive to suppressor geometry. The level of performance, on the other hand, is governed largely by the suppressor afterbody drag for tube lengths compatible with the stowable tube concept. The ejector geometry, particularly the ventilation area $A_S$, and the paths between the tubes regulate the distribution of pressure on the base. The static pressure reduction caused by the secondary air entering the ejector increases the drag by shifting the entire base pressure distribution to a higher value. Increasing tube length, though it increases $A_S$, does not substantially contribute to an increase in secondary air. Instead, the principal benefit of increased tube length is the distance necessary to provide a larger static pressure gradient between the ejector lip and baseplate. Since present installation constraints dictate tube length, it is recommended that base drag be minimized by placing tubes on radial lines and by using the fewest number of tubes that will satisfy the suppression requirements while providing 12 to 15 jet diameters of ejector length within the installation requirement. Elliptical tubes converging to round exits are recommended because they afford good external ventilation, produce small internal losses, and still provide structural hoop strength. While the use of a suppressor ramp has been shown to be beneficial, the shape of the ramp does not appear to be very important. More effort is needed to quantify the effective inlet area. Sufficient trends and experimental results are presented to afford reasonably accurate assessment of the inlet area required for the suppressor/ejectors similar to those investigated. Unfortunately, it is not yet possible to nondimensionalize the effective inlet area as a general function of each of the parameters.

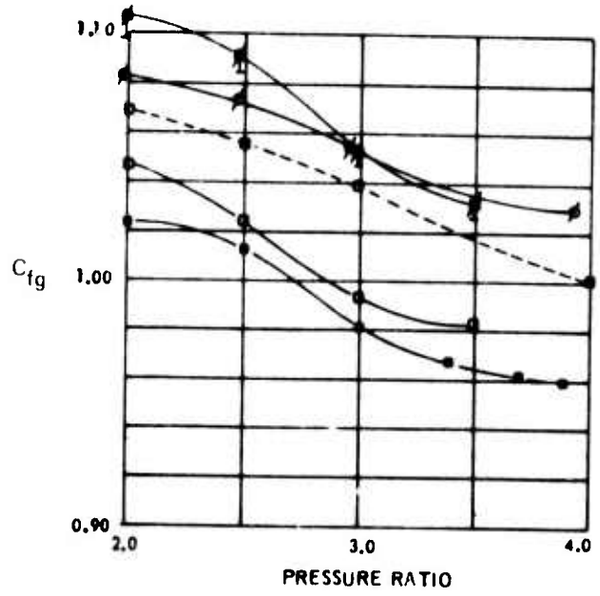


OPEN SYMBOLS = AMBIENT TEMPERATURE

SOLID SYMBOLS = 1150°F

| EAR 3.1 | EAR 3.7 | $L_T/D_{eq}$ |
|---|---|---|
| △ | ◭ | 1.0 |
| ○ | ◯ | .75 |
| □ | ◱ | .50 (*$L_E/D_{eq} = 6$) |
| ◇ | ◮ | .25 |

SETBACK (S.B./Deq)

——— 0

– – ——— .125

——— ——— .250

$L_E/D_{eq}$ = 2 EXCEPT WHERE NOTED

ACCURACY: ± 0.25% OR SHOWN WITH ERROR BAR

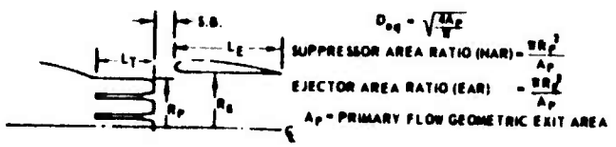


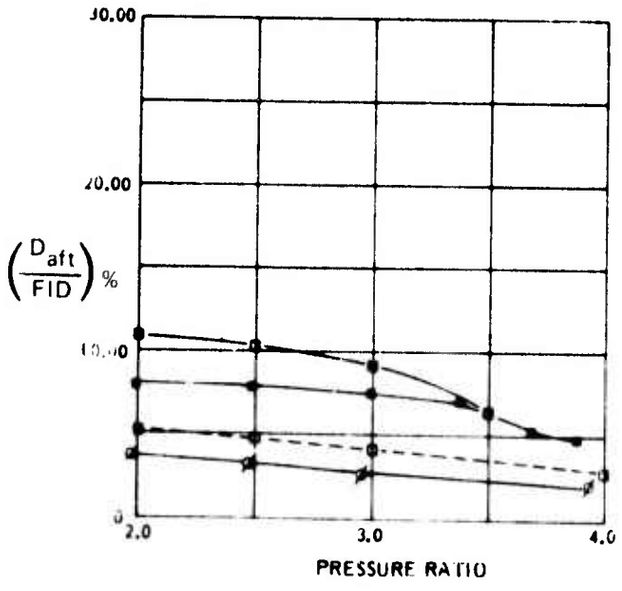


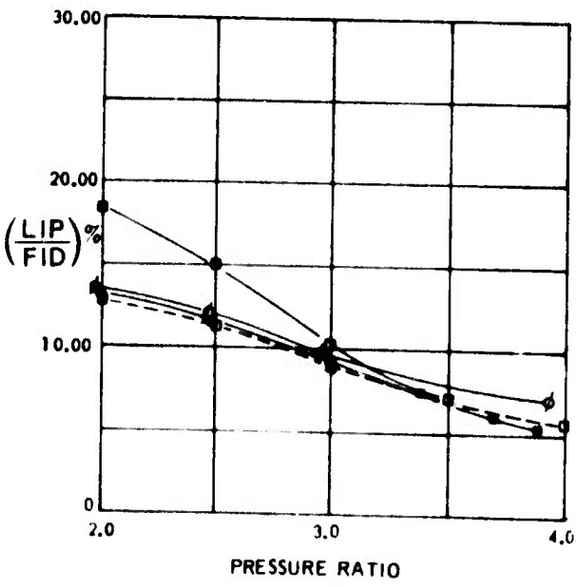


*Figure 1.—Gross Thrust Coefficient and Body Forces for 37-Tube, NAR = 3.3, EAR = 3.1, Close-Packed, Elliptical Ramp, Elliptical Convergent Tubes*

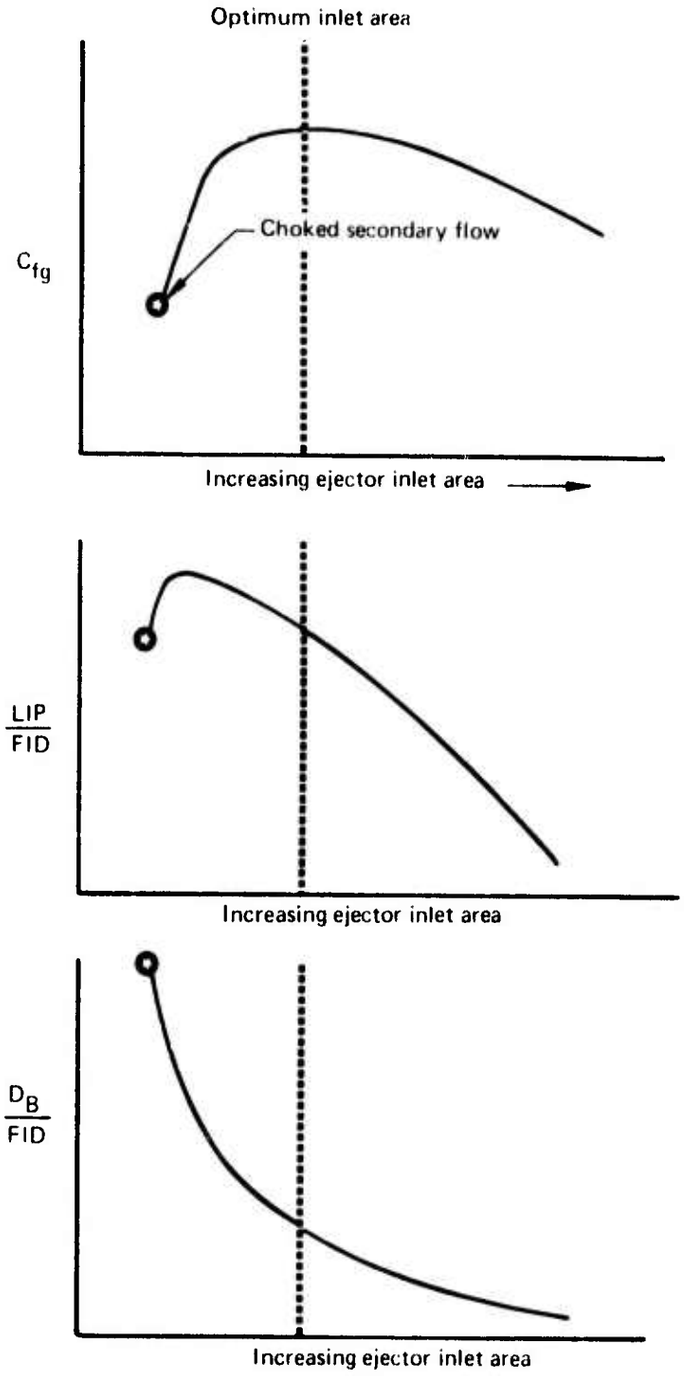


*Figure 2.—Effect of Ejector Inlet Area on the Performance Suppressor/Ejectors*

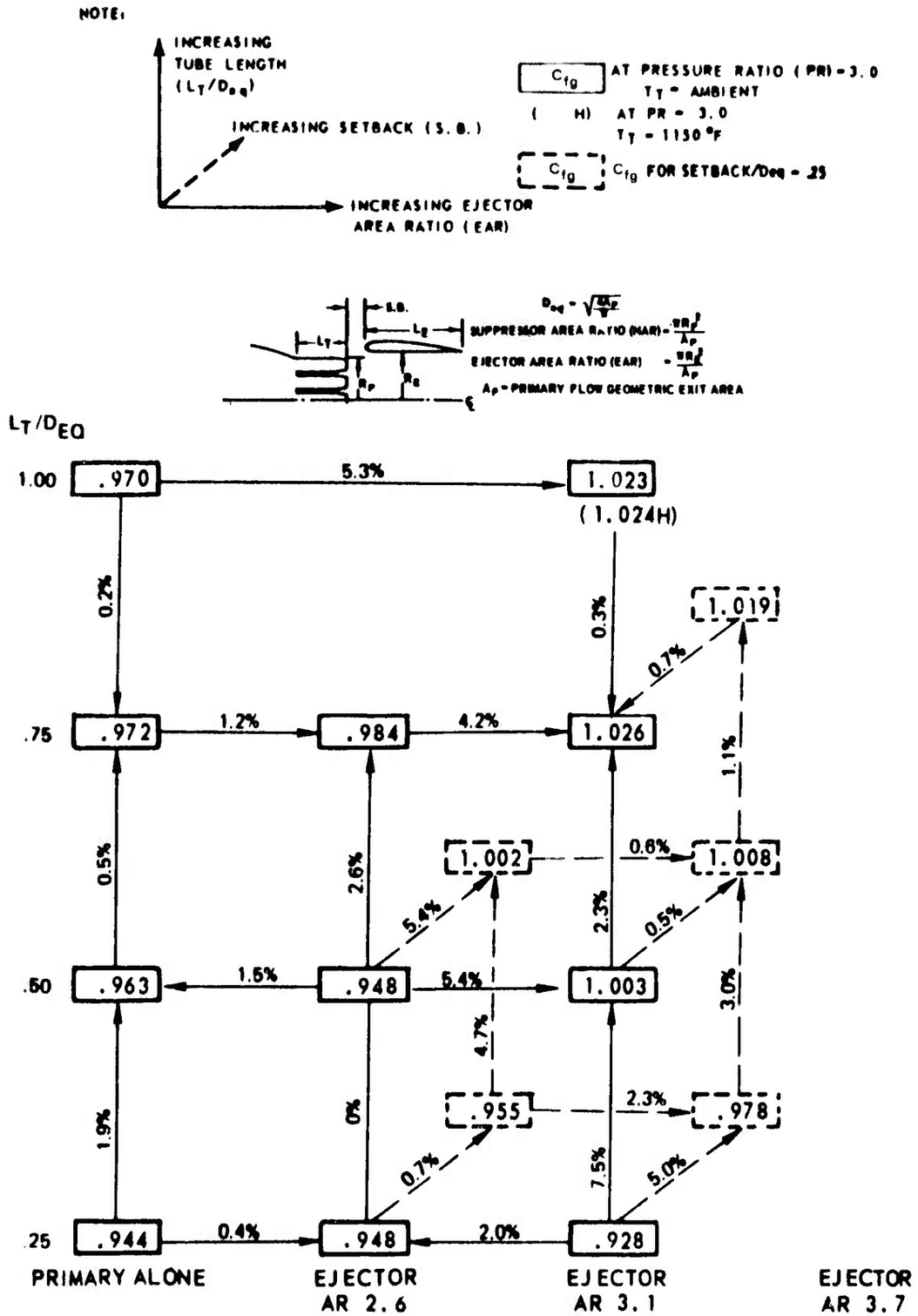


*Figure 3.—Performance Matrix for 37 Elliptical Convergent Tubes: NAR = 2.75—Close-Packed Array—Elliptical Ramp*

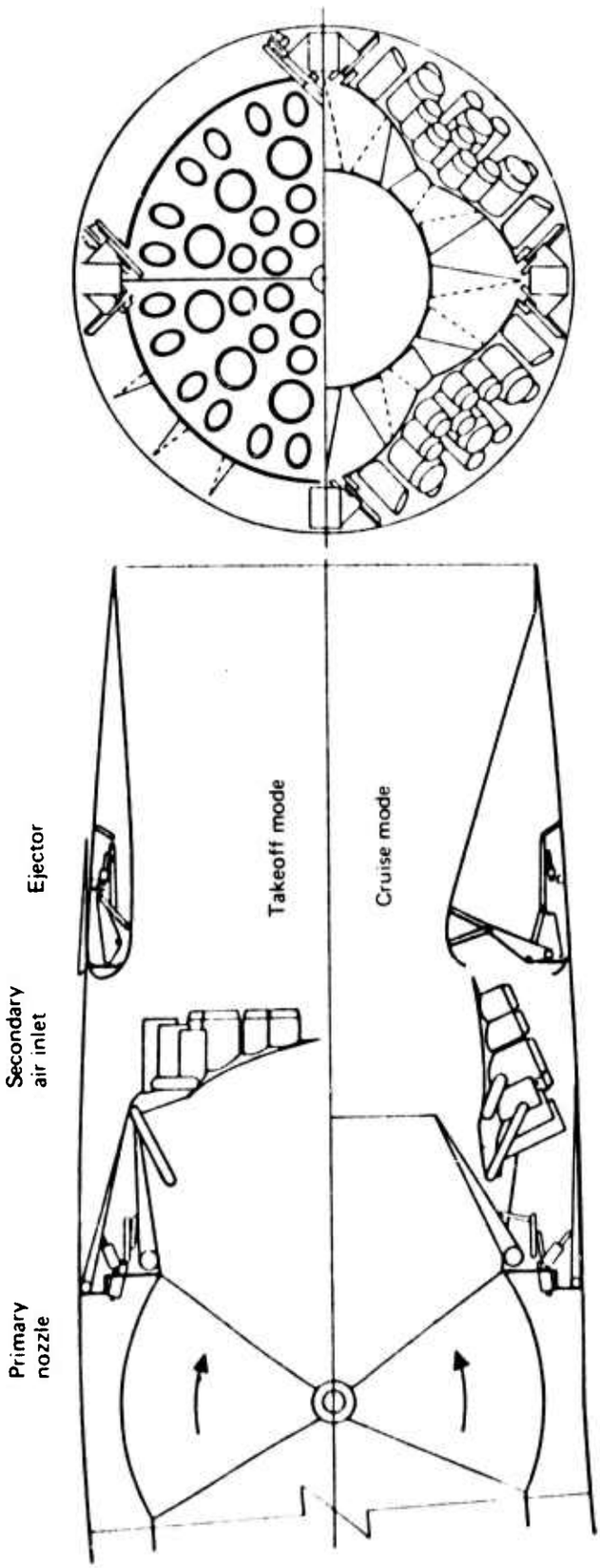


*Figure 4.–Application of Stowable Suppressor to an Advanced SST Exhaust System*

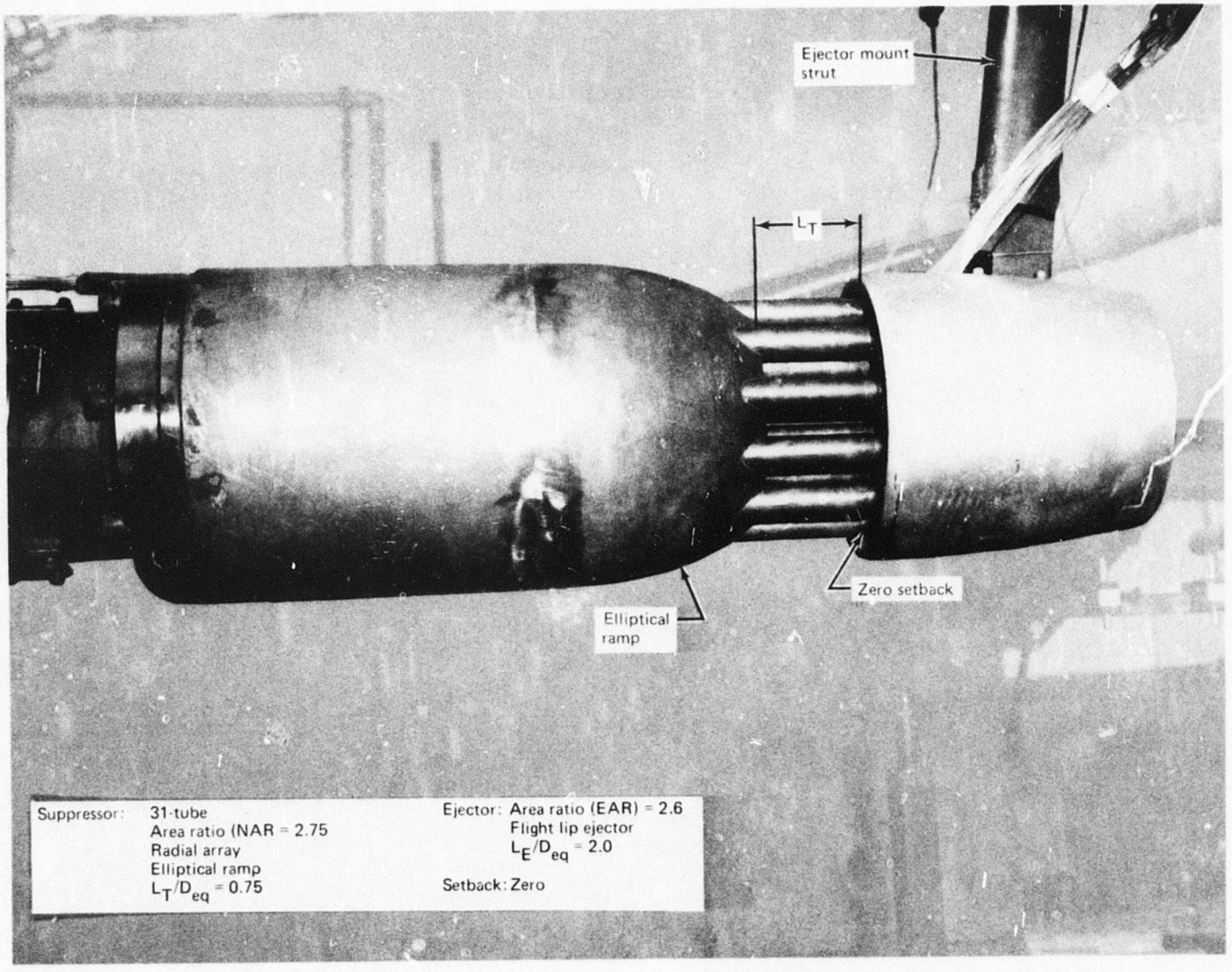


*Figure 5.—Typical Suppressor/Ejector Installation*

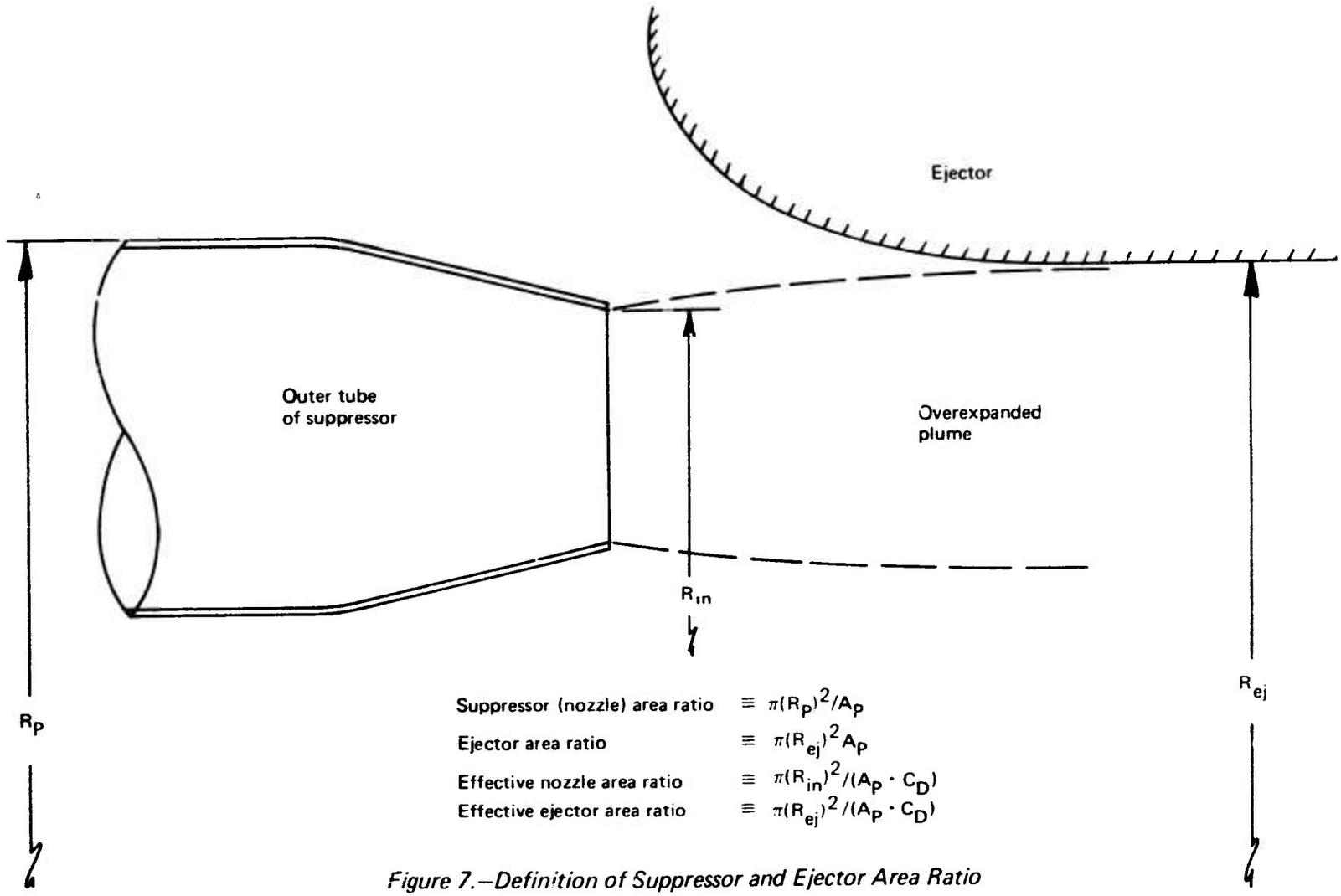


Suppressor (nozzle) area ratio $\equiv \pi(R_P)^2/A_P$

Ejector area ratio $\equiv \pi(R_{ej})^2 A_P$

Effective nozzle area ratio $\equiv \pi(R_{in})^2/(A_P \cdot C_D)$

Effective ejector area ratio $\equiv \pi(R_{ej})^2/(A_P \cdot C_D)$

*Figure 7.—Definition of Suppressor and Ejector Area Ratio*

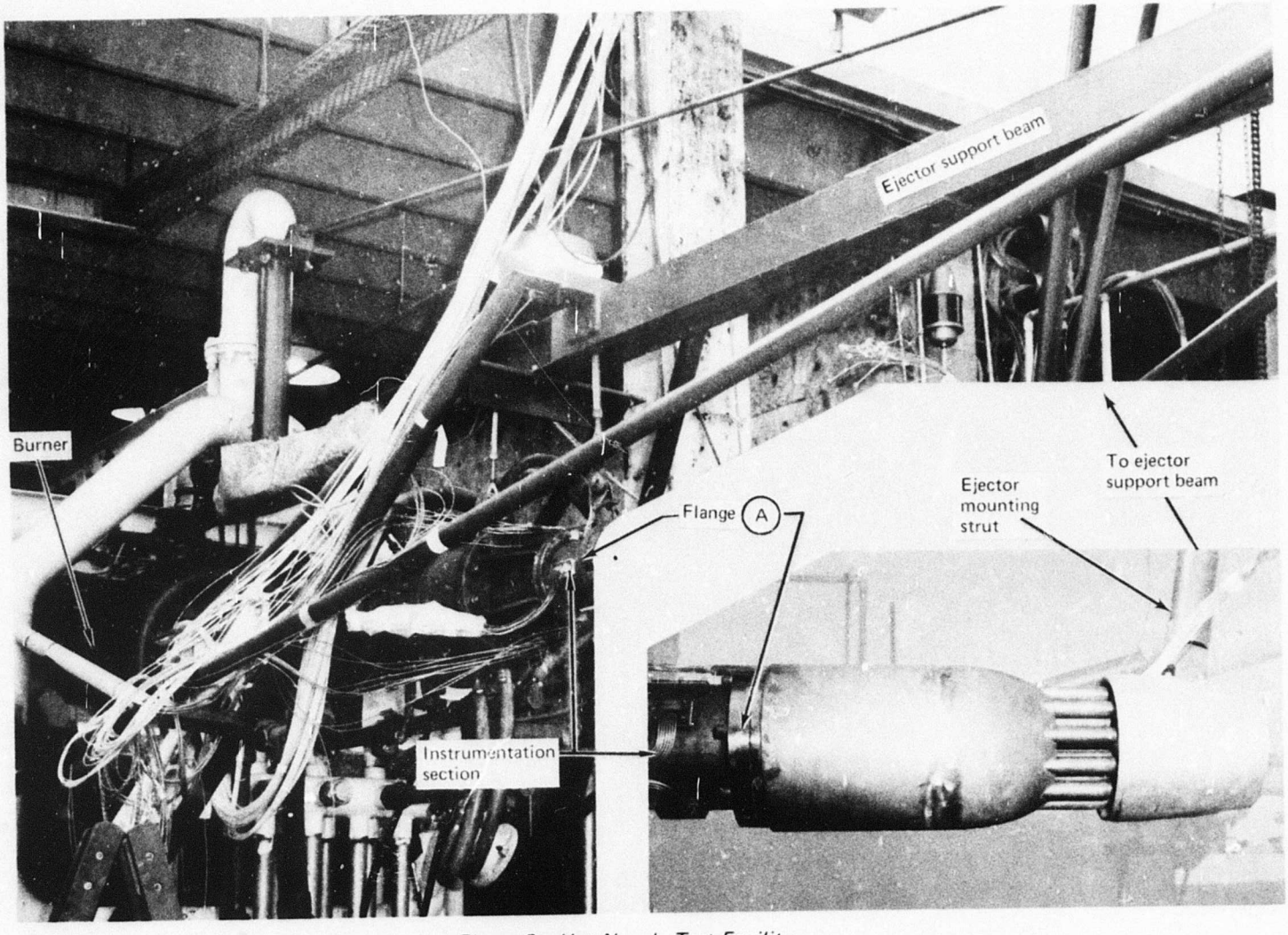


*Figure 8.–Hot Nozzle Test Facility*

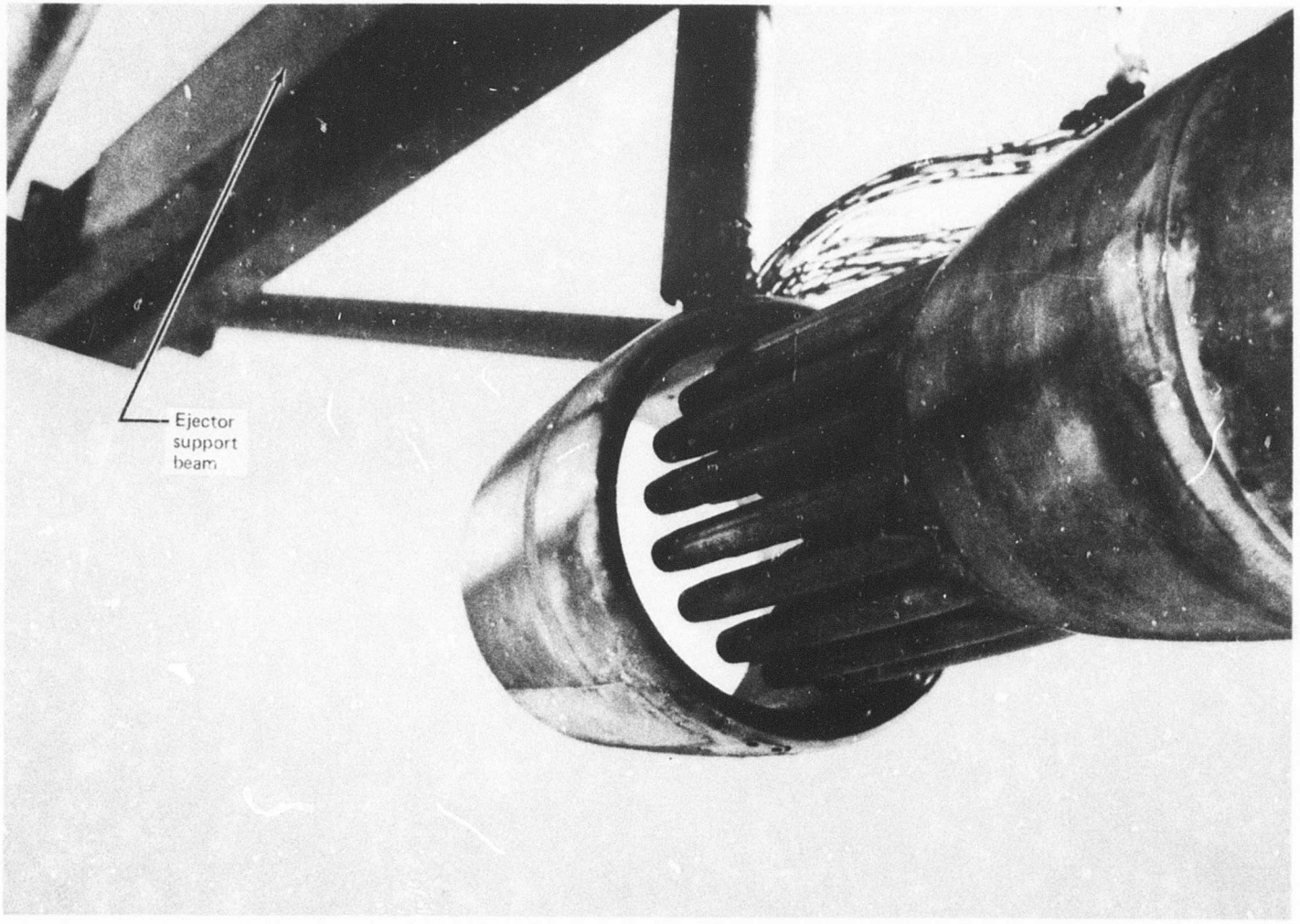


*Figure 9.—R/37 and 3.7 Area Ratio Flightlip Ejector*

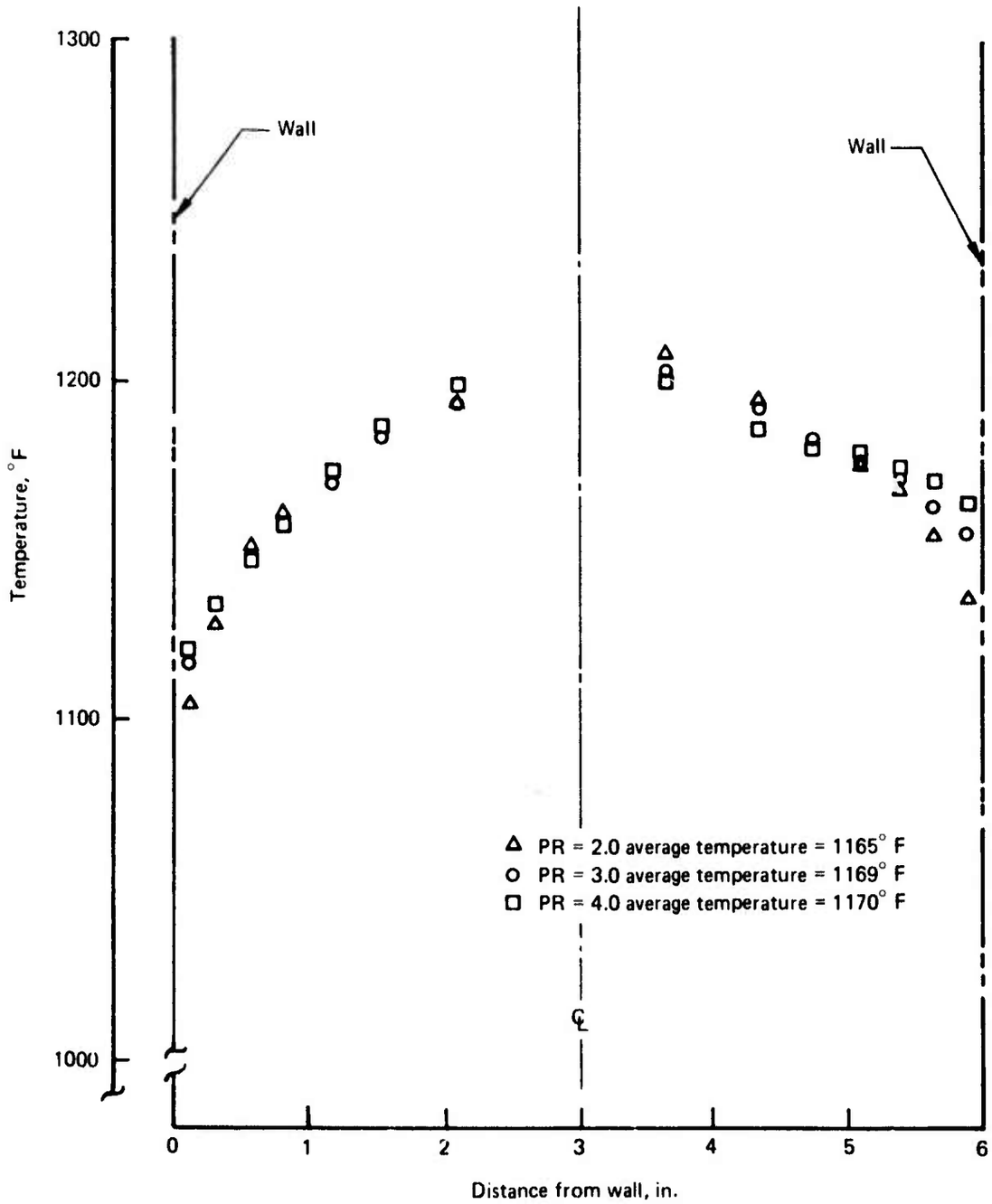


*Figure 10.—Typical Temperature Profile*

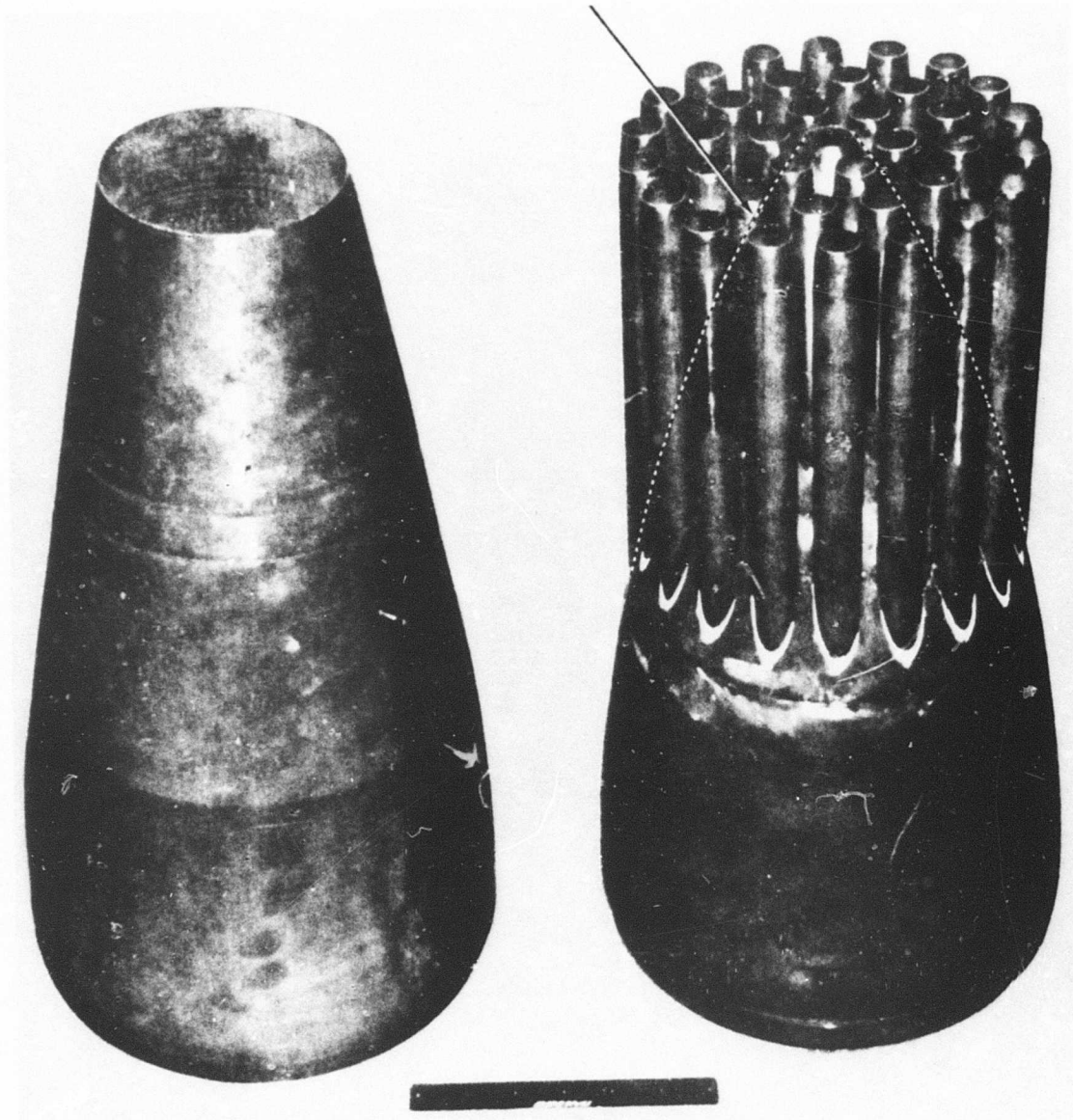

R/C nozzle

Round convergent
reference nozzle

R/37 nozzle

37 tube, area ratio = 33,
close-packed with
round convergent tubes

*Figure 11.--R/C and R/37 Nozzles*

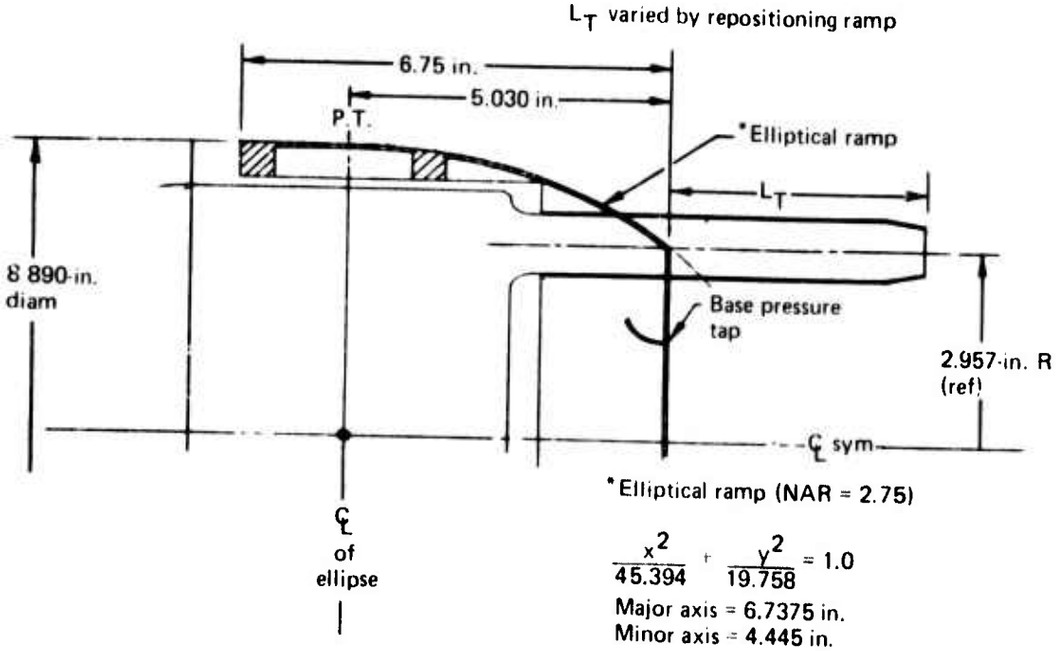


**NAR 2.75**

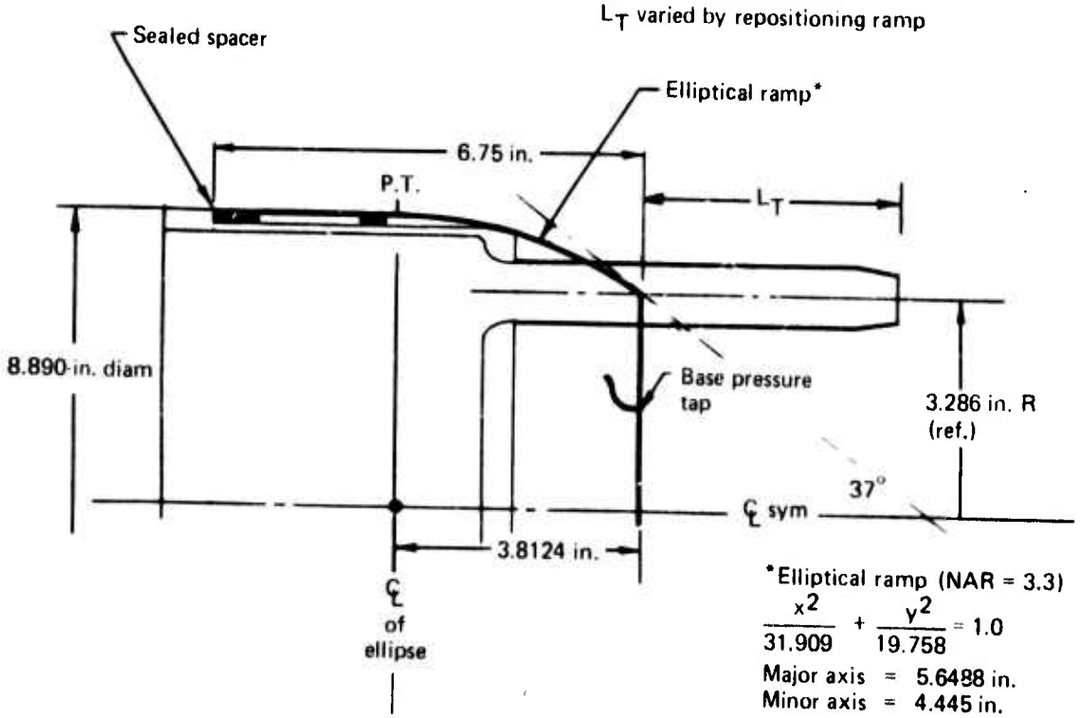


**NAR 3.3**

*Figure 12.—Elliptical Ramps*

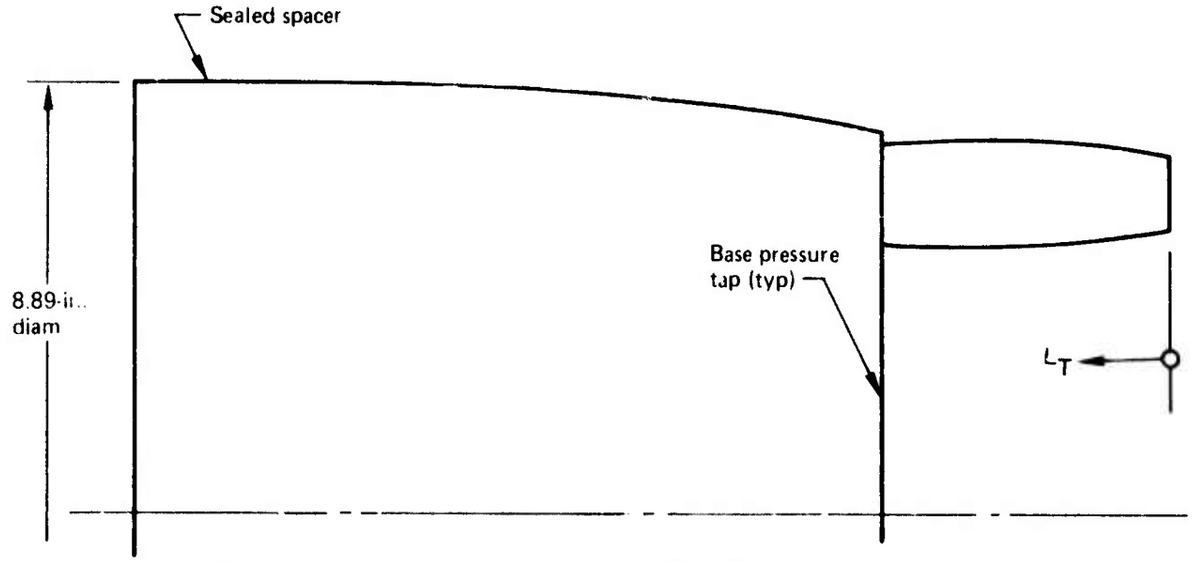


*Figure 13.–Circular Arc Ramp and Method for Varying External Tube Length, $L_T$ (Constant Internal Tube Length)*

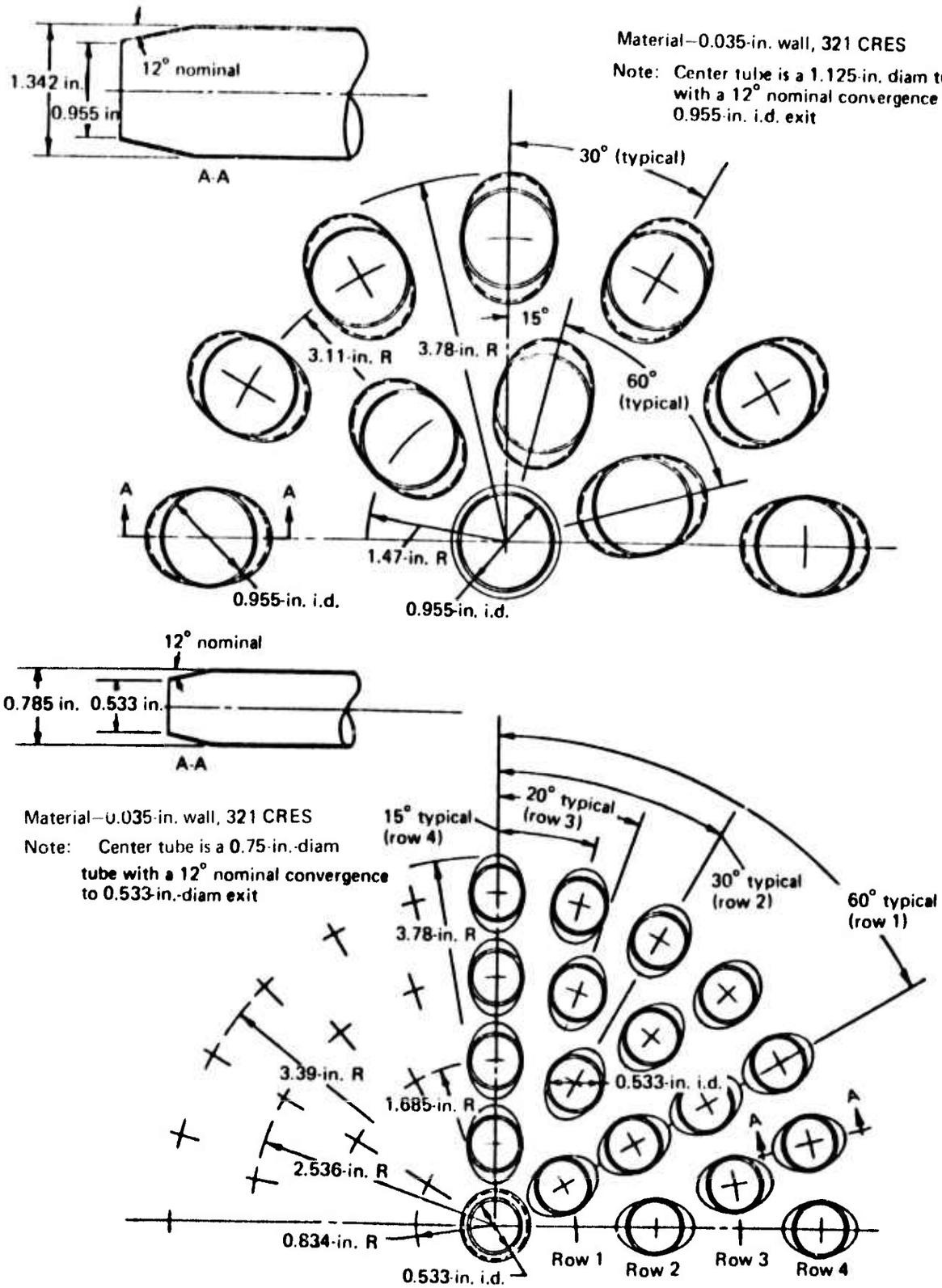


*Figure 14.—19- and 61-Tube, Area Ratio = 3.3 Suppressors*

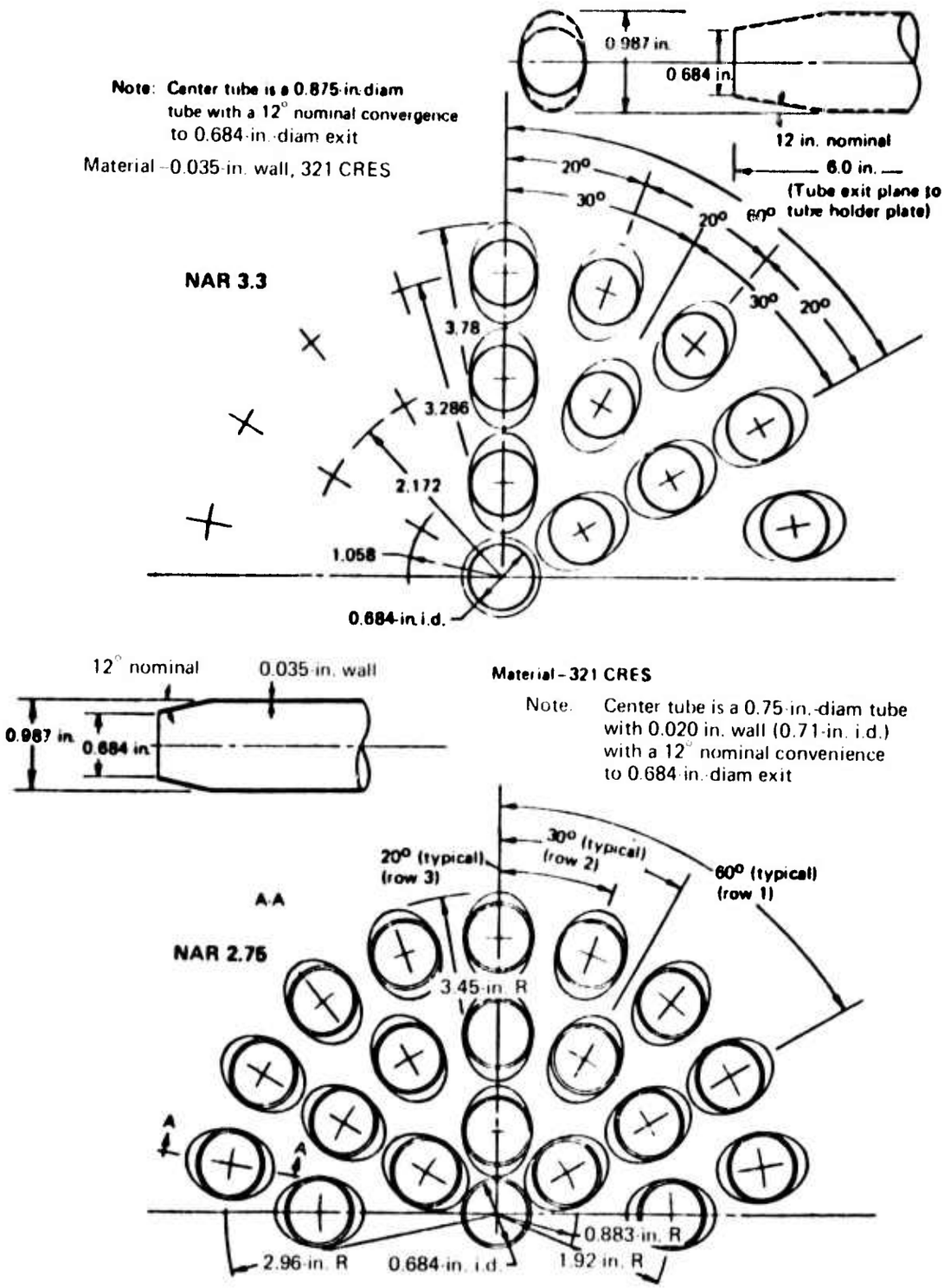


*Figure 15.—37-Tube, Close-Packed Suppressors, NAR = 2.75 and 3.3*

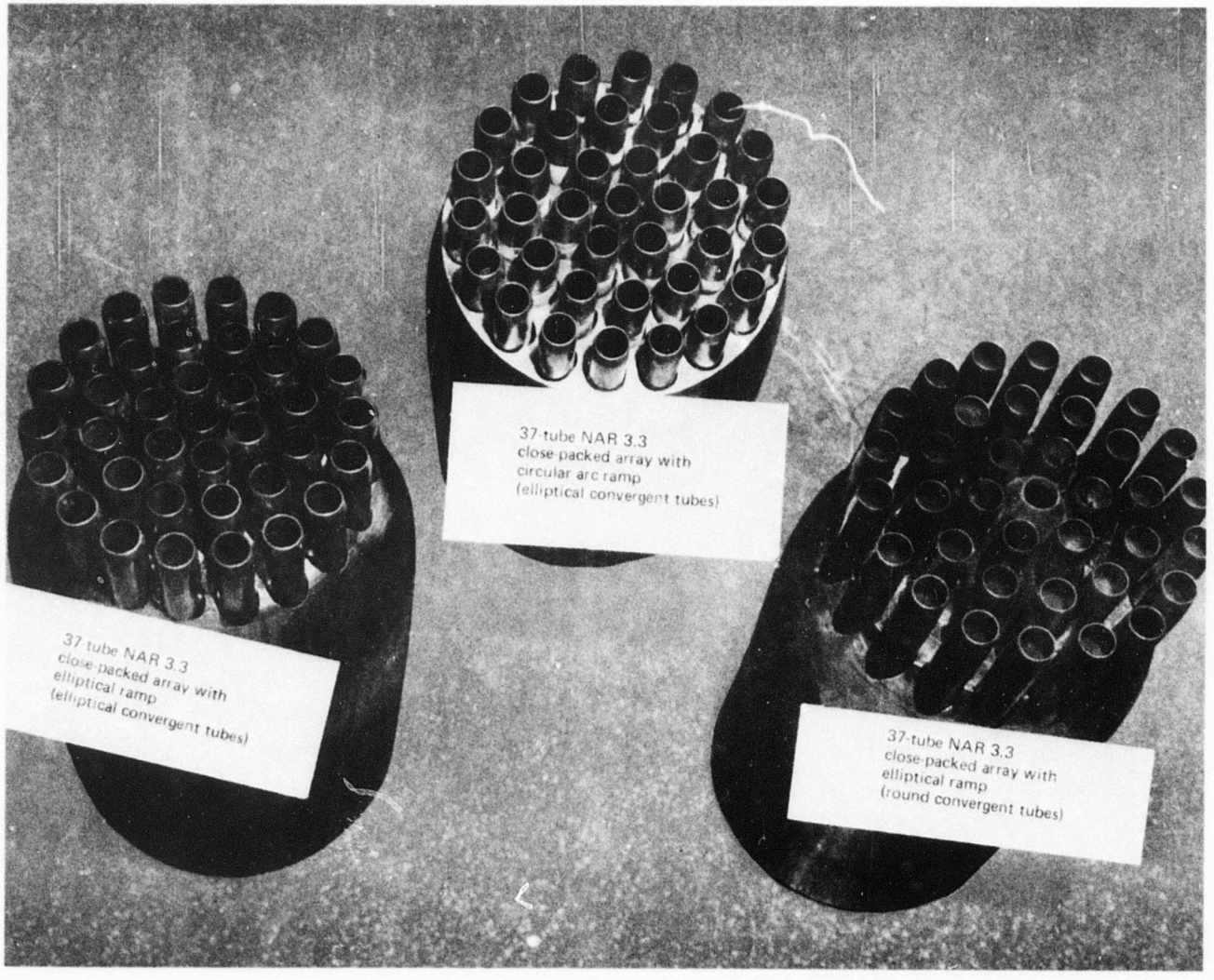


*Figure 16.—Comparison of 37-Tube, Area Ratio = 3.3 Nozzles*

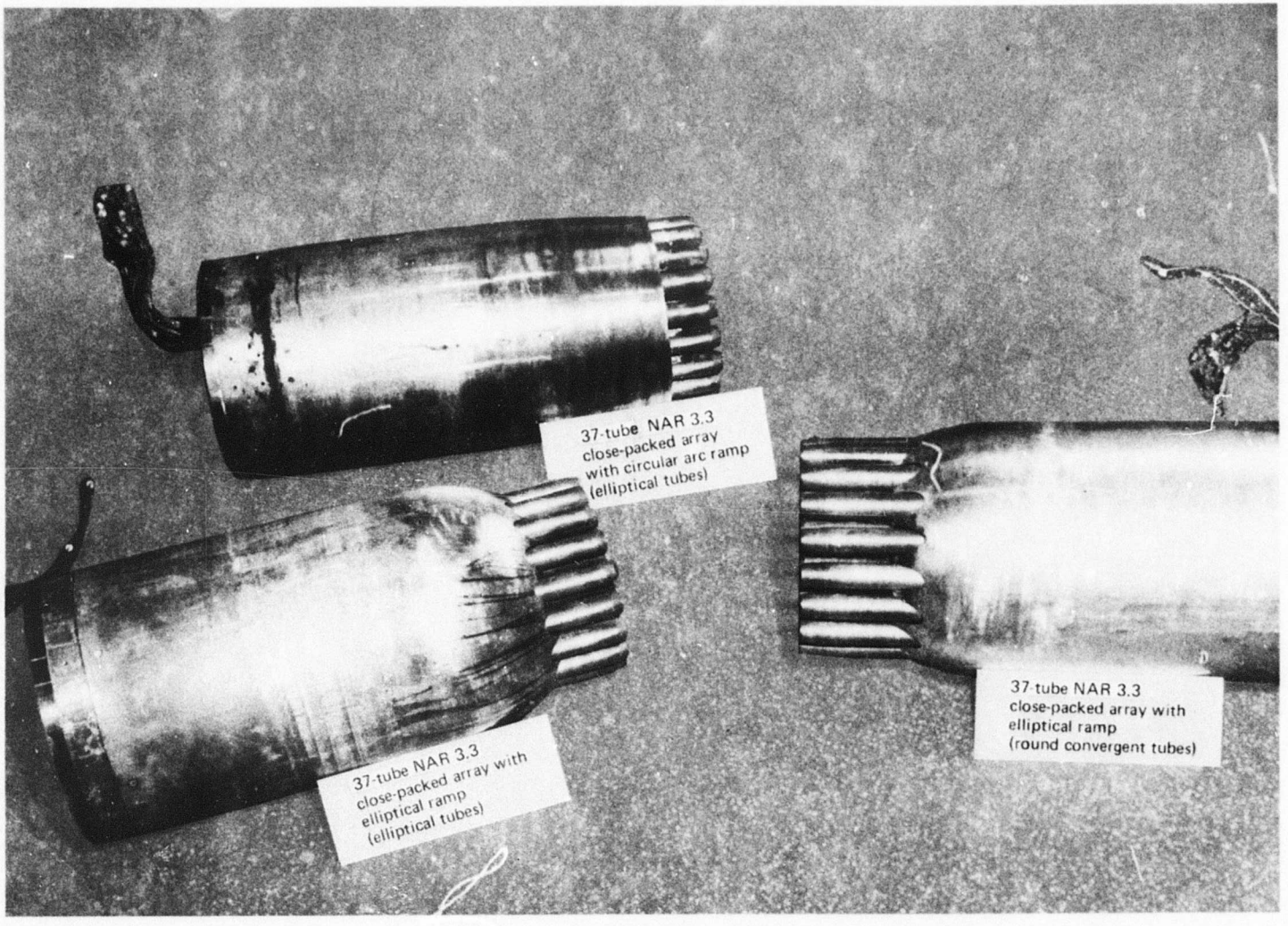


*Figure 17.—37-Tube, Area Ratio = 3.3, Close-Packed Arrays With Various Ramps and Tube Shapes*

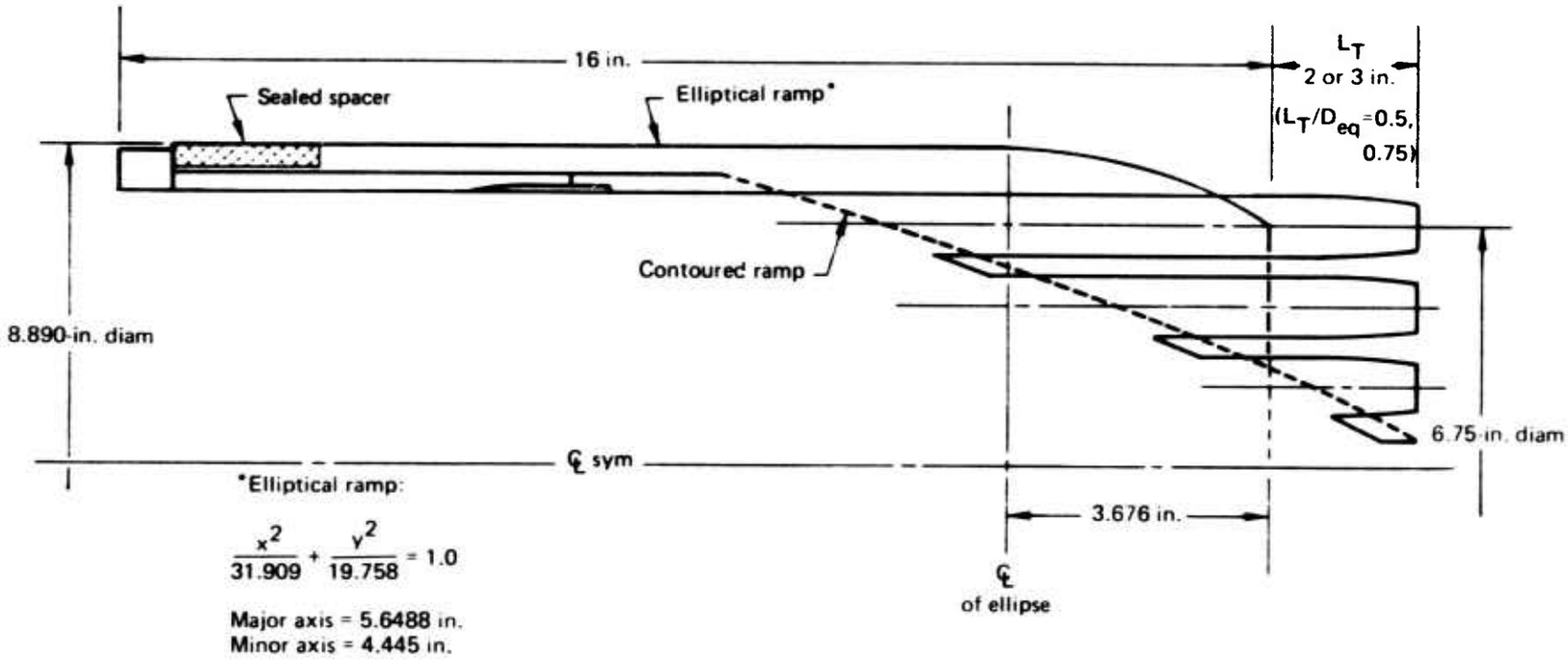


*Figure 18.—Elliptical Ramp for 37-Tube, NAR = 3.3, Close-Packed Array With Round Convergent Tubes*

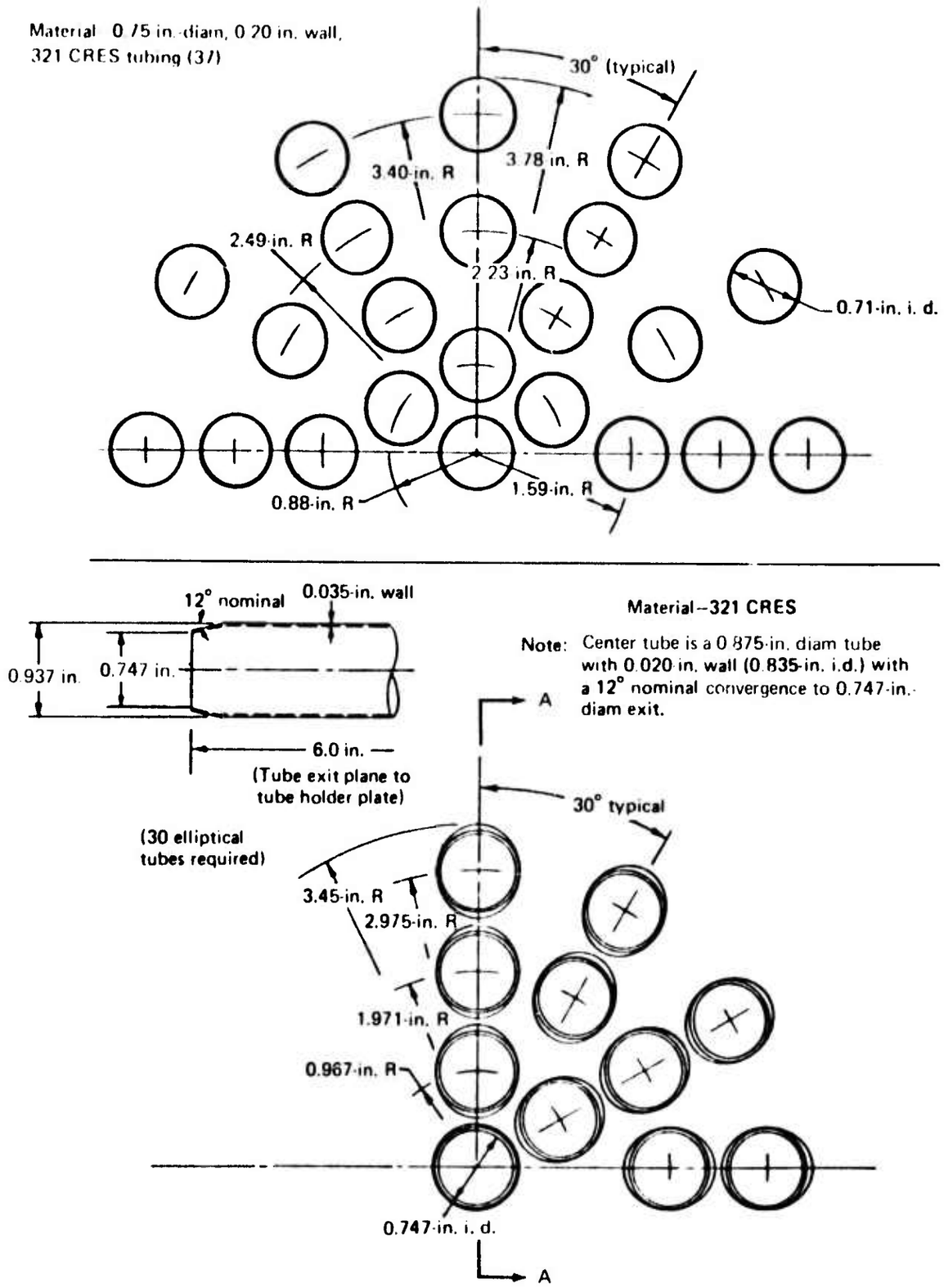


*Figure 19.–Radial Array Nozzles*

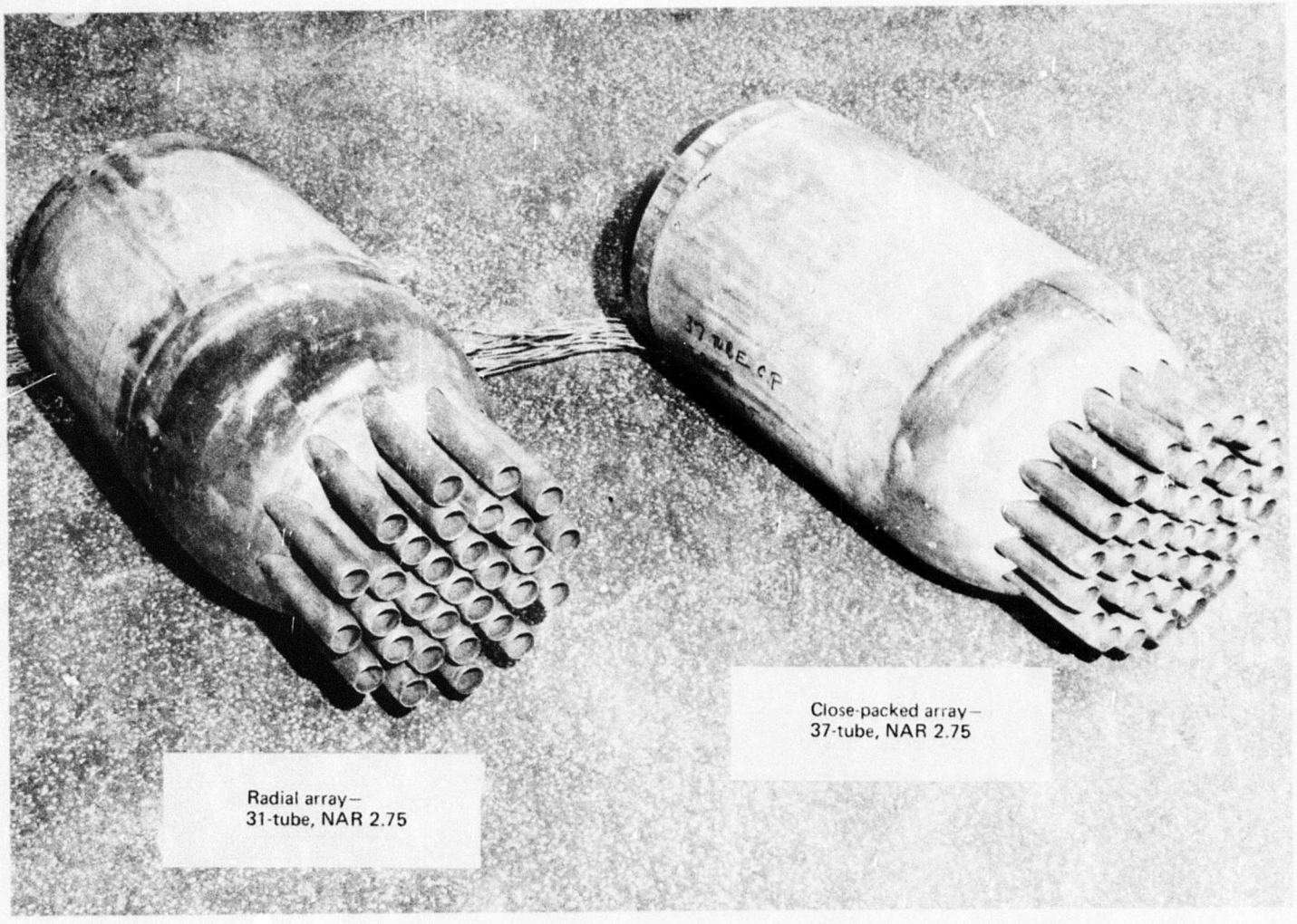


*Figure 20.–Radial and Close-Packed NAR = 2.75 Suppressors*

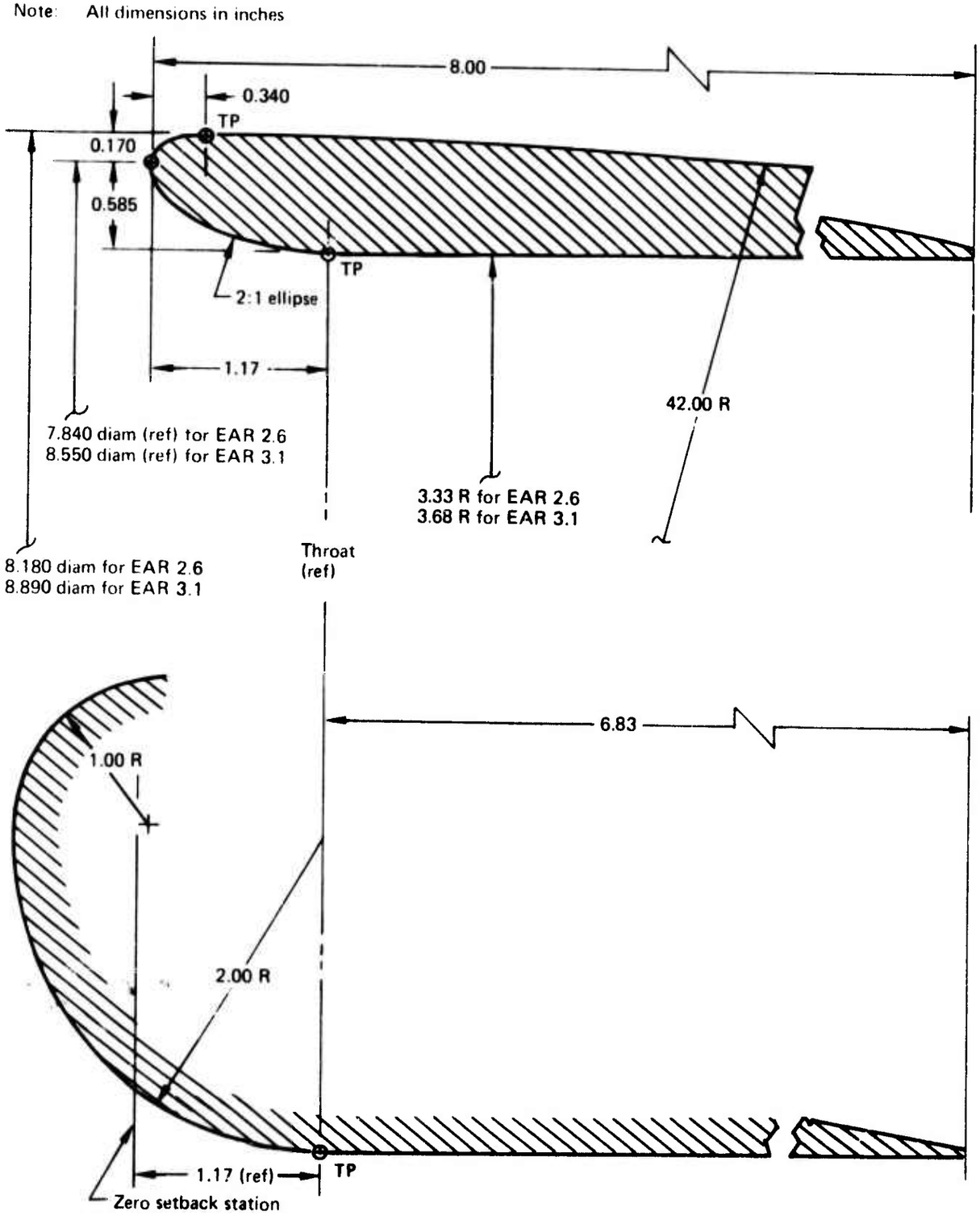


*Figure 21.—Area Ratio = 2.6 and 3.1 Bellmouth and Flightlip Ejectors*

Note: All dimensions in inches

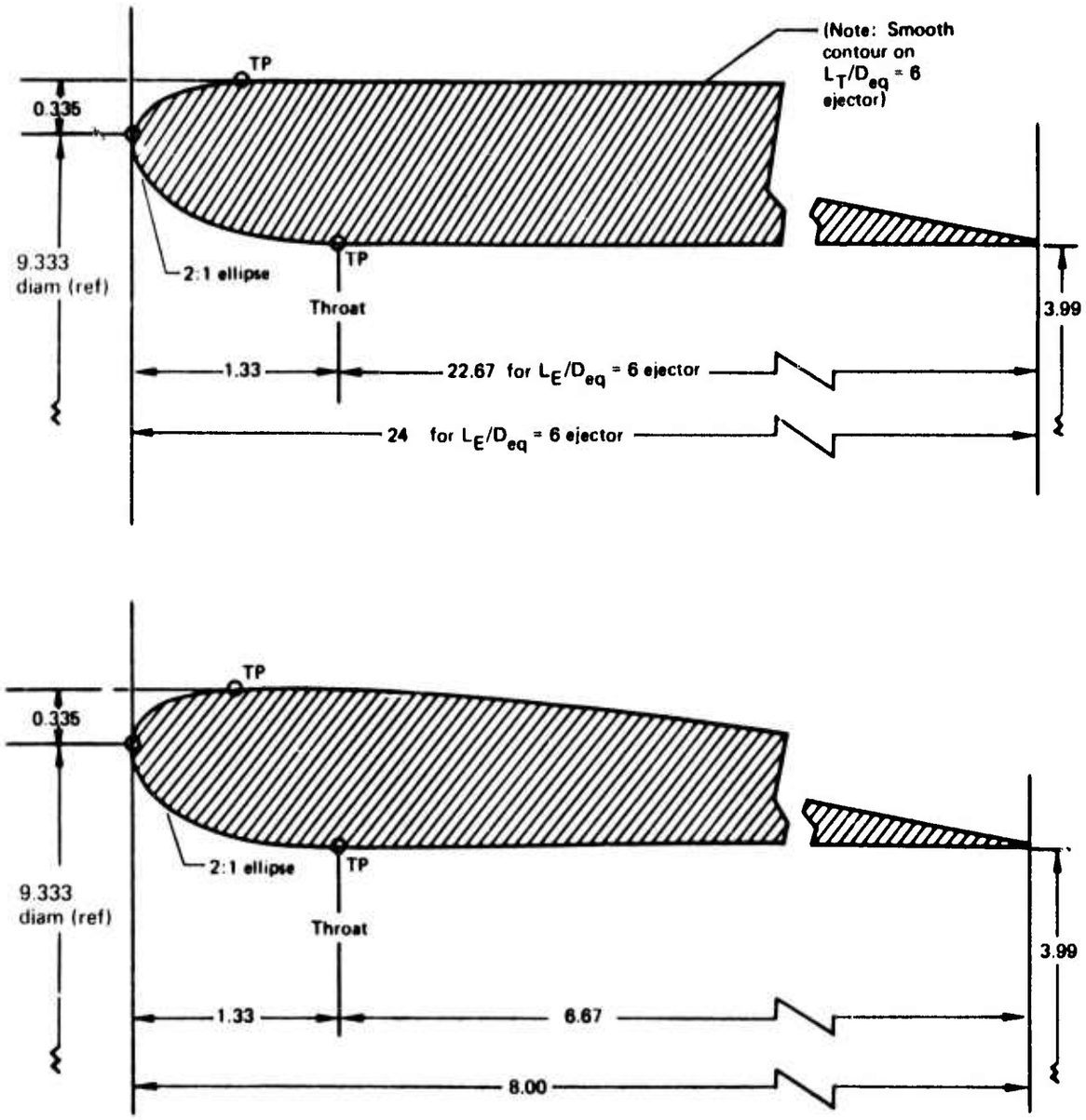


*Figure 22.–Area Ratio (EAR) = 3.7 Flightlip Ejectors, $L_E/D_{eq}$ = 2 and 6*


*Figure 23.–$L_E/D_{eq}$ = 2.0 Flightlip Ejectors*

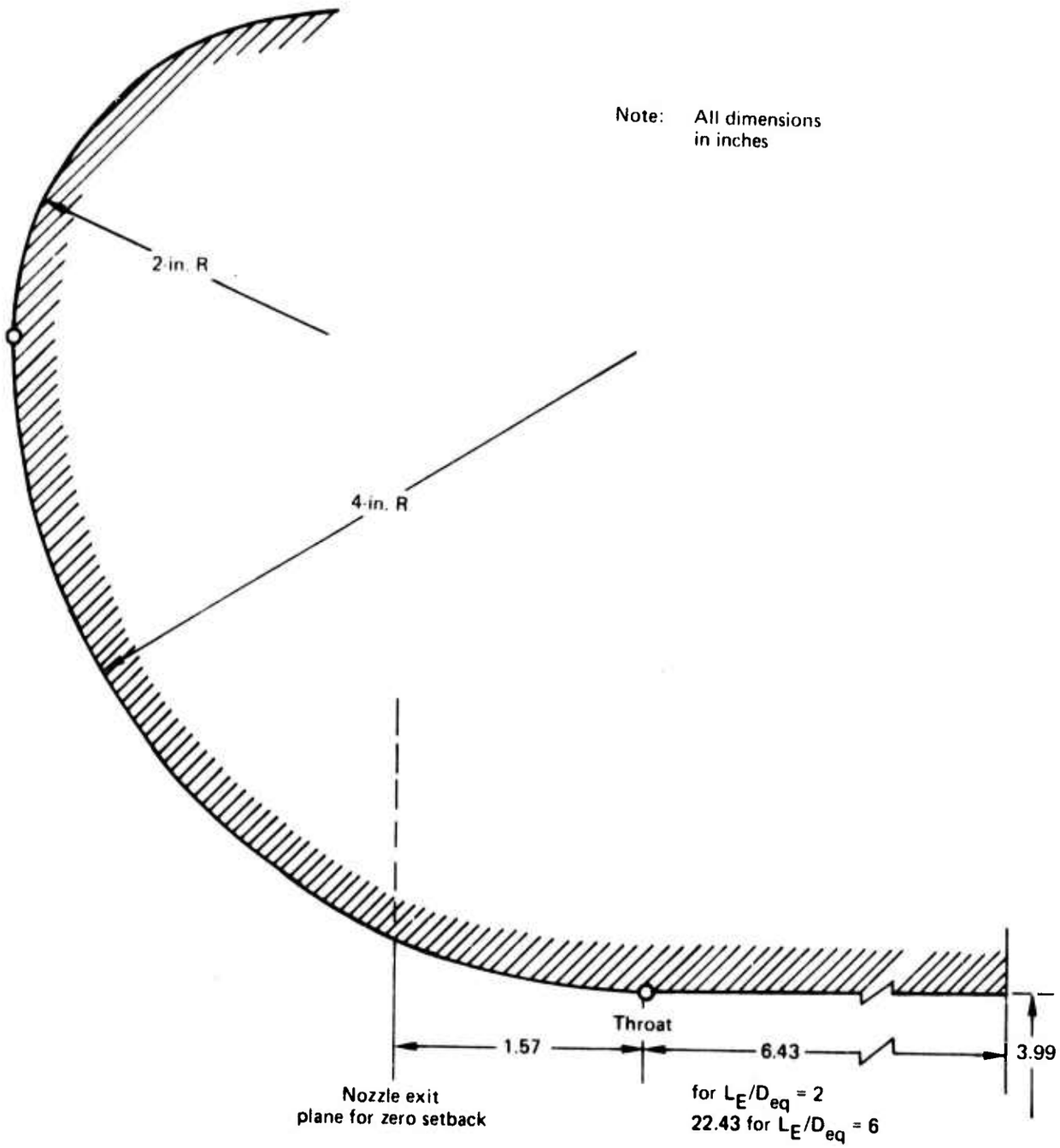


*Figure 24.—Area Ratio (EAR) = 3.7 Bellmouth Ejectors, $L_E/D_{eq}$ = 2 and 6*

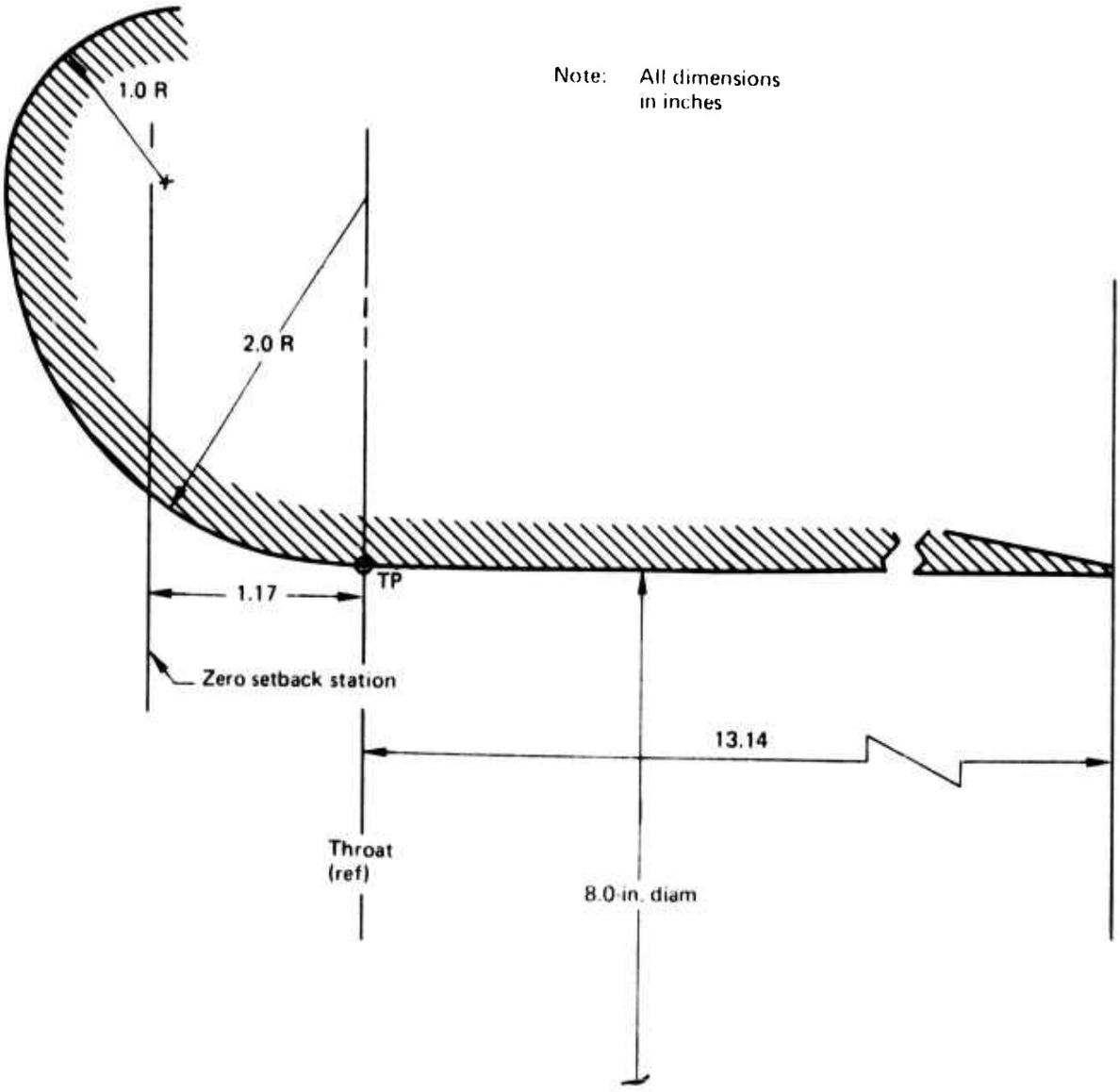


*Figure 25.—Area Ratio (EAR) = 3.7 Bellmouth Ejectors, $L_E/D_{eq}$ = 3.6 (14.3 in.)*

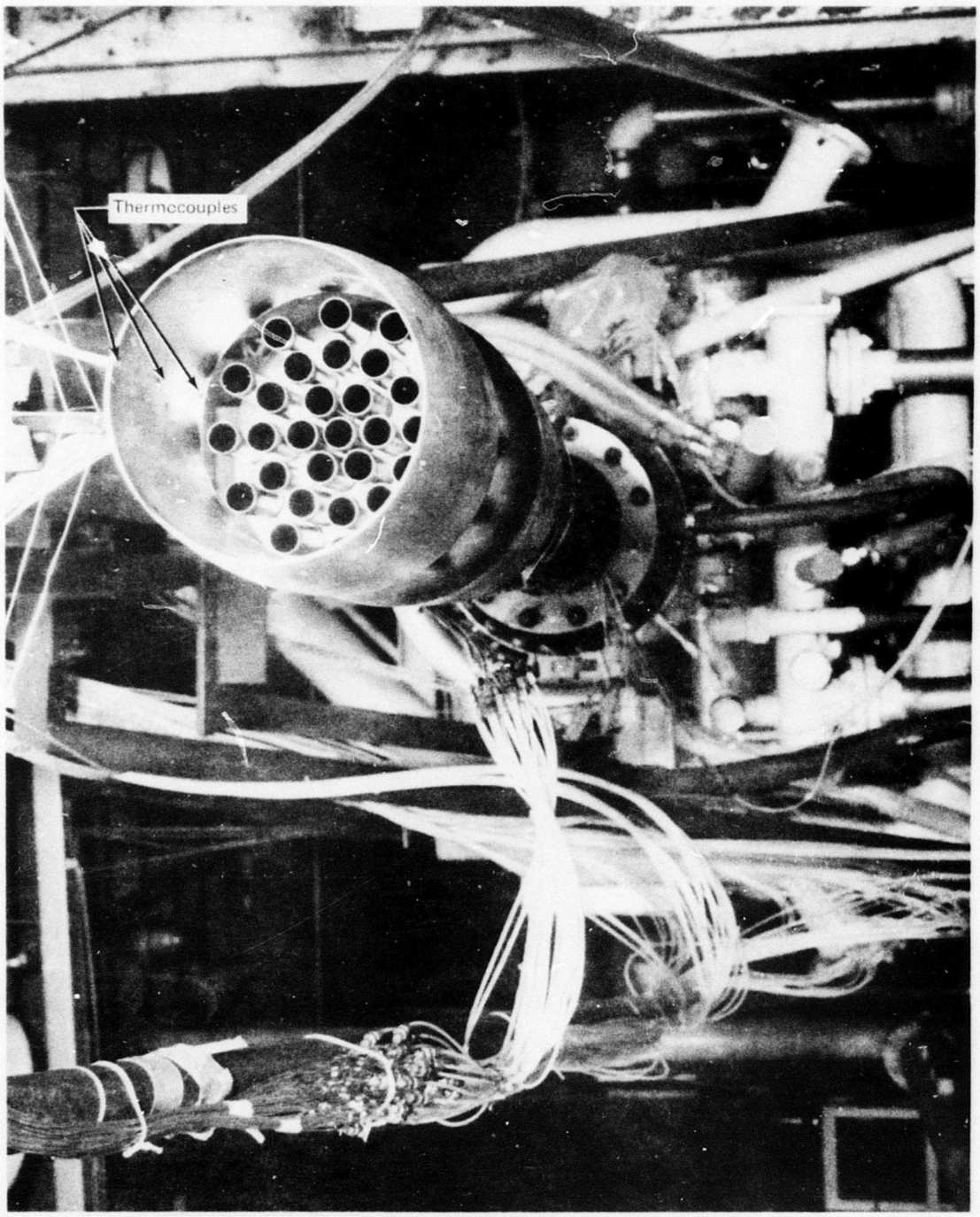


*Figure 26.—Typical Thermocouple Placement*

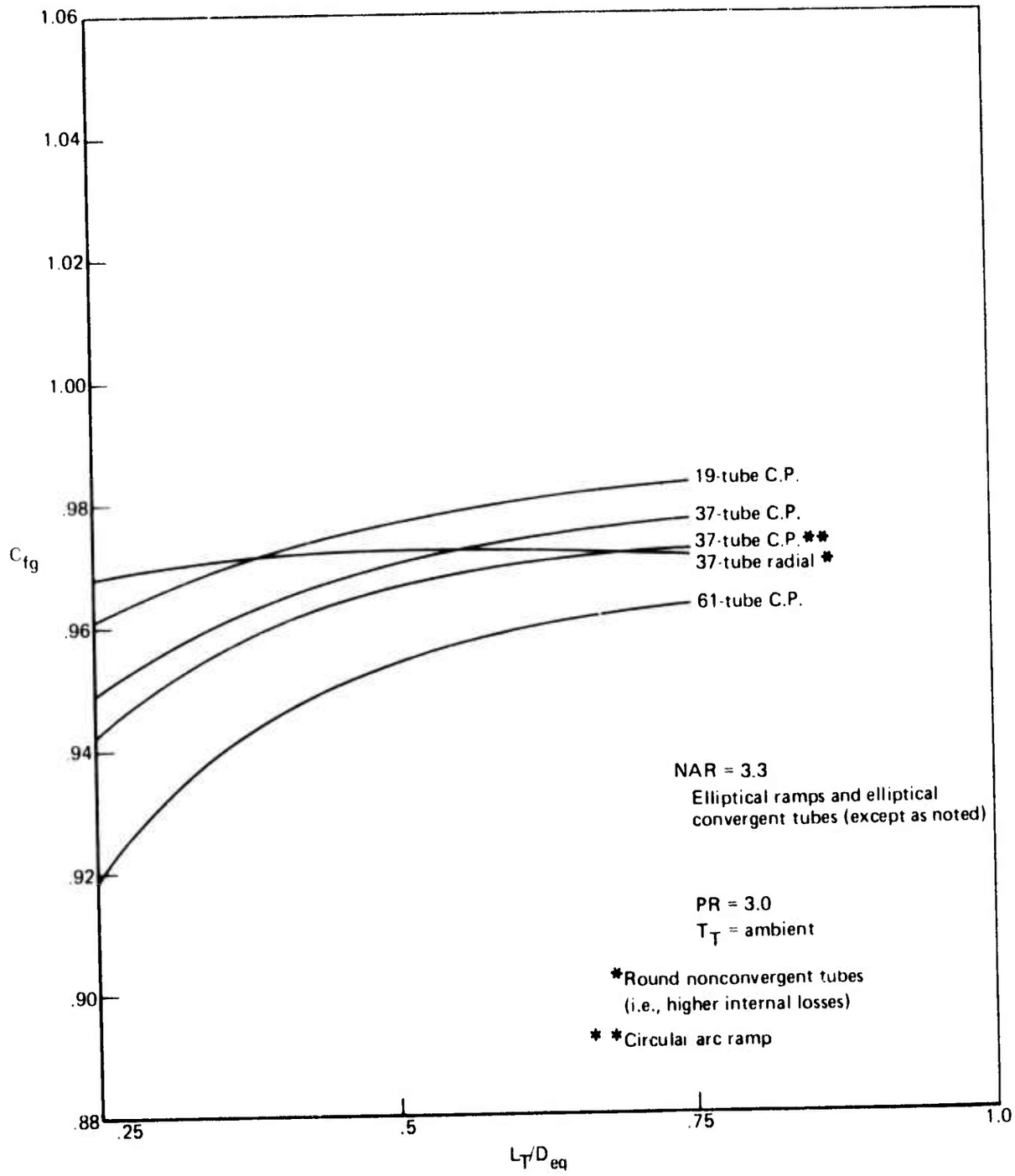


*Figure 27.–Performance Versus Tube Length for Various NAR = 3.3 Suppressors Without Ejectors*

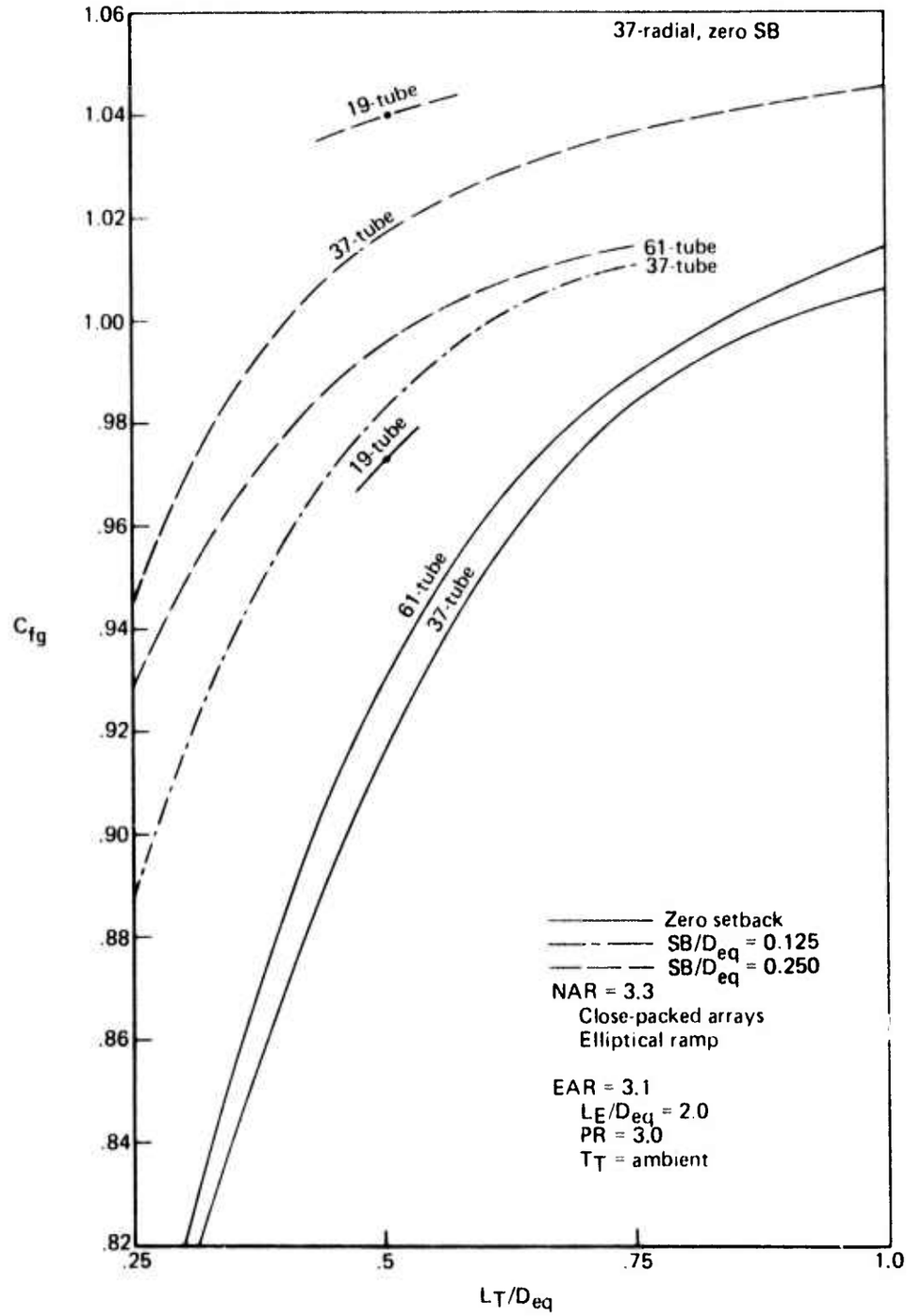


*Figure 28.—Performance as a Function of Tube Length for Various NAR = 3.3 Suppressors With EAR = 3.1 Ejectors*

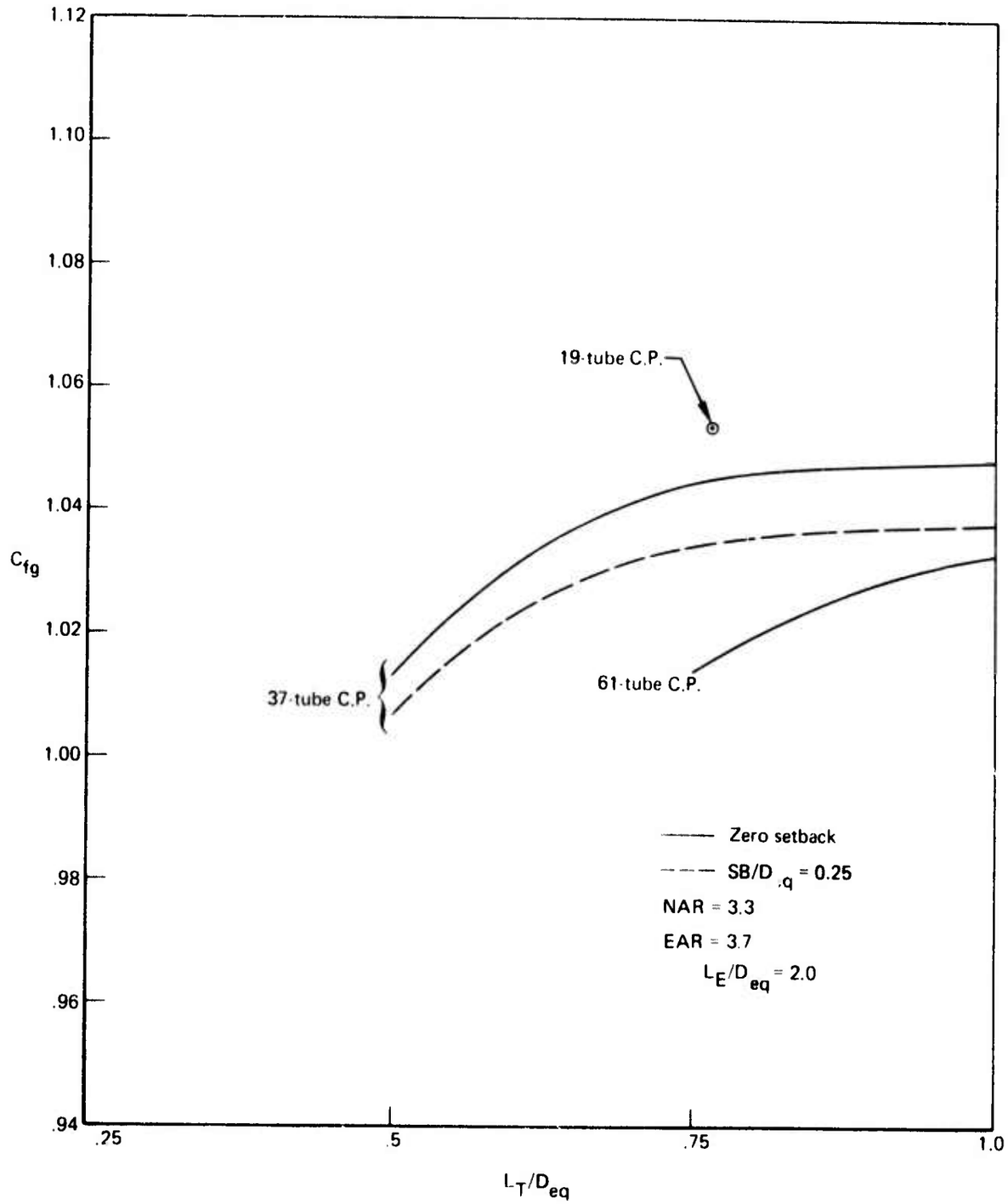


*Figure 29.—$C_{fg}$ Versus Tube Length for Various NAR = 3.3 Suppressors With EAR = 3.7 Ejectors*

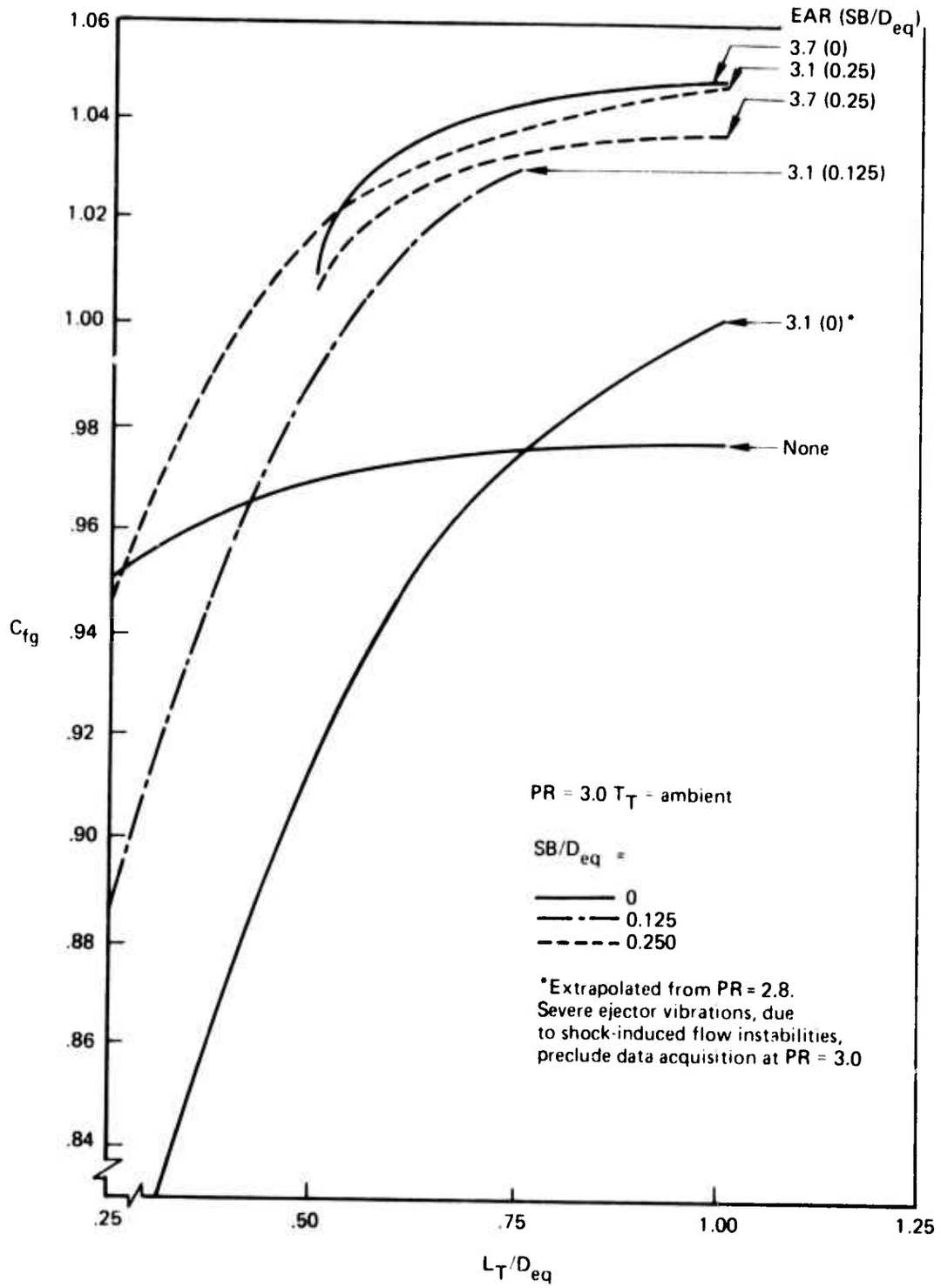


*Figure 30.–$C_{fg}$ Versus Tube Length for a 37 Tube, NAR = 3.3, Close-Packed Suppressor With Various Ejectors*

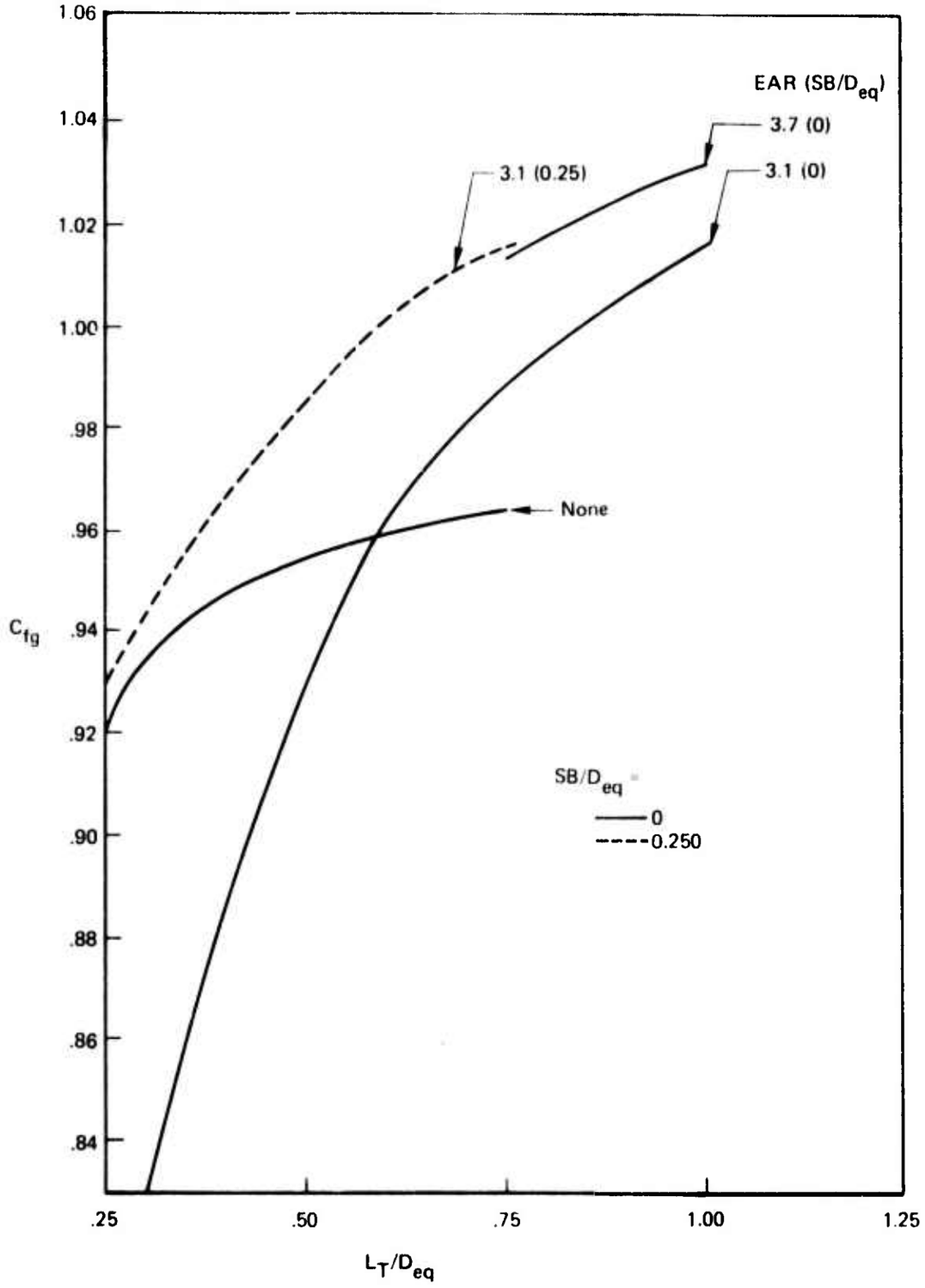


*Figure 31.—$C_{fg}$ Versus Tube Length for a 61-Tube, NAR = 3.3, Close-Packed Suppressor With Various Ejectors*

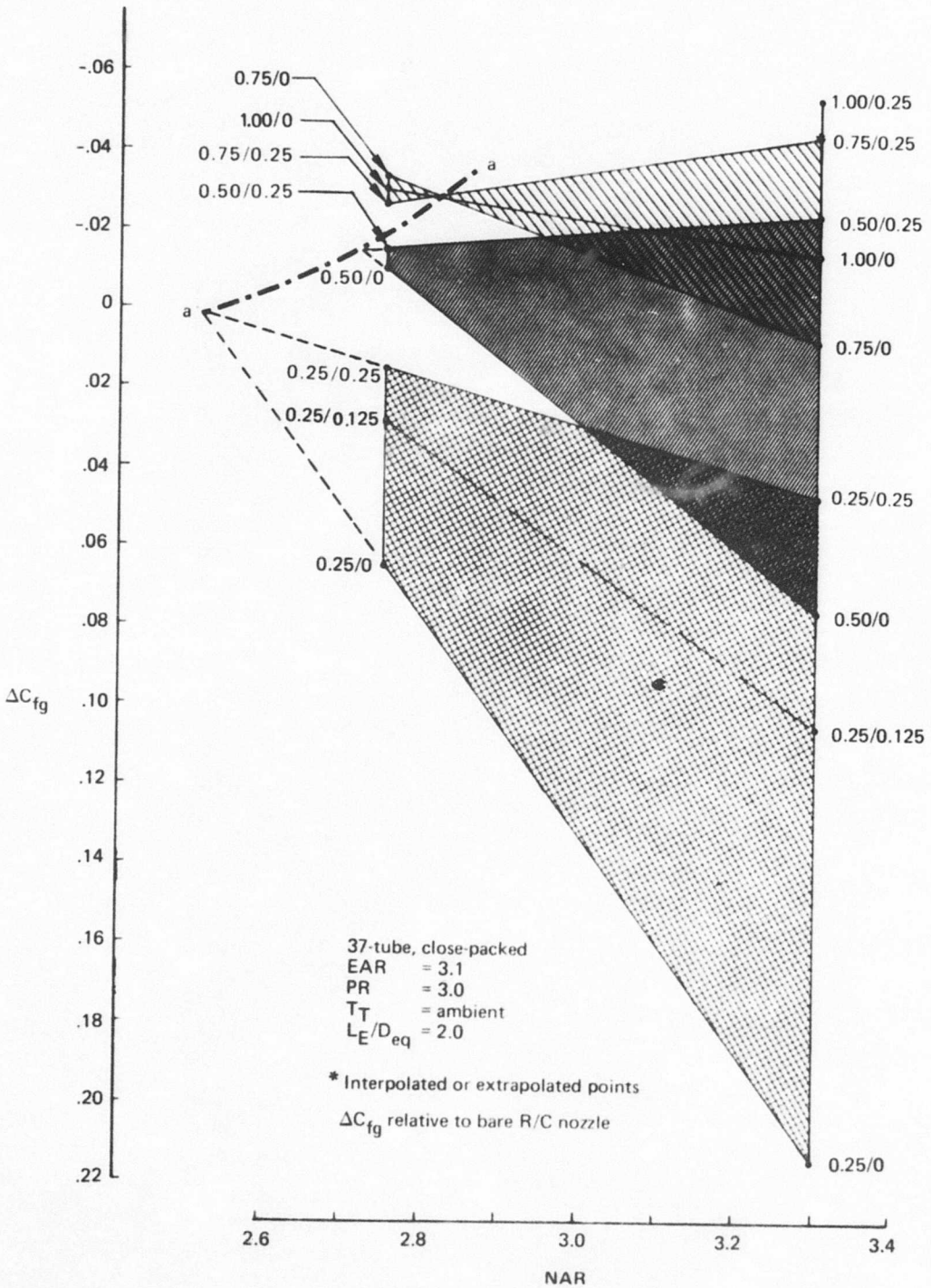


*Figure 32.—Primary Nozzle Pressure Ratio*

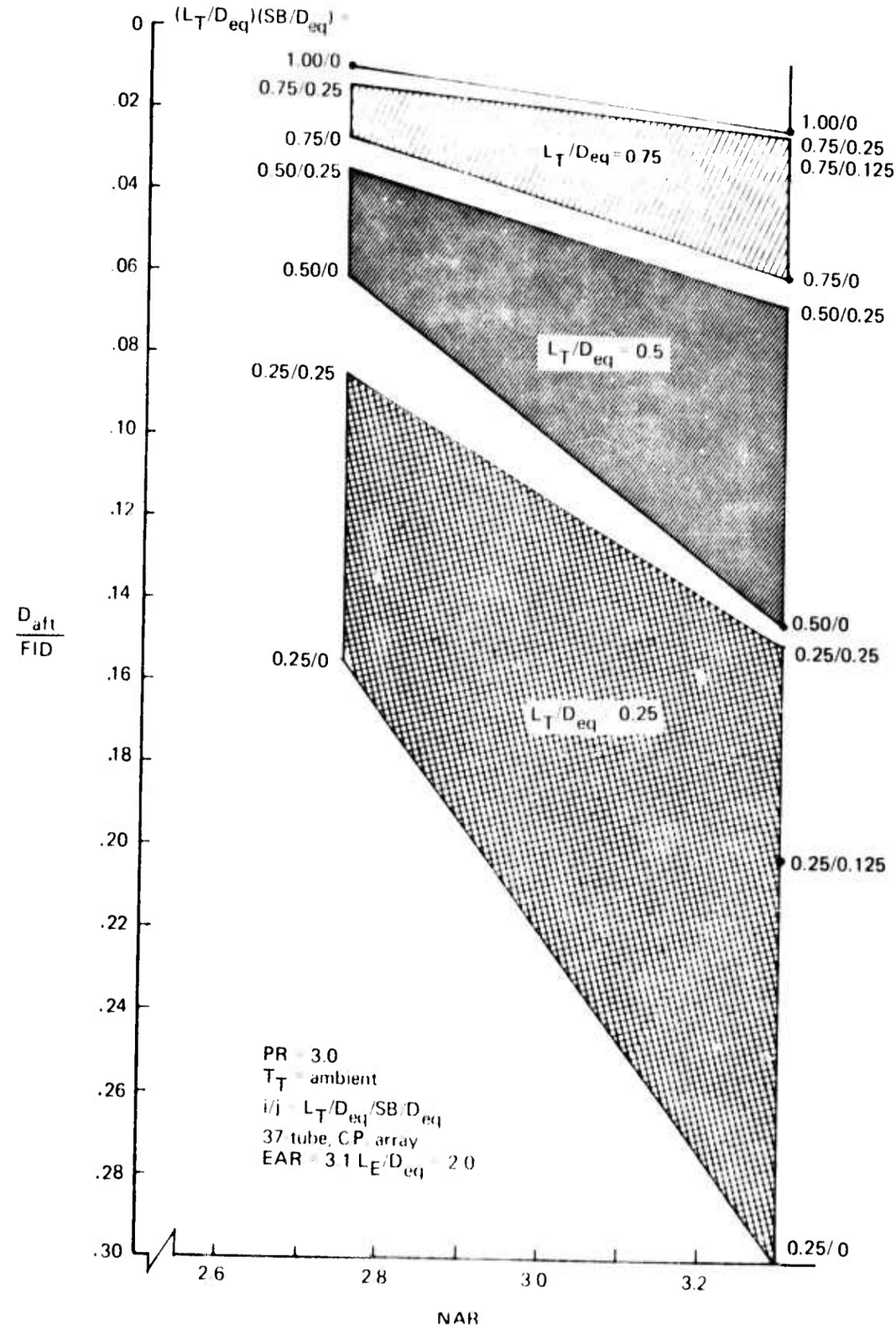


*Figure 33. Effect of Nozzle Area Ratio, Tube Length, and Setback on Afterbody Drag*

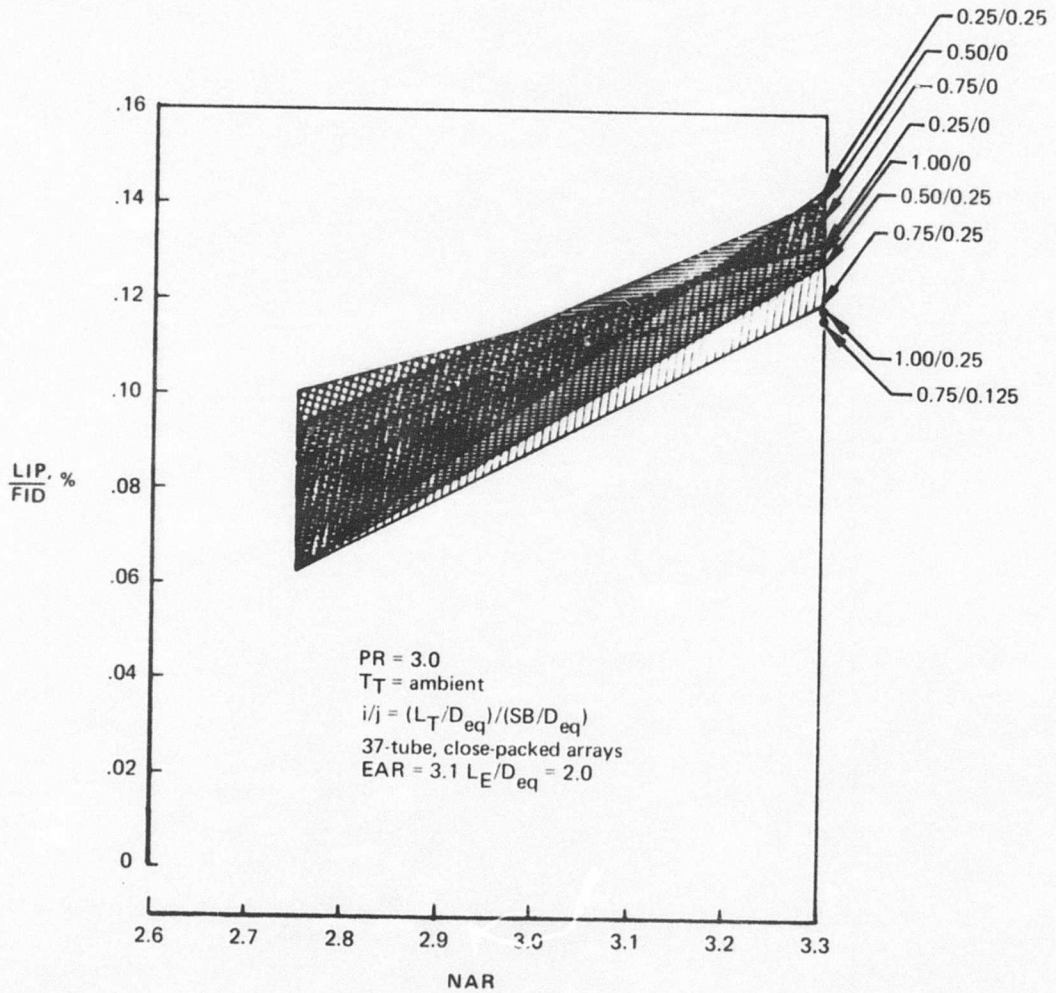


*Figure 34.—The Effect of Nozzle Area Ratio, Tube Length, and Setback on Lip Suction*

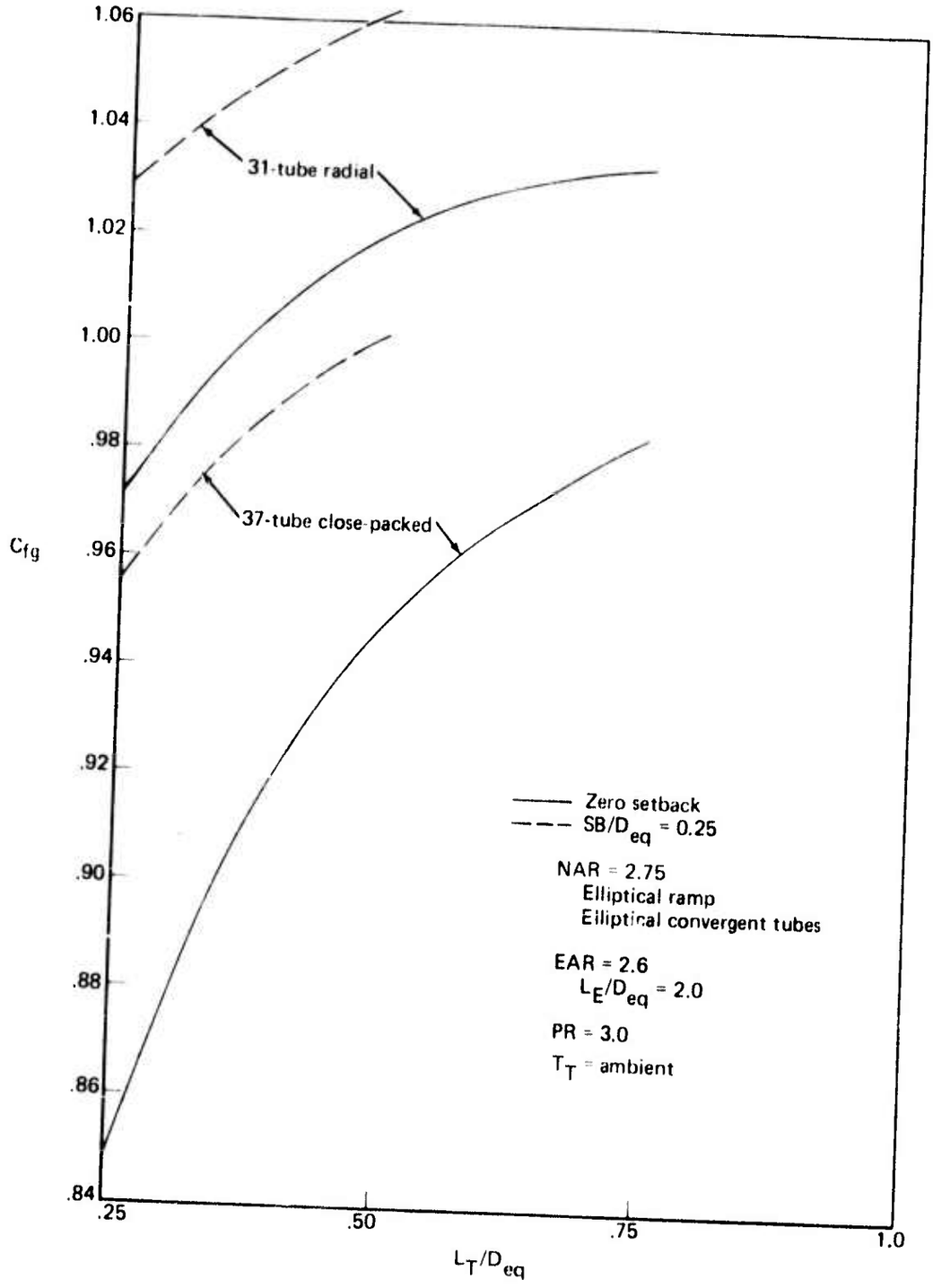


*Figure 35.—Performance as a Function of Tube Length for Various NAR = 2.75 Suppressors With EAR = 2.6 Ejectors*

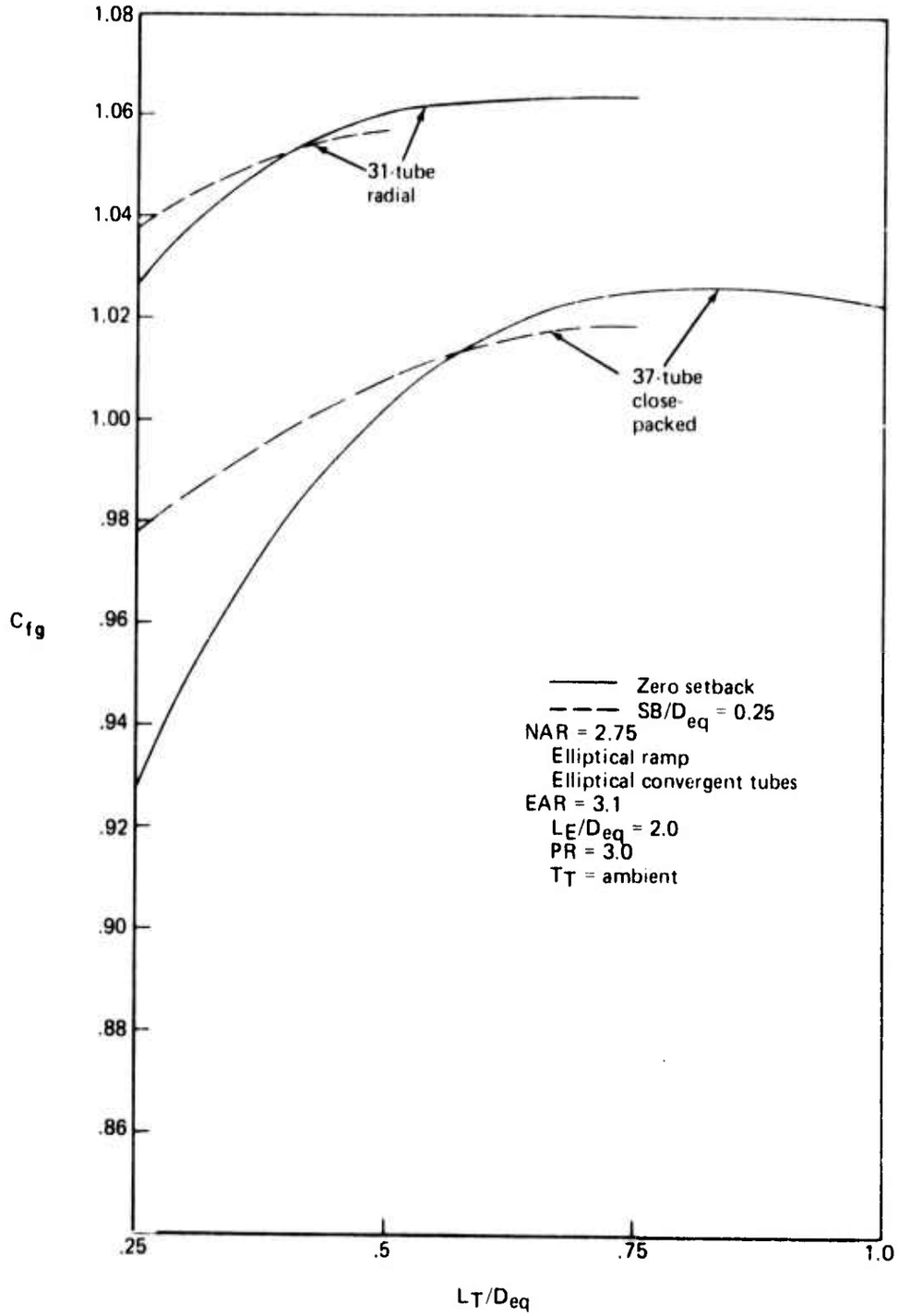


*Figure 36.—Performance as a Function of Tube Length for Various NAR = 2.75 Suppressors With EAR = 3.1 Ejectors*

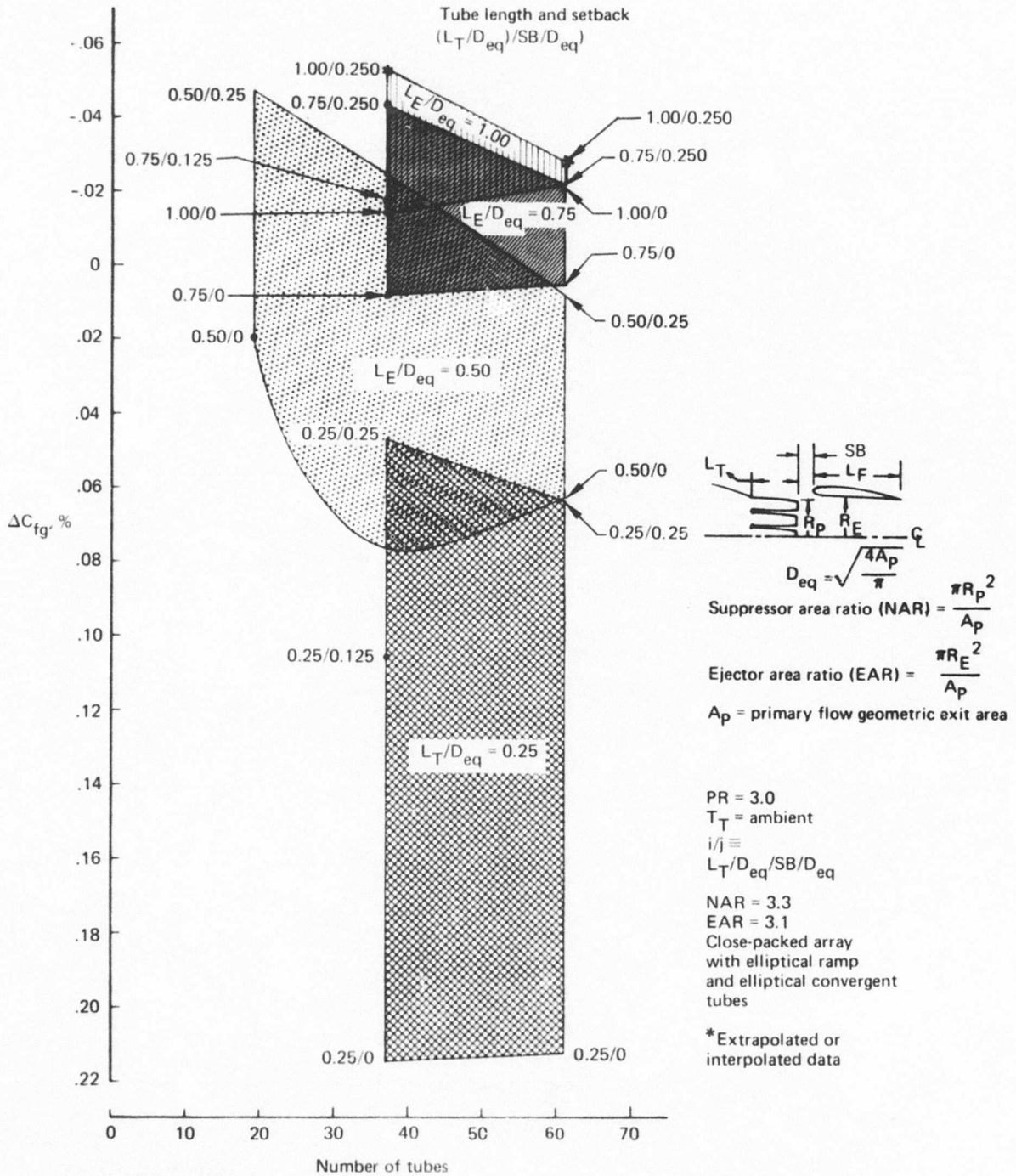


*Figure 37.—Thrust Loss Relative to R/C Nozzle as a Function of Tube Number, Tube Length, and Ejector Setback*

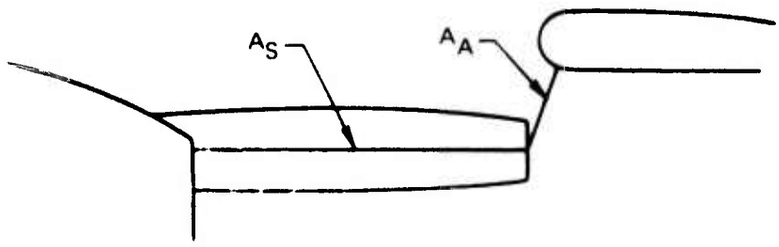


Detail X-X

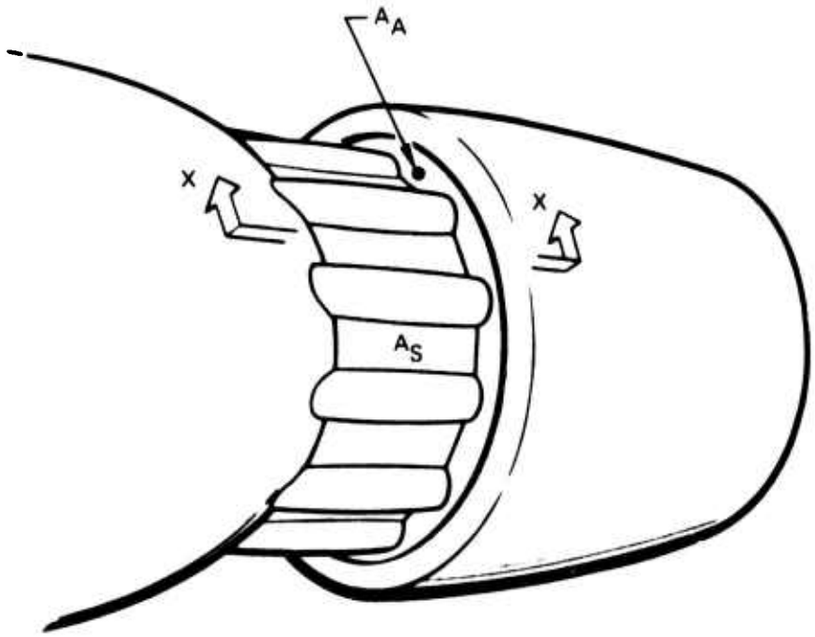


*Figure 38.–Ejector Inlet Area $A_A$ and $A_S$*

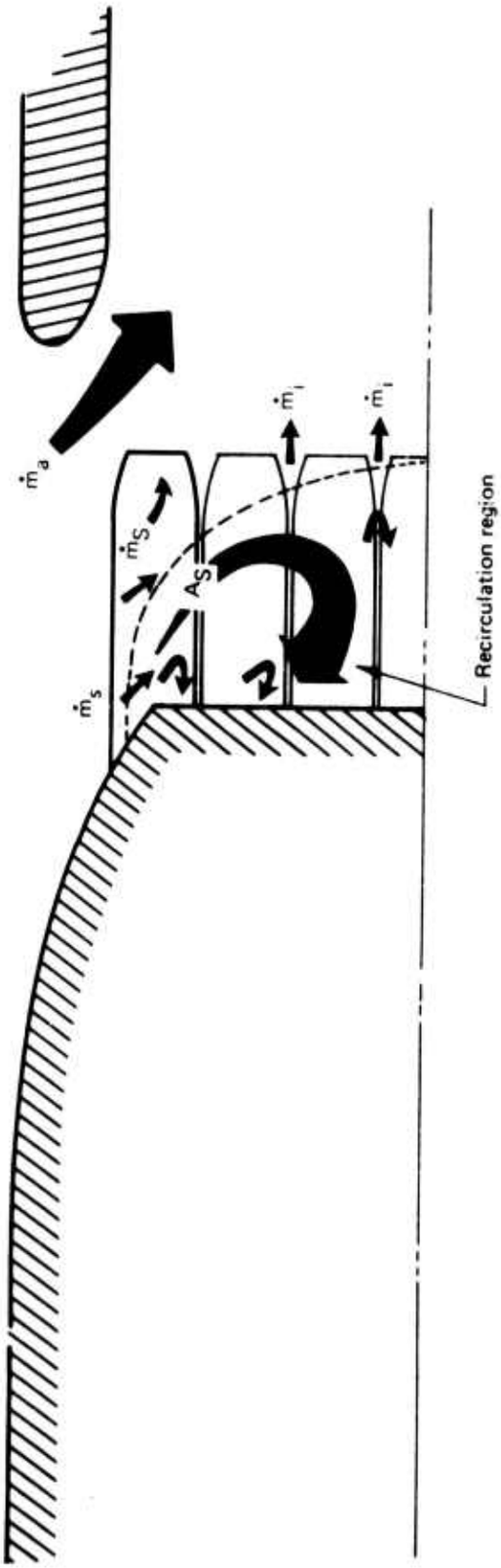


*Figure 39.—Schematic for Suppressor/Ejector Inlet Flow Field*

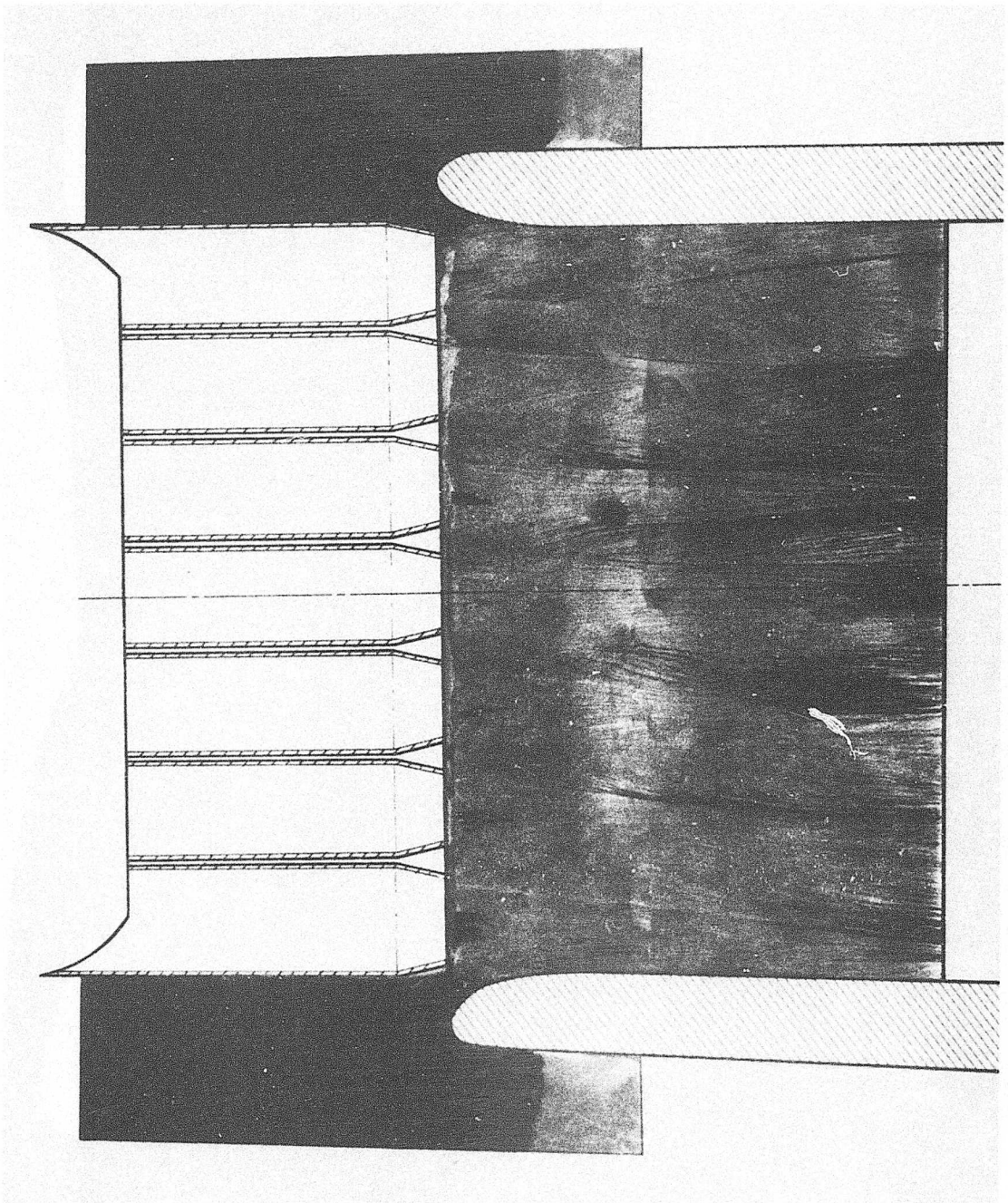

*Figure 40.—Oil Flow on a Plate Bisecting EAR = 3.1 Ejector on the 37-Tube, NAR = 3.3, Close-Packed Array*

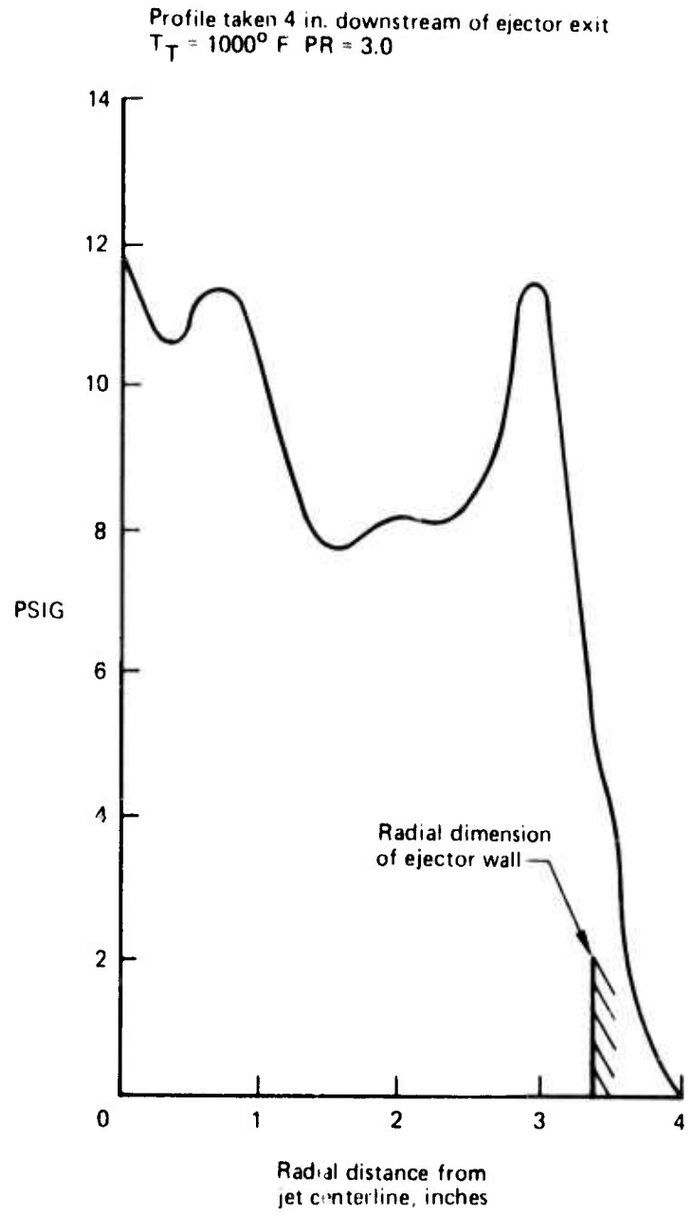


*Figure 41.—Total Pressure Exit Profile for 37-Tube, NAR = 3.3, Close-Packed Array With EAR = 3.1 Ejector*

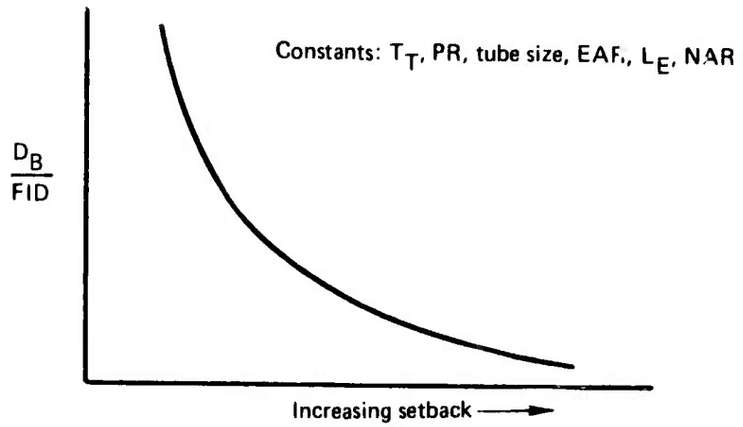


*Figure 42.—Typical Base Drag Versus Setback for Suppressor Ejector*

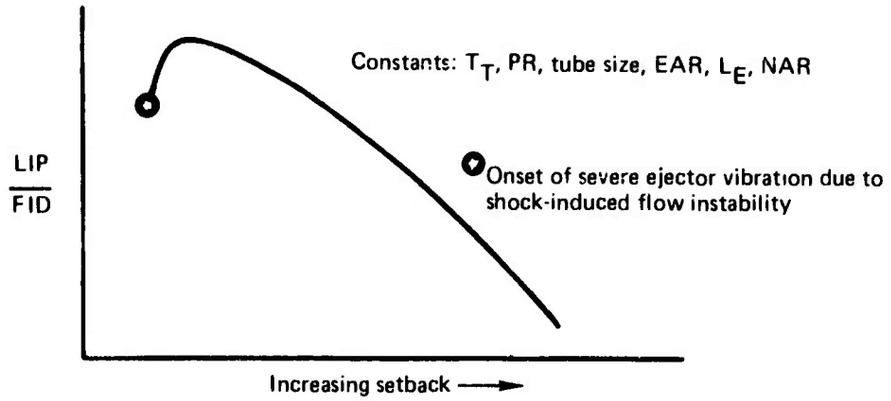


*Figure 43.—Typical Lip Suction as a Function of Setback*

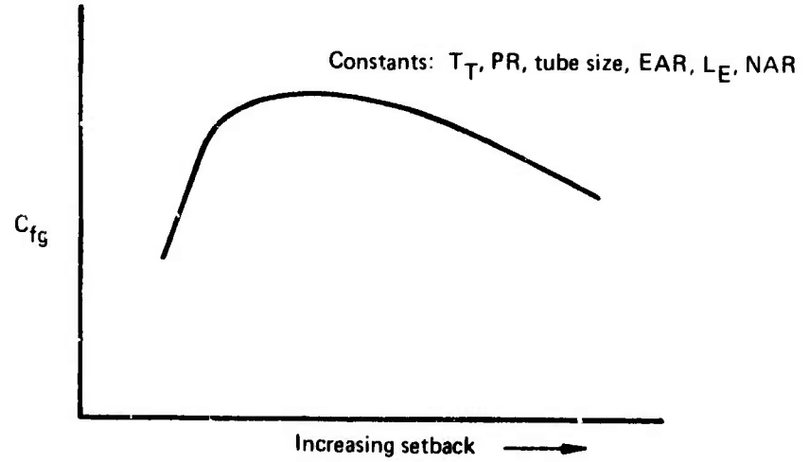


*Figure 44.—Typical Suppressor/Ejector Performance as a Function of Setback*

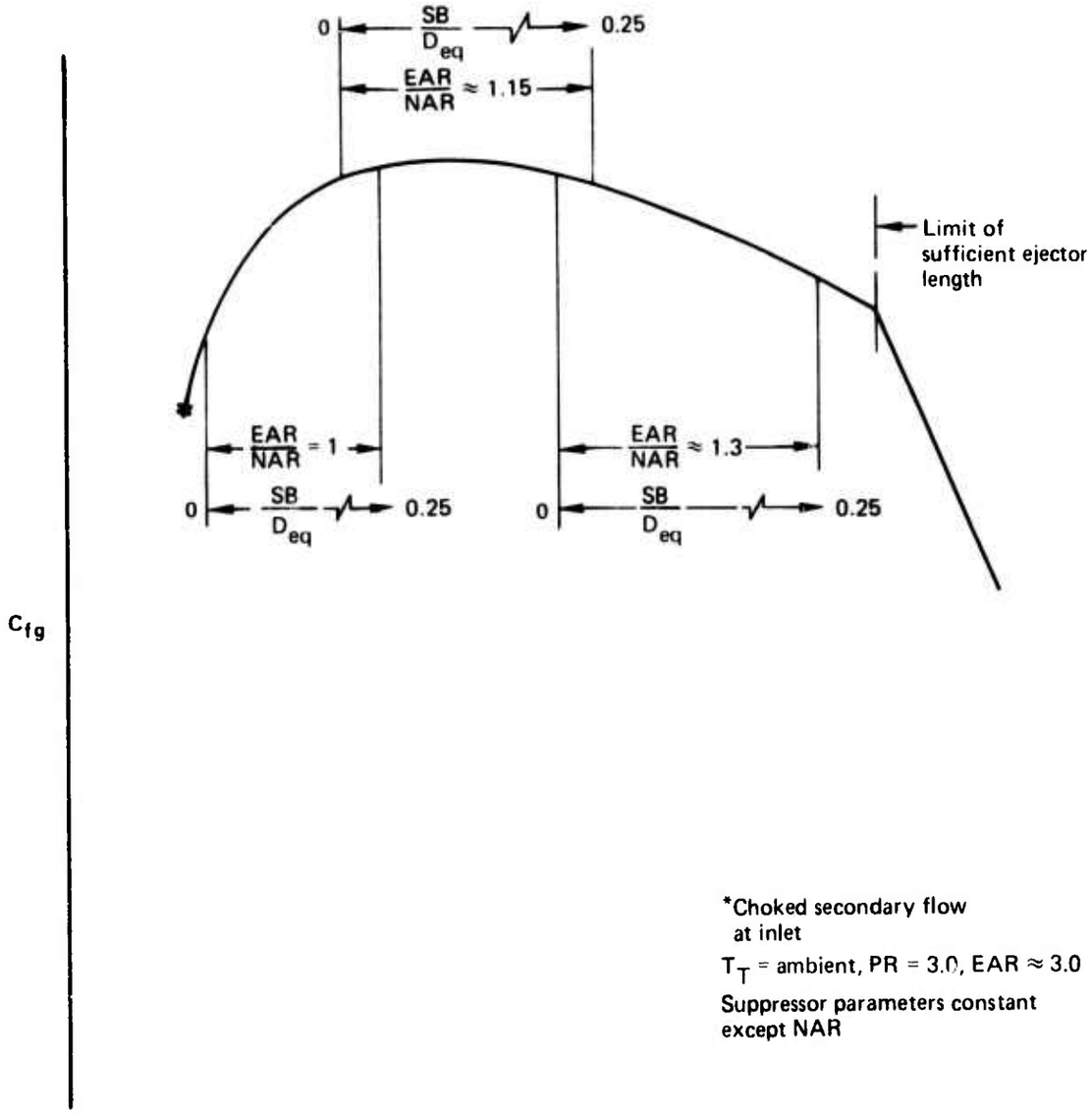


*Figure 45.–Gross Thrust Coefficient as a Function of Effective Inlet Area, Setback, and EAR/NAR Ratio*

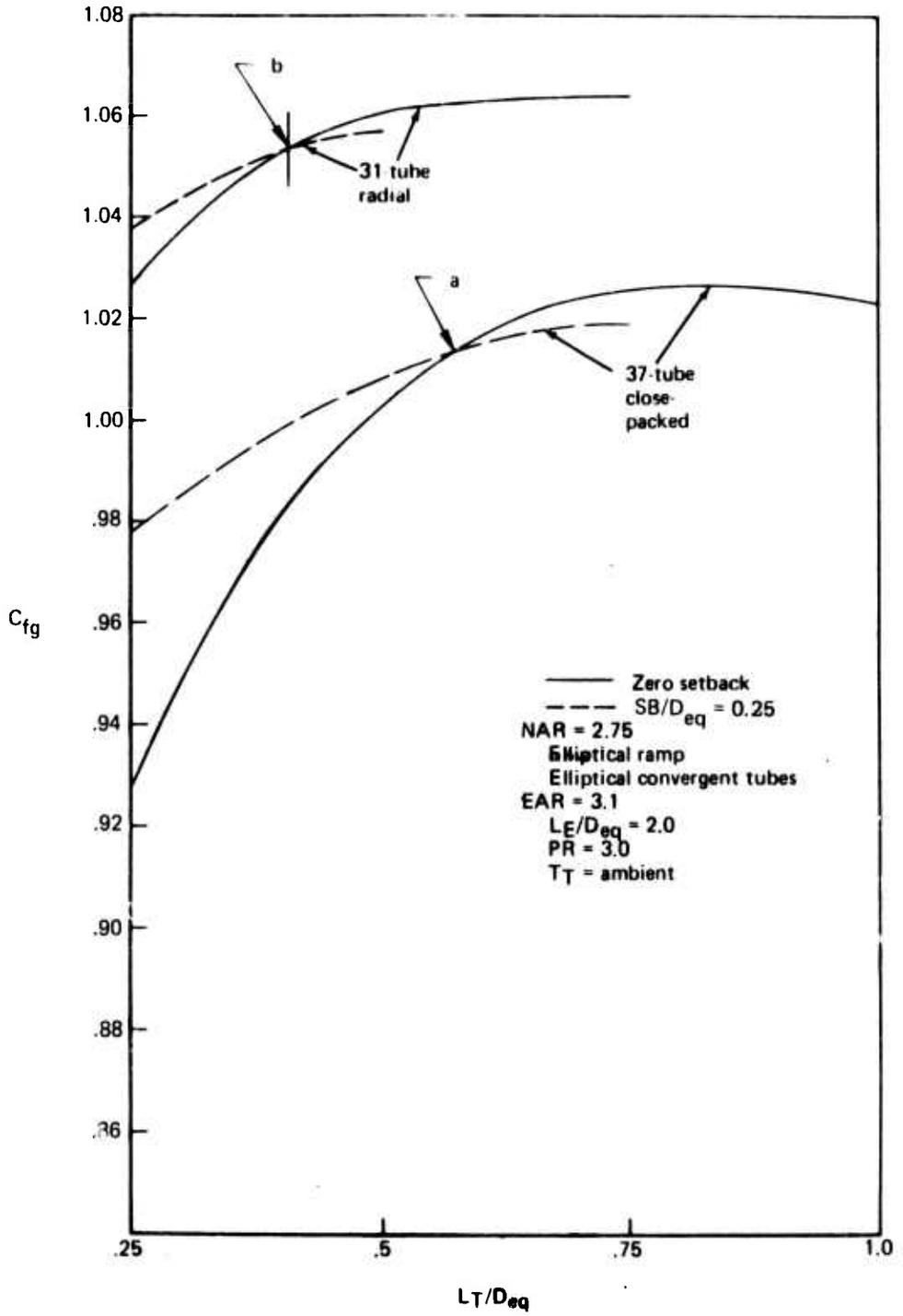


*Figure 46.–Performance as a Function of Tube Length for Various NAR = 2.75 Suppressors With EAR = 3.1 Ejectors*

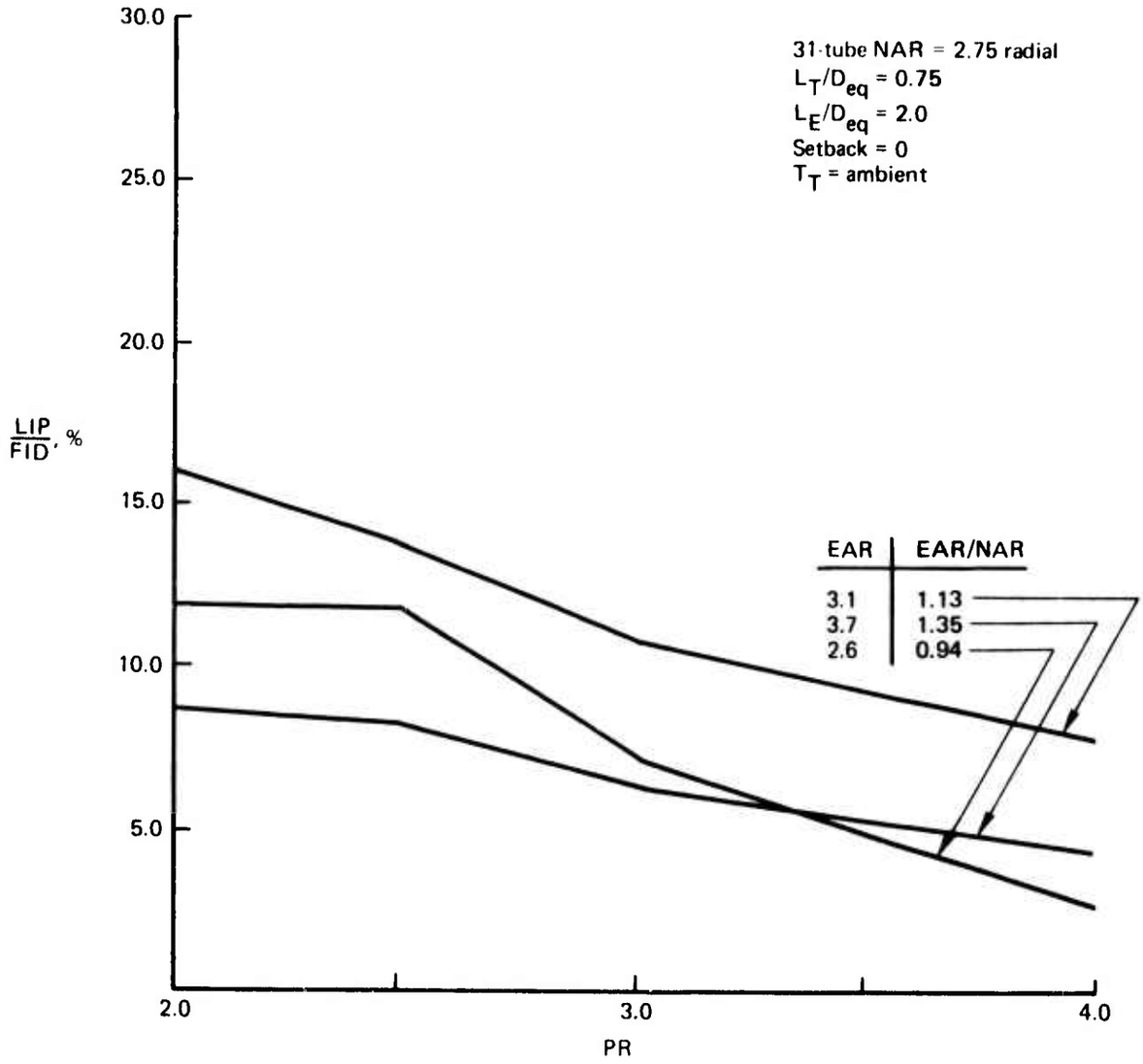


*Figure 47.—Lip Suction/FID as a Function of Ejector Area Ratio and Pressure Ratio*

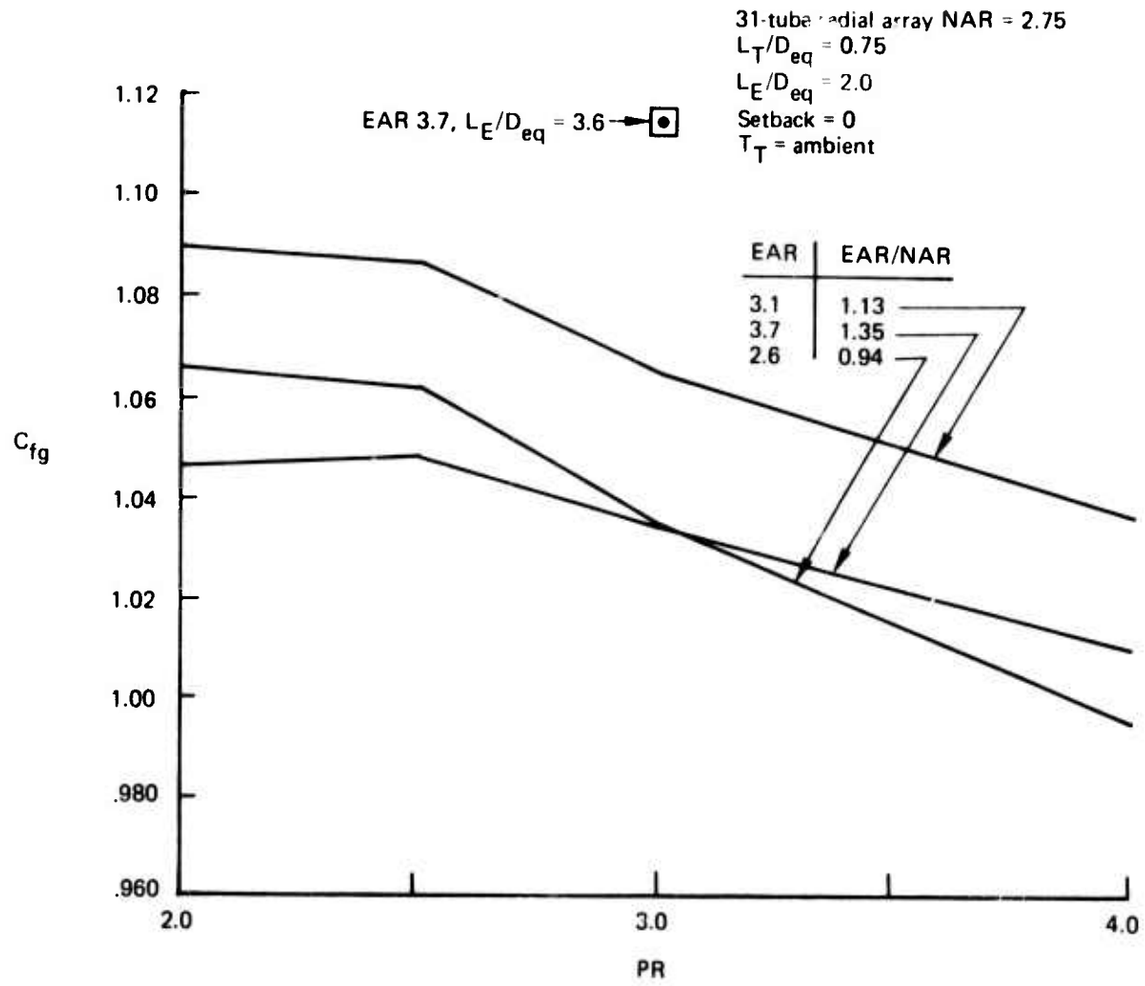


*Figure 48.--Performance as a Function of EAR, PR, and Ejector Length*

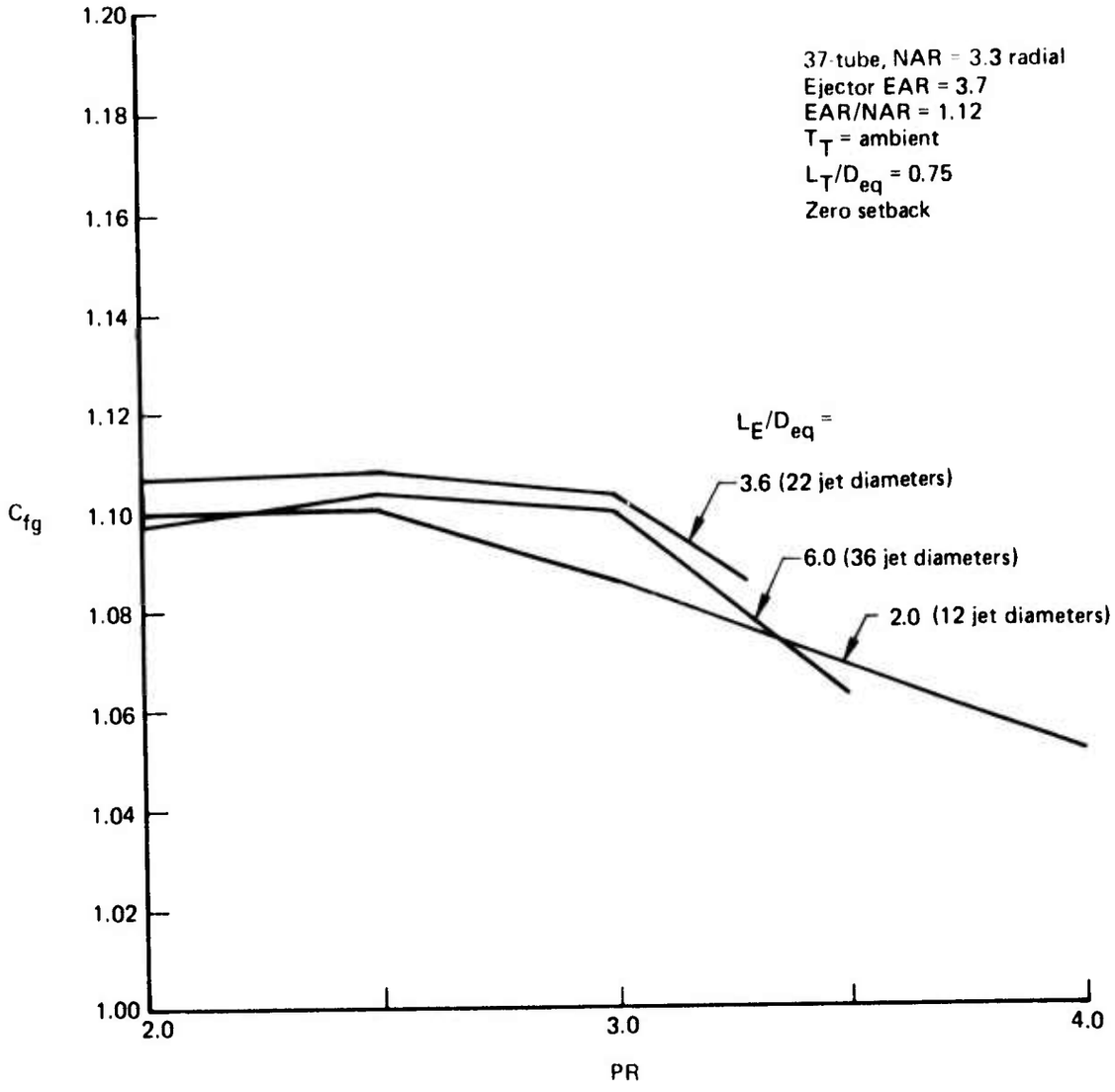


*Figure 49.—Performance as a Function of Ejector Length for EAR/NAR = 1.12*

| Number of Tubes | NAR | EAR | Circumferential Location of Thermocouples Relative to Jet |
|---|---|---|---|
| 61-tube | 3.3 | 3.1 | In line with jet |
| 37-tube | 3.3 | 3.1 | ¼ of distance between jets |
| 31-tube | 2.75 | 2.6 | ¼ of distance between jets |
| 19-tube | 3.3 | 3.1 | ½ of distance between jets |
| R/37 | 3.3 | 3.1 | ¼ of distance between jets |

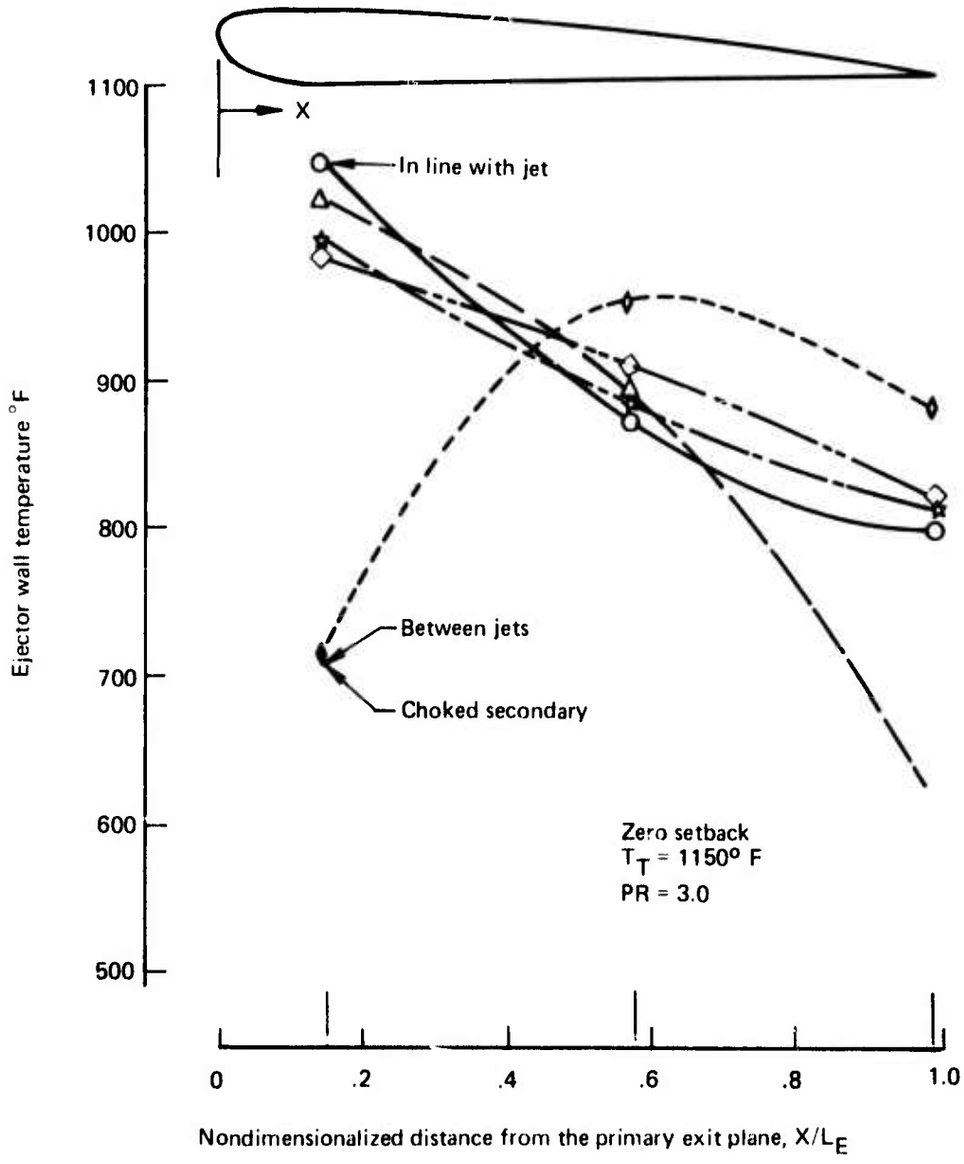


*Figure 50.—Ejector Wall Temperatures*

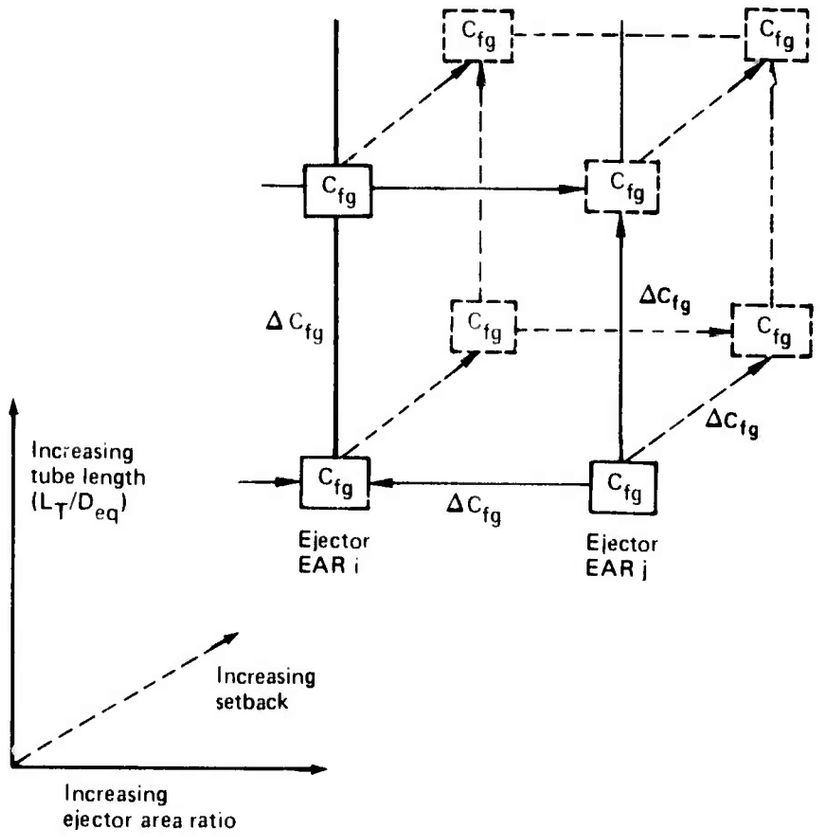


Note:

- All boxes contain the value of $C_{fg}$ at pressure ratio = 3.0 ($T_T$ ambient) for the configuration described by the intersection of tube length, ejector area ratio, and setback lines. The $C_{fg}$ for setback ($SB/D_{eq}$ = 0.25) uses dashed boxes.
- Increasing setback is represented by a set of orthographic projections "into the page" (at 45°) to produce a plane of constant setback = 0.25 using all dashed lines.
- Arrows between boxes point in the direction of the geometry producing maximum performance.
- Numbers in parenthesis are $C_{fg}$ values at 1150° F and pressure ratio = 3.0.

*Figure 51.—General Formats for Summary Performance Plots as a Function of Ejector Area Ratio, Tube Length, and Ejector Setback*

## Performance Matrix Curves (Pressure Ratio = 3.0)

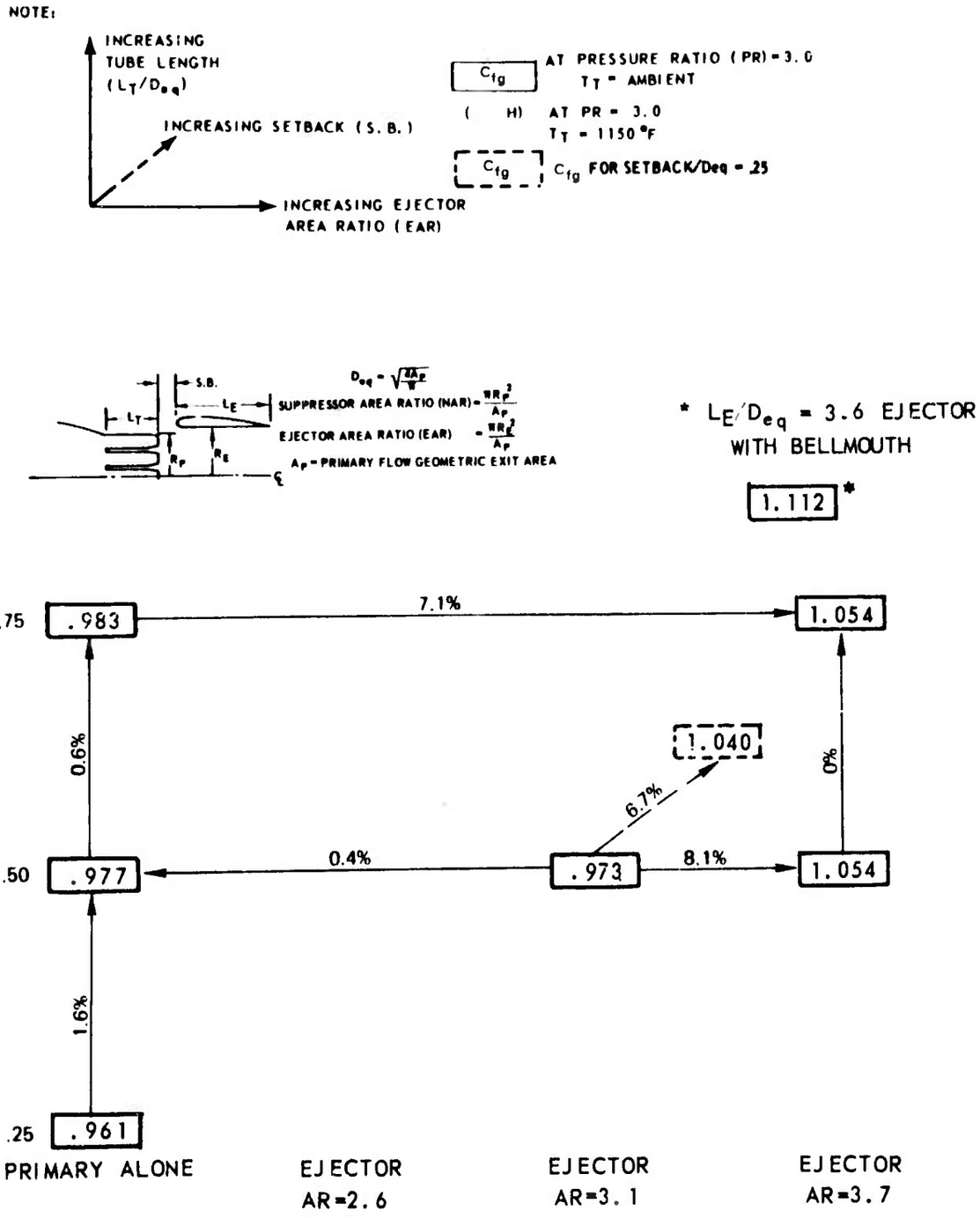


*Figure 52.—Performance Matrix for 19 Elliptical Convergent Tubes: NAR = 3.3— Close-Packed Array—Elliptical Ramp*

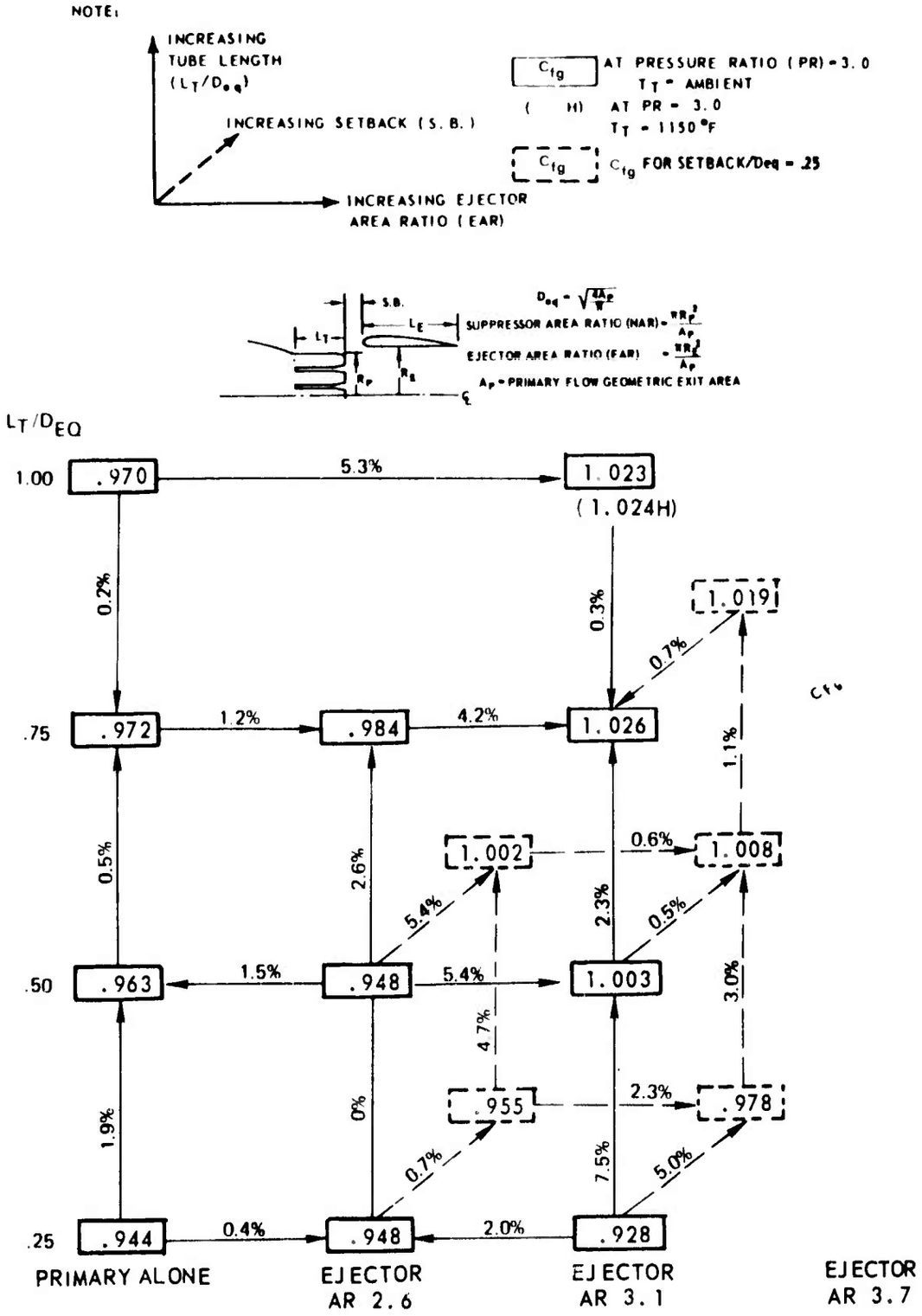


*Figure 53.—Performance Matrix for 37 Elliptical Convergent Tubes: NAR = 2.75— Close-Packed Array—Elliptical Ramp*

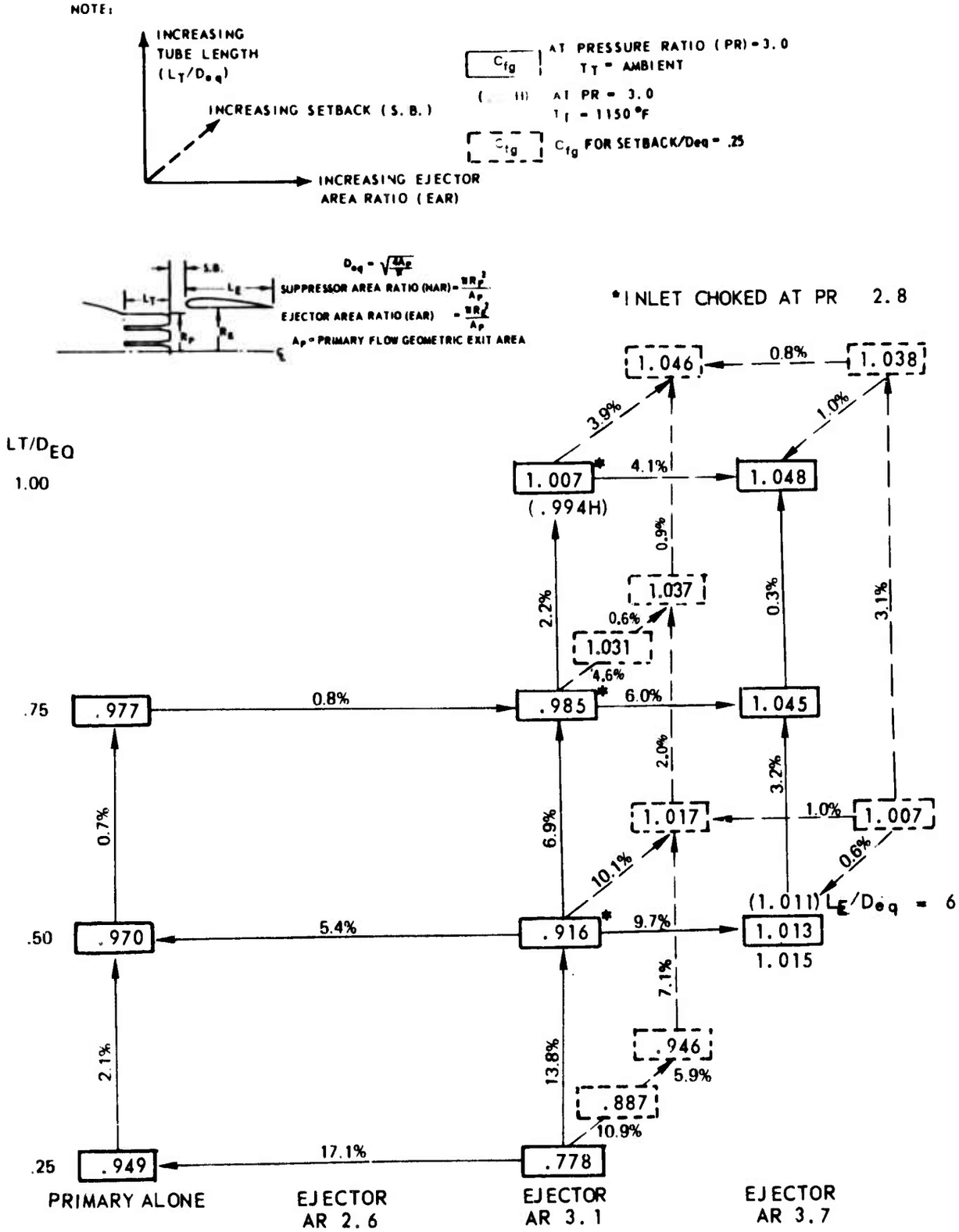


*Figure 54.—Performance Matrix for 37 Elliptical Convergent Tubes: NAR = 3.3— Close-Packed Array—Elliptical Ramp*

NOTE:

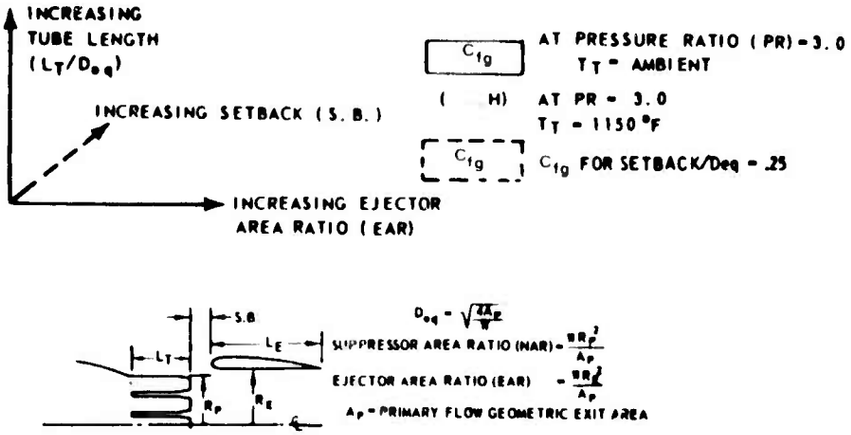


$L_T/D_{EQ}$

1.00

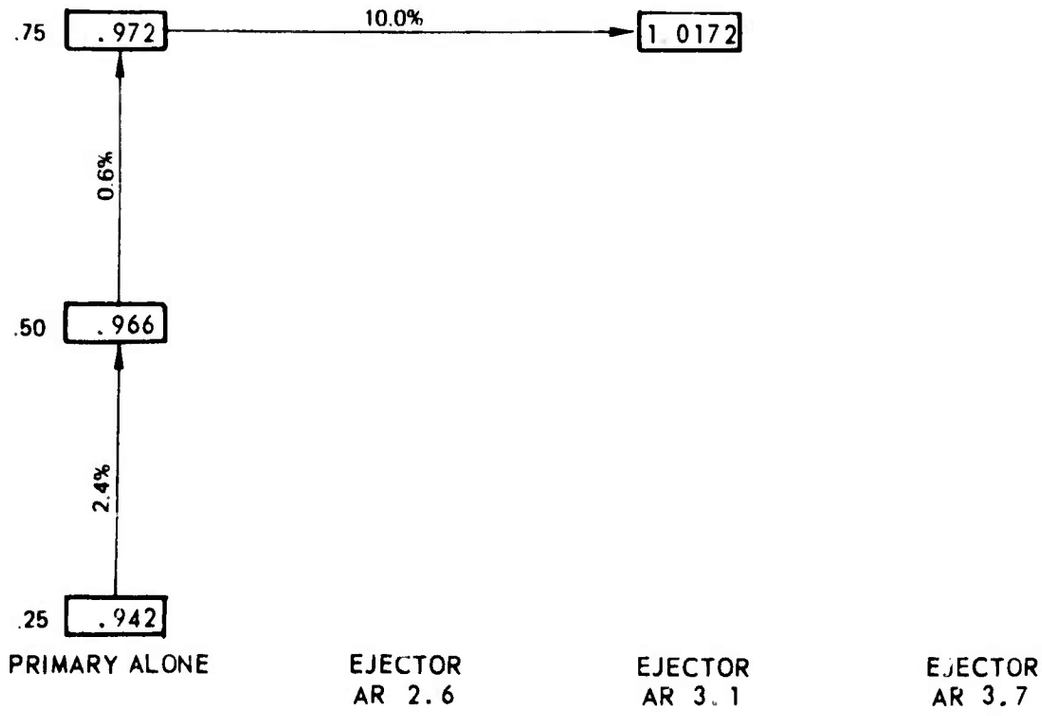


*Figure 55.—Performance Matrix for 37 Elliptical Convergent Tubes: NAR = 3.3— Close-Packed Array—Circular Arc Ramp*

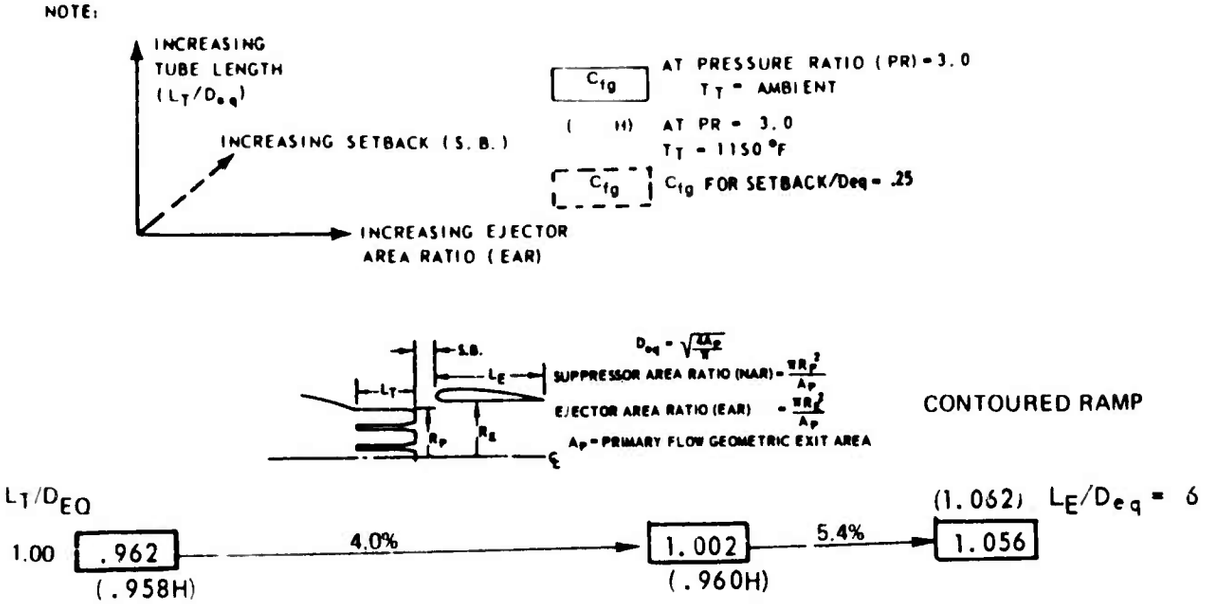


*Figure 56.—Performance Matrix for 37 Round Convergent Tubes: NAR = 3.3—Close-Packed Array—Contoured Ramp*

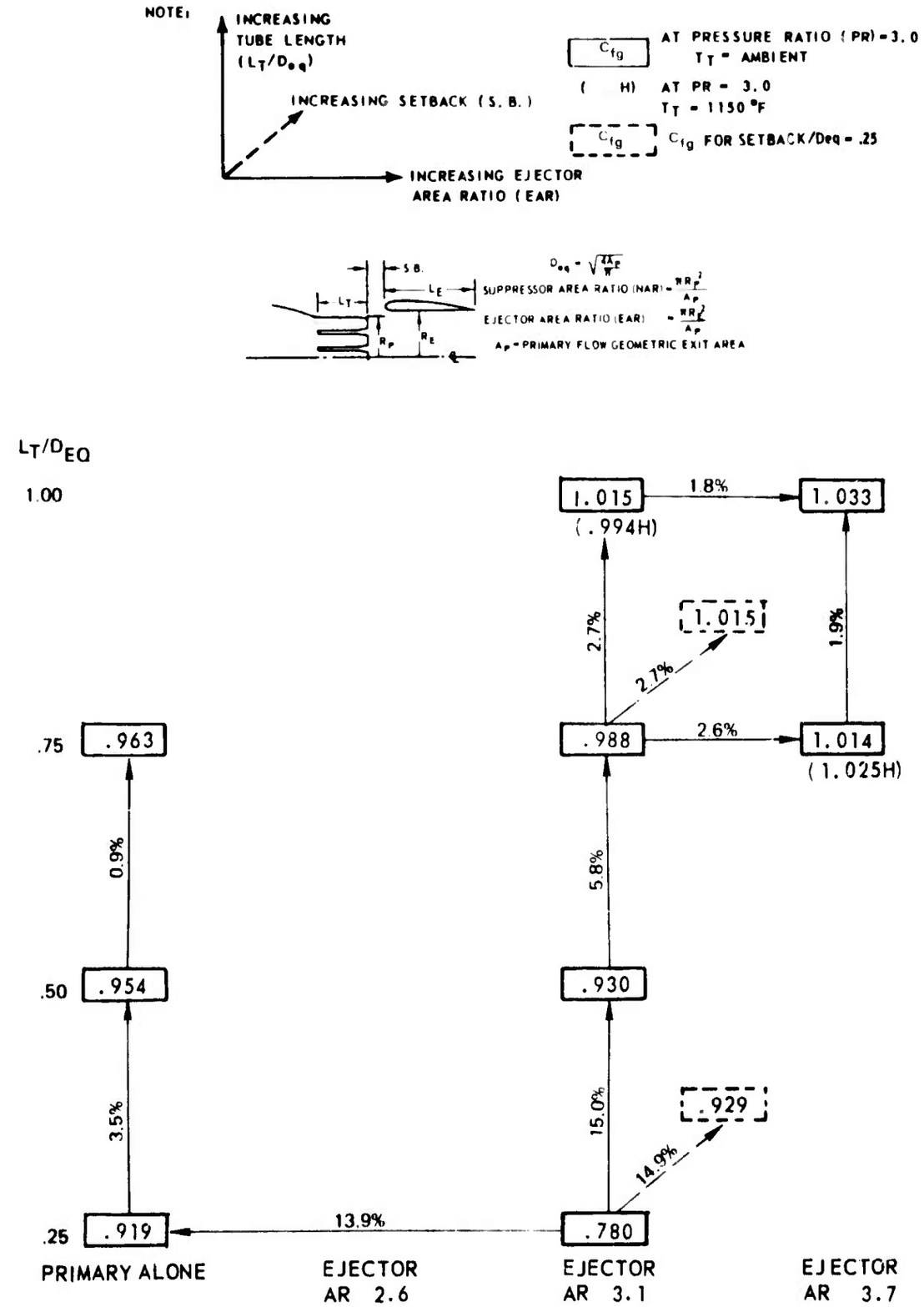


*Figure 57.—Performance Matrix for 61 Elliptical Convergent Tubes: NAR = 3.3— Close-Packed Array—Elliptical Ramp*

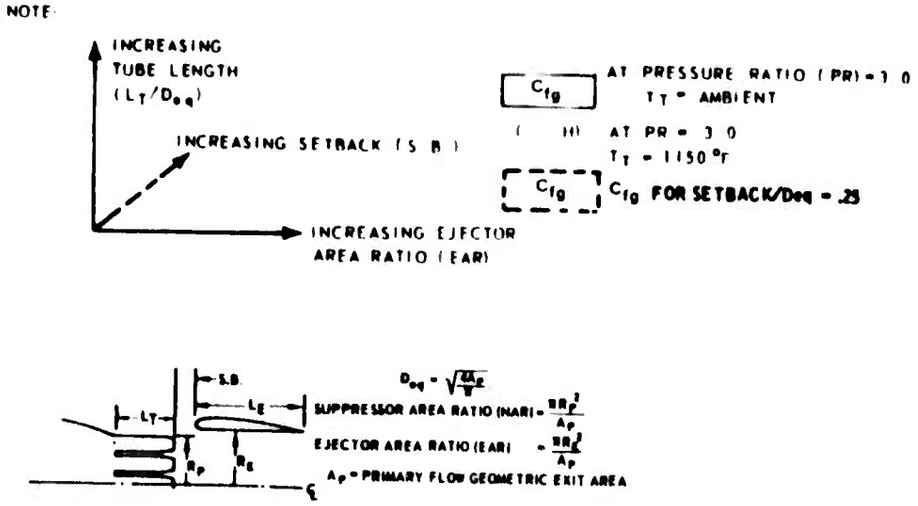


$L_T/D_{eq}$

1.00

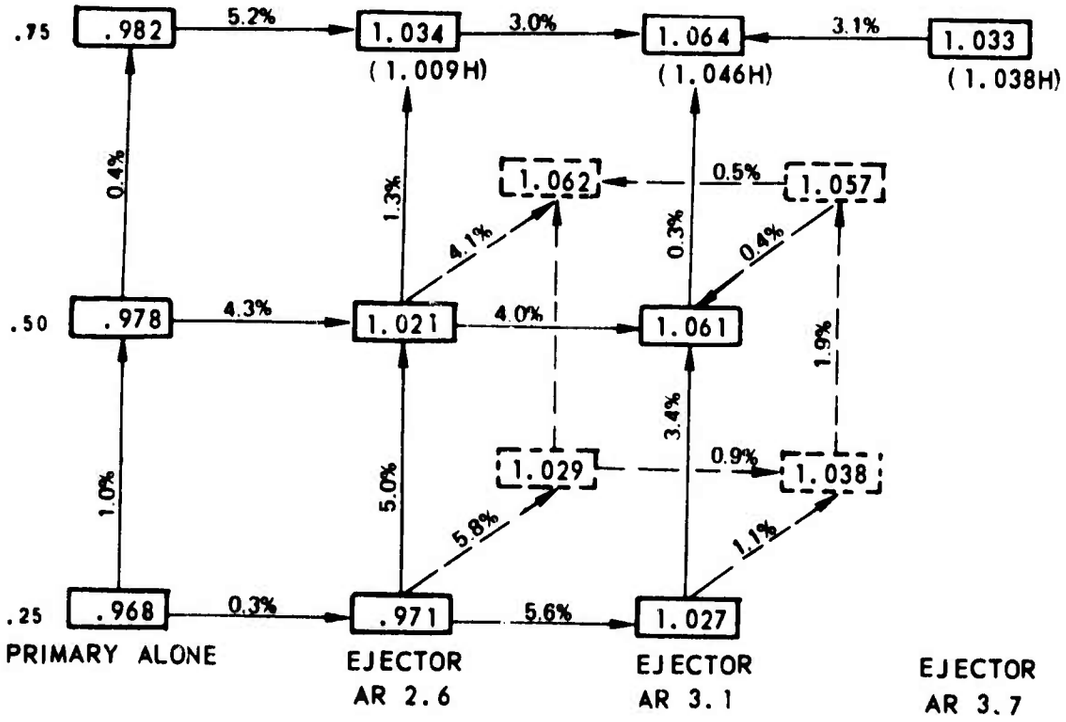


*Figure 58.—Performance Matrix for 31 Elliptical Convergent Tubes: NAR = 2.75— Radial Array—Elliptical Ramp*

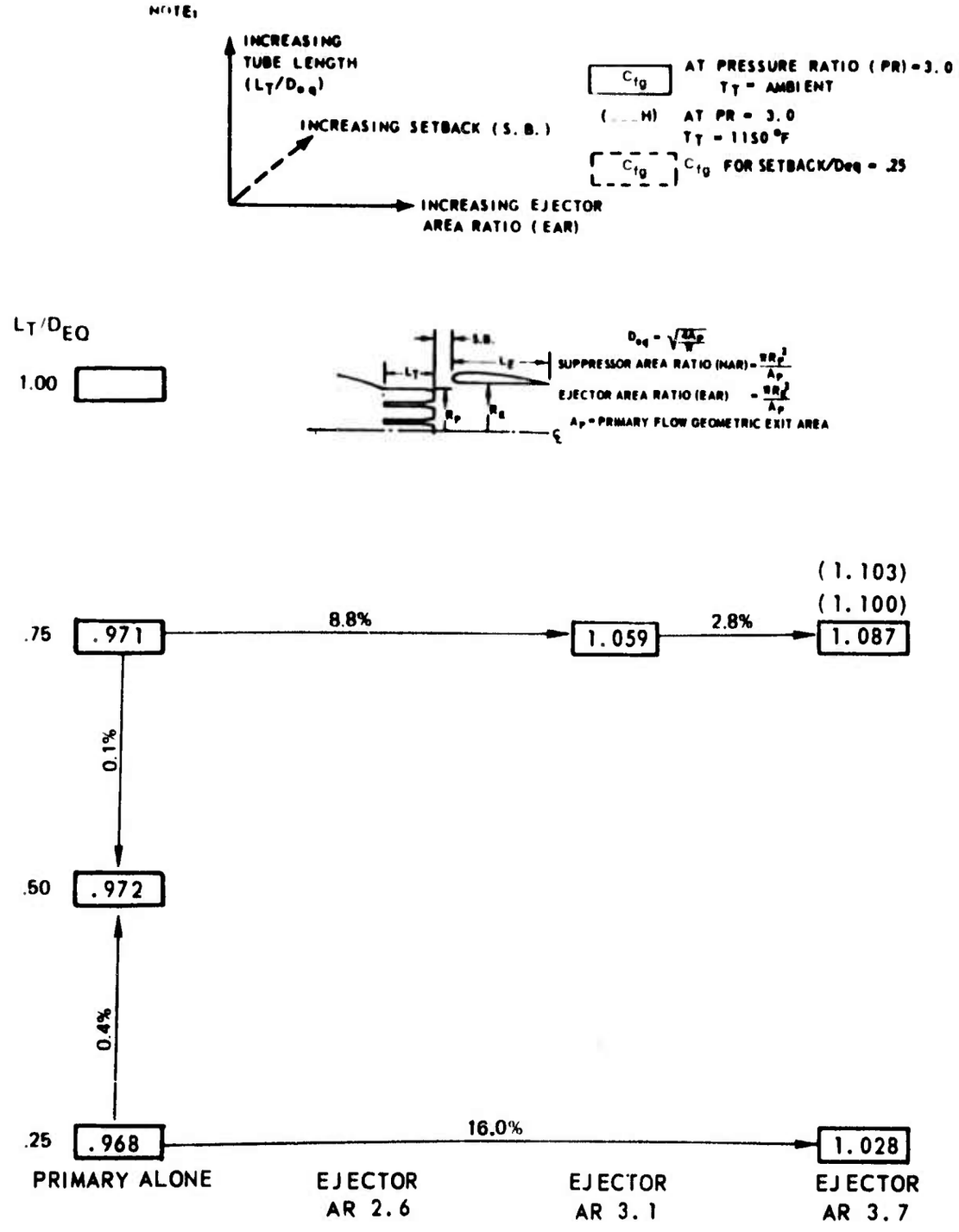


*Figure 59.–Performance Matrix for 37 Round Nonconvergent Tubes: NAR = 3.3– Radial Array–Elliptical Ramp*

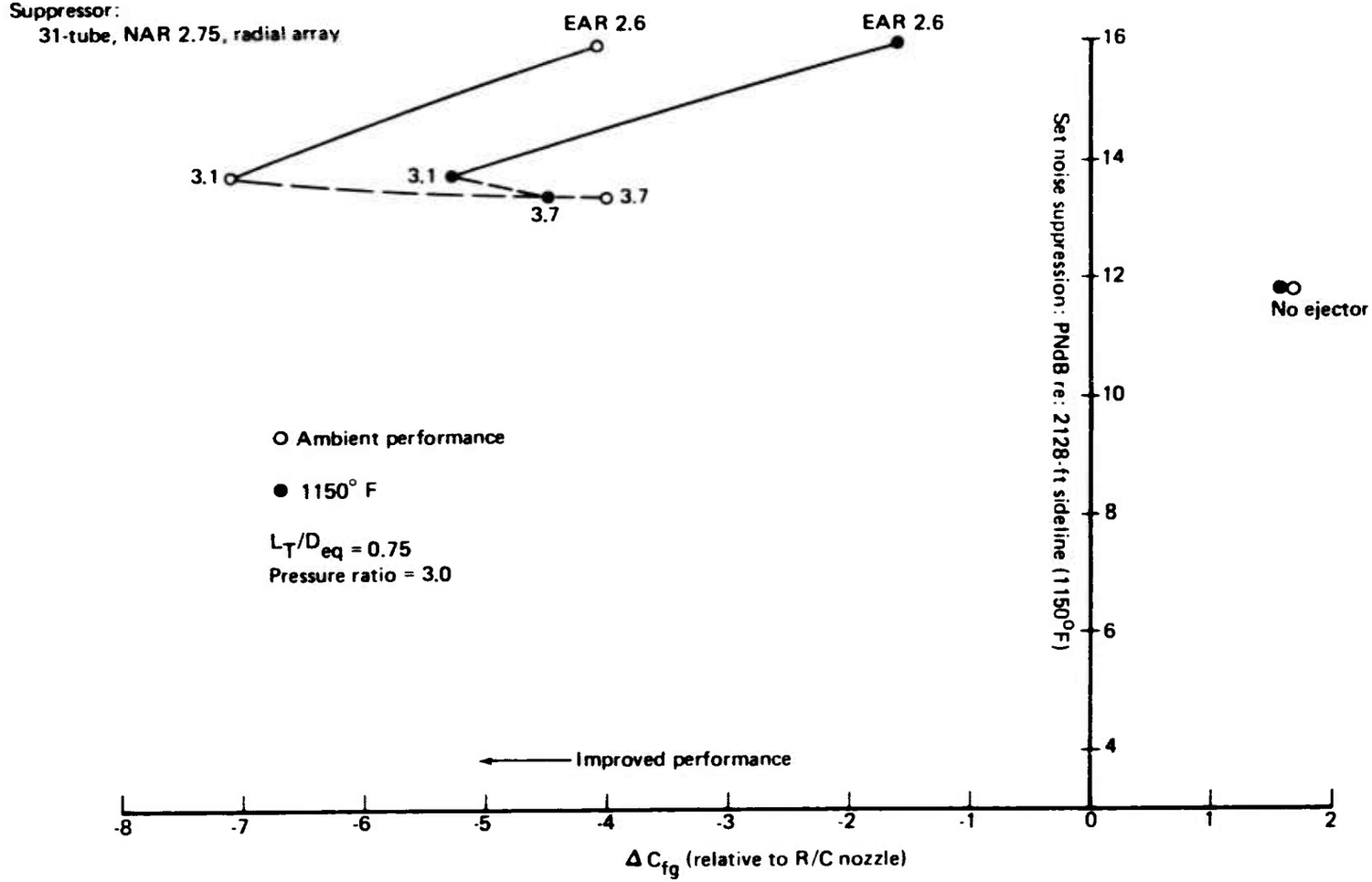


*Figure 60.—The Effect of Ejector Area Ratio on Suppression and Thrust Loss for a 31-Tube, NAR = 2.75, Radial Array*

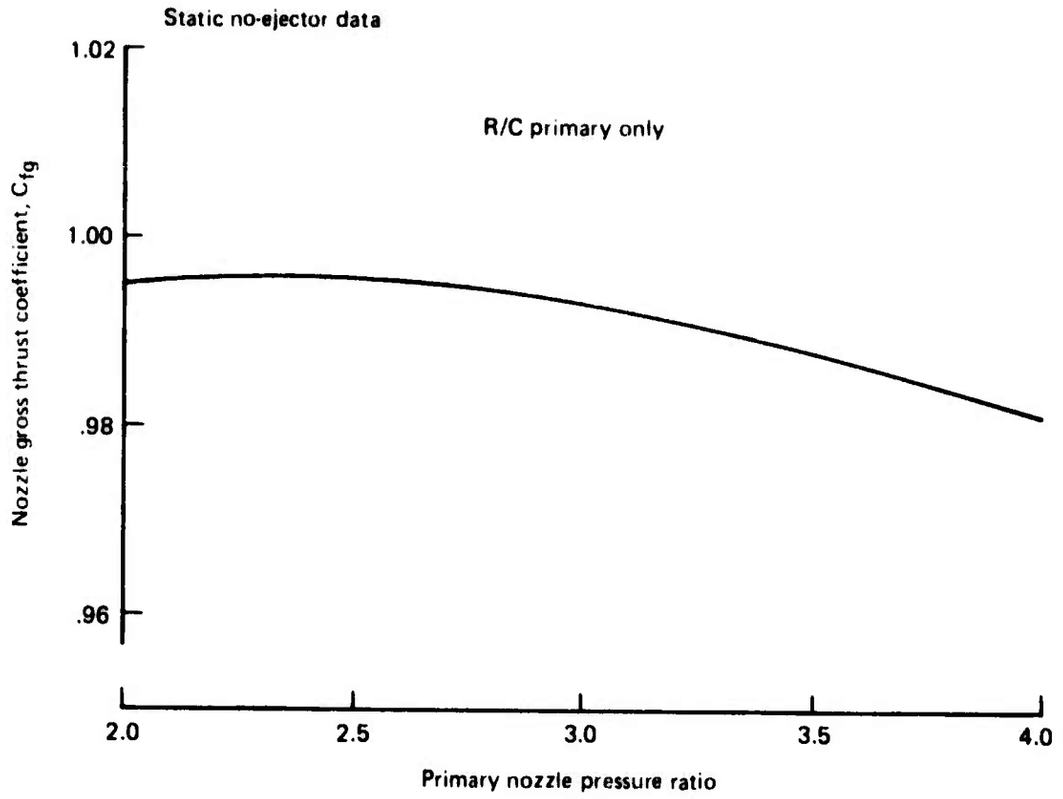


*Figure 61.—Gross Thrust Coefficient Versus Pressure Ratio for R/C Nozzle*

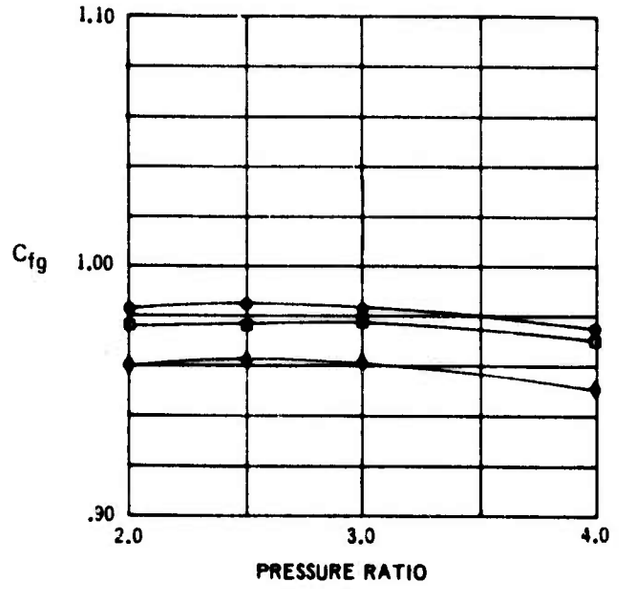


Open symbols = ambient temperature
Solid symbols = 1150° F

| $L_T/D_{eq}$ | |
|---|---|
| △ | 1.00 |
| ○ | 0.75 |
| □ | 0.50 |
| ◇ | 0.25 |

Accuracy: ± 0.25%

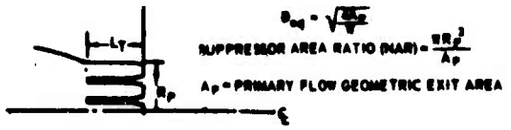


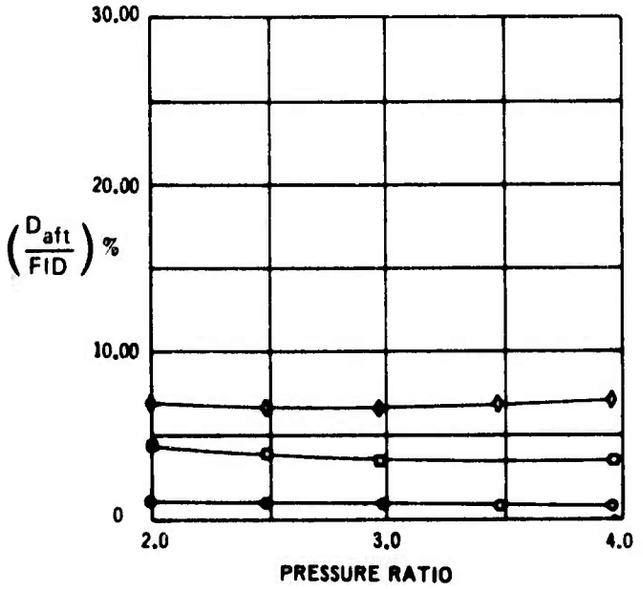


*Figure 62.—Gross Thrust Coefficient and Afterbody Drag for 19-Tube, NAR = 3.3, Close-Packed Array, Elliptical Ramp, Elliptical Convergent Tubes*

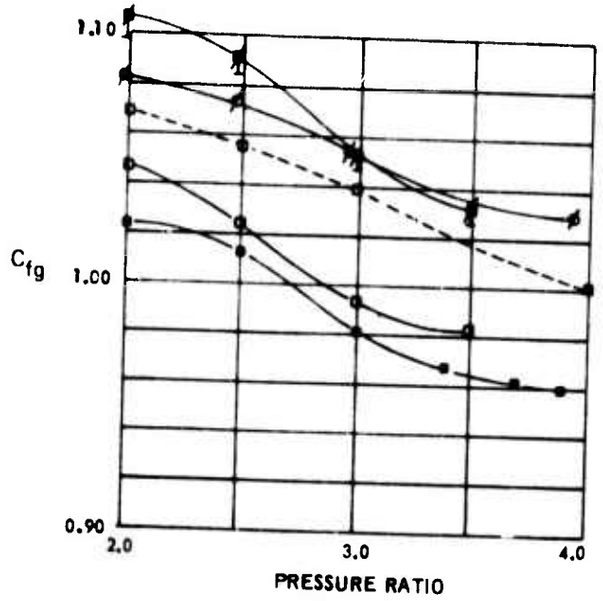


OPEN SYMBOLS = AMBIENT TEMPERATURE

SOLID SYMBOLS = 1150°F

| EAR 3.1 | EAR 3.7 | $L_T/D_{eq}$ |
|---|---|---|
| △ | ◭ | 1.0 |
| ○ | ⌀ | .75 |
| □ | ◰* | .50 *($L_E/D_{eq} = 6$) |
| ◇ | ◮ | .25 |

SETBACK (S.B./$D_{eq}$)

———— 0

– – ——— .125

—— —— .250

$L_E/D_{eq}$ = 2 EXCEPT WHERE NOTED

ACCURACY: ± 0.25% OR SHOWN WITH ERROR BAR

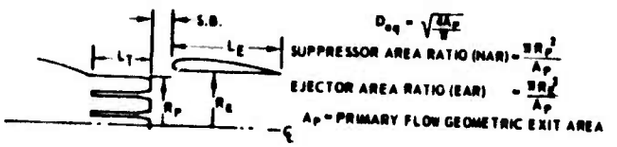


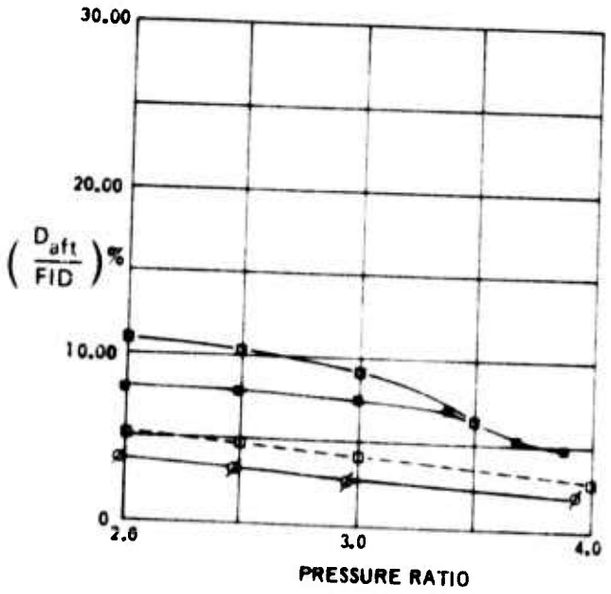


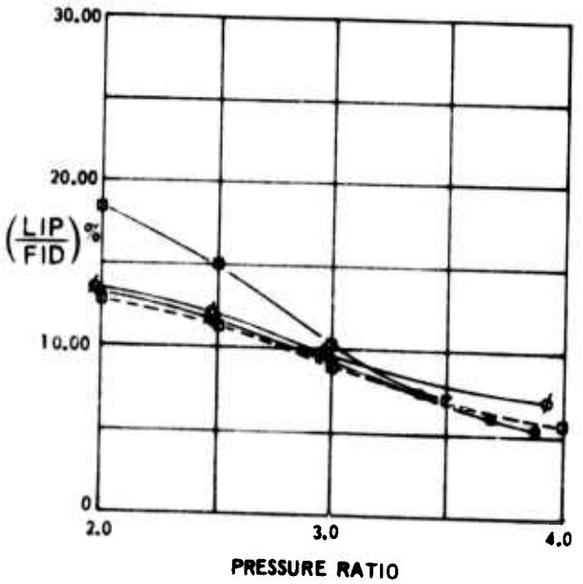


*Figure 63.–Gross Thrust Coefficient and Body Forces for 19-Tube, NAR = 3.3, EAR = 3.1 and 3.7, C.P. Array, Elliptical Ramp, Elliptical Convergent Tubes*

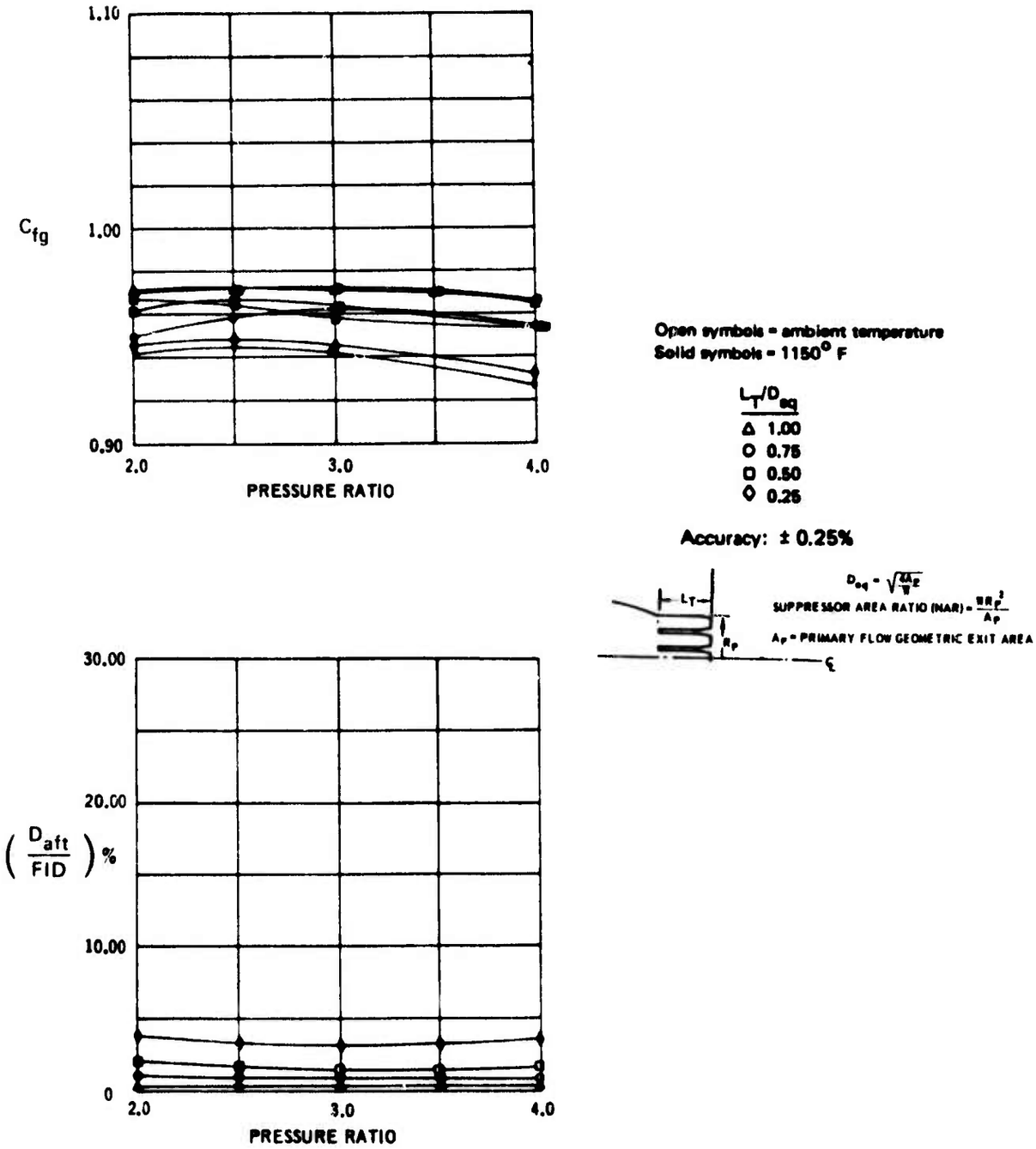


*Figure 64.—Gross Thrust Coefficient and Afterbody Drag for 37-Tube, NAR = 2.75, Close-Packed Array, Elliptical Ramp, Elliptical Convergent Tubes*

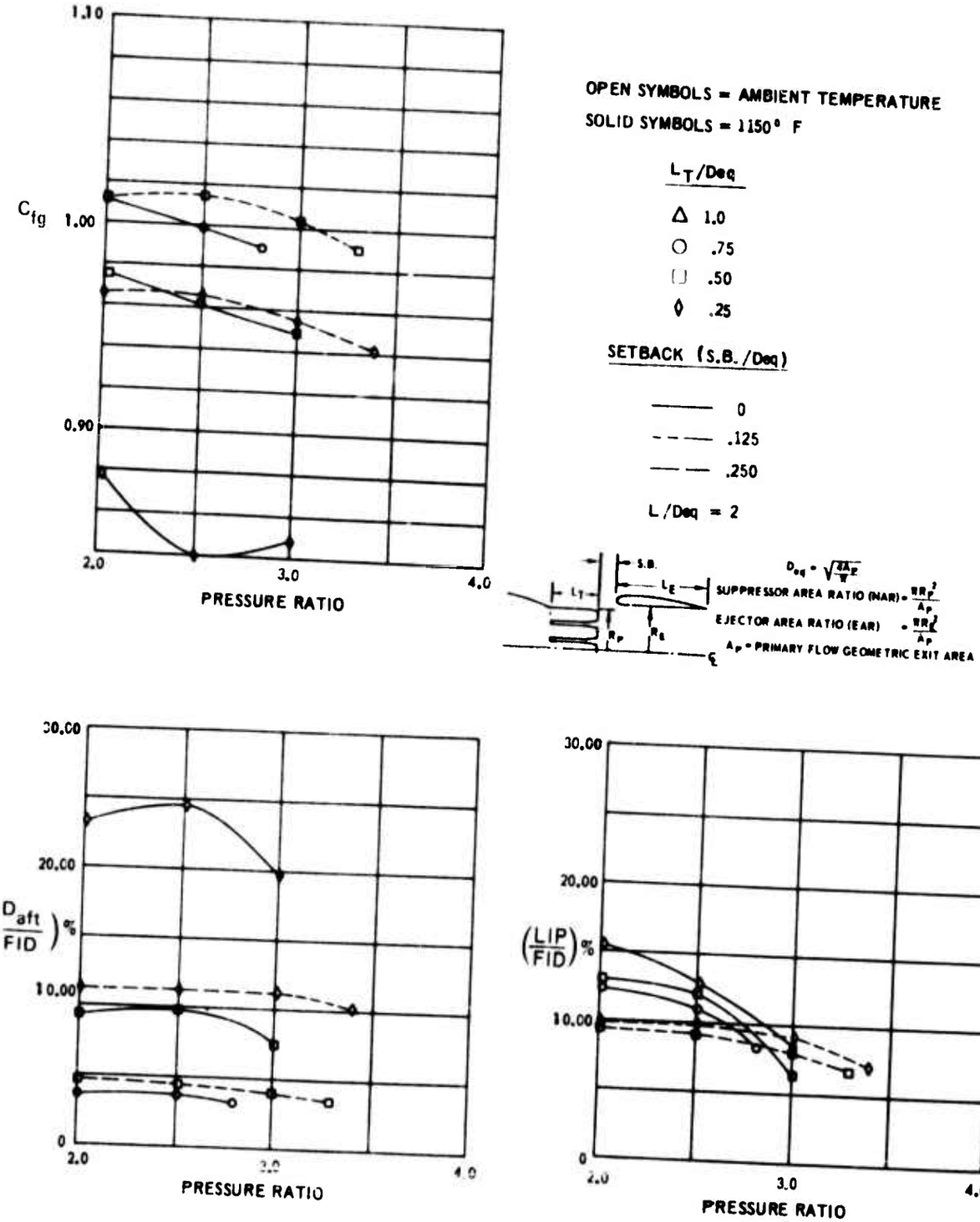


*Figure 65.—Gross Thrust Coefficient and Body Forces for 37-Tube, NAR = 2.75, EAR = 2.6, Close-Packed Elliptical Ramp, Elliptical Convergent Tubes*

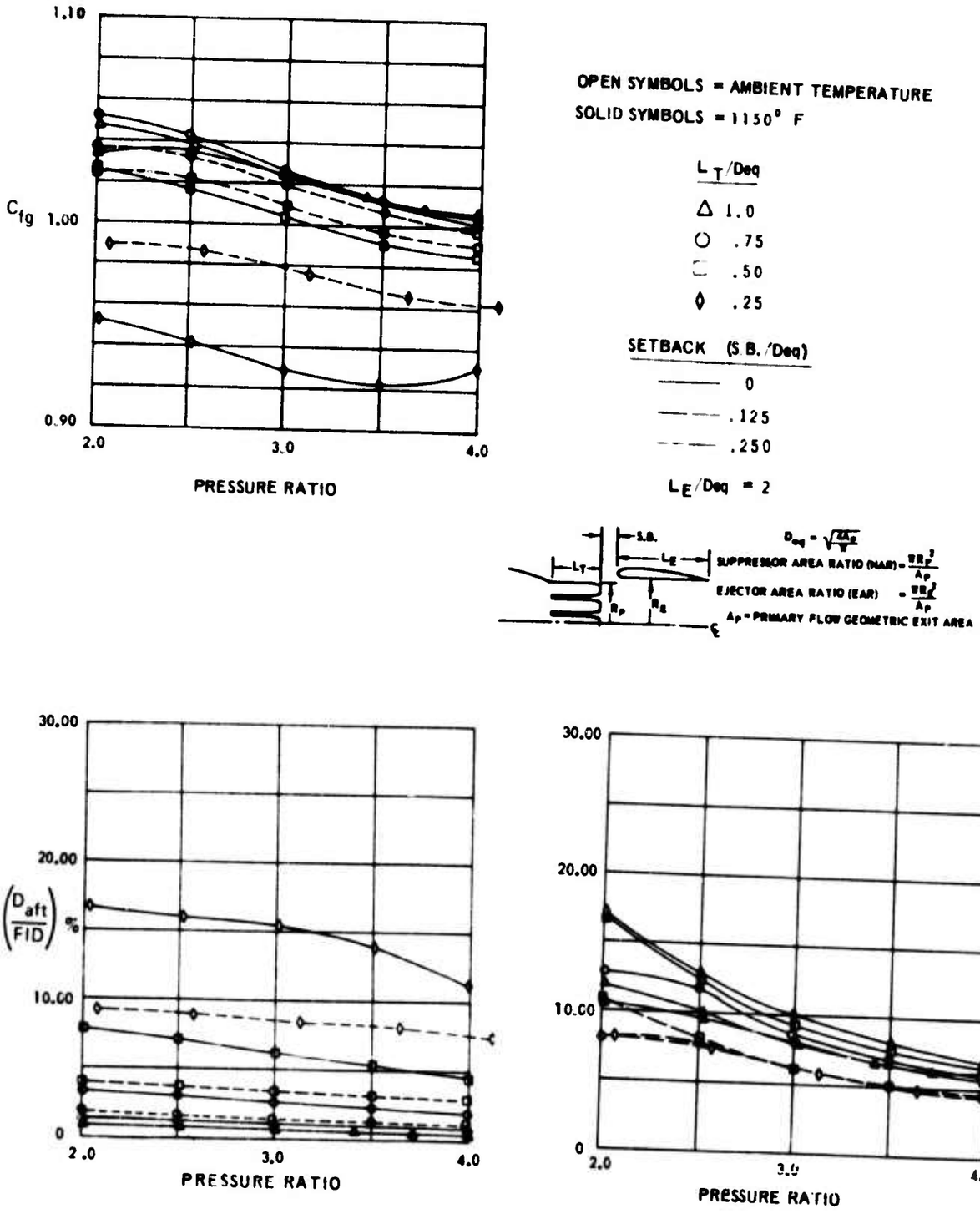


*Figure 66. Gross Thrust Coefficient and Body Forces for 37-Tube, NAR = 2.75, EAR = 3.1, Close-Packed, Elliptical Ramp, Elliptical Convergent Tubes*

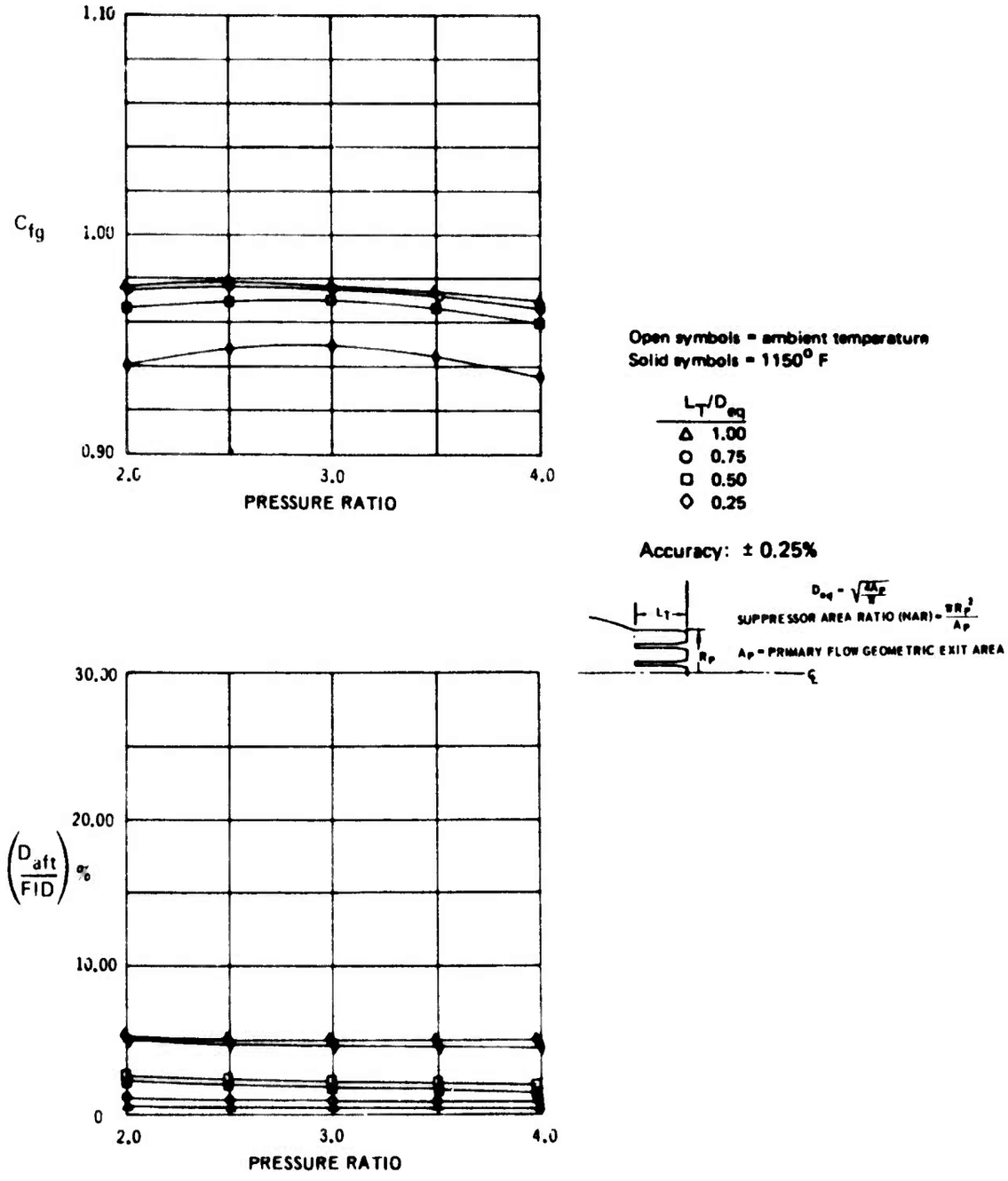


*Figure 67.—Gross Thrust Coefficient and Afterbody Drag for 37-Tube, NAR = 3.3, Close-Packed Array, Elliptical Ramp, Elliptical Convergent Tubes*

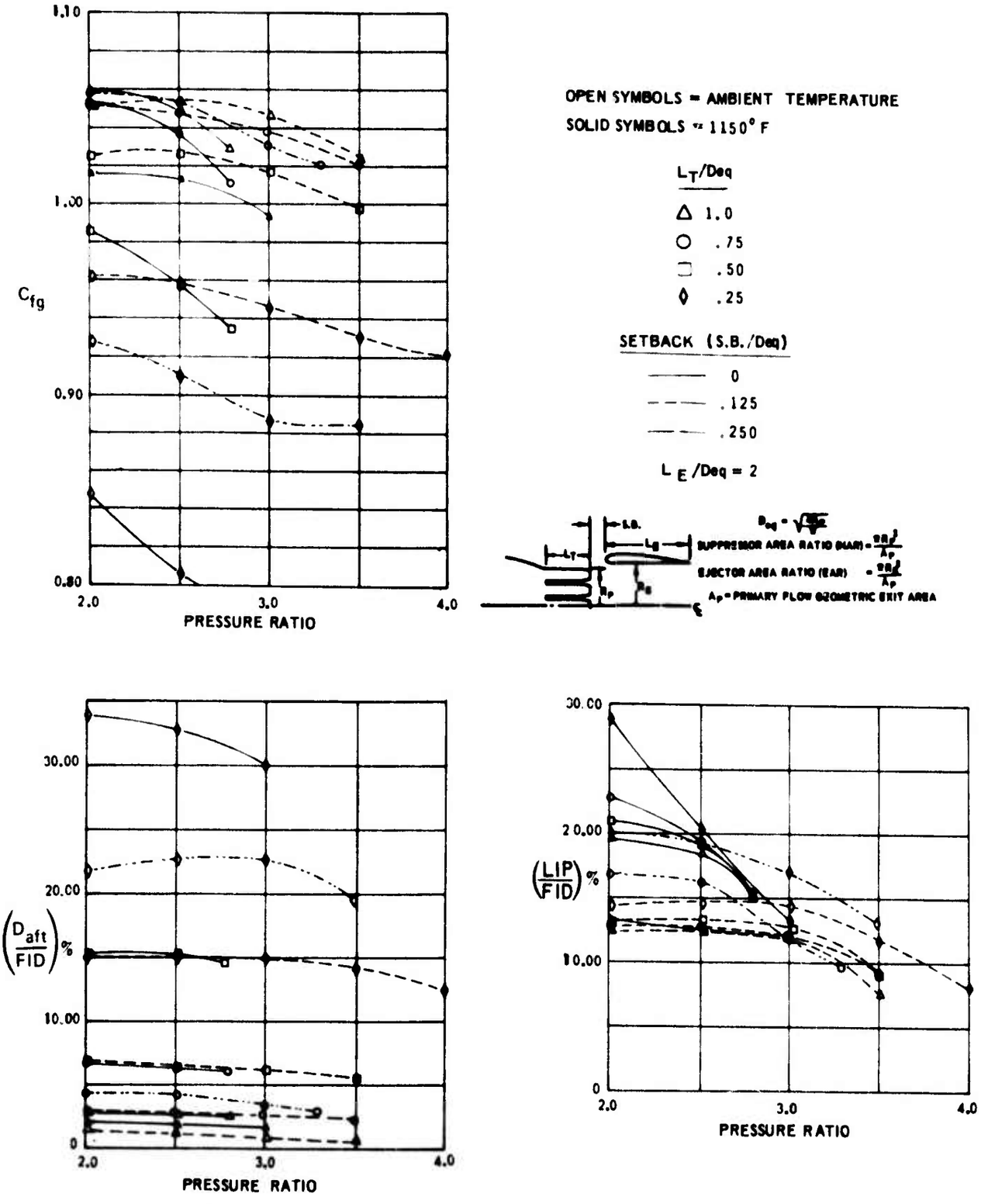


*Figure 68.—Gross Thrust Coefficient and Body Forces for 37-Tube, NAR = 3.3, EAR = 3.1, Close-Packed, Elliptical Ramp, Elliptical Convergent Tubes*

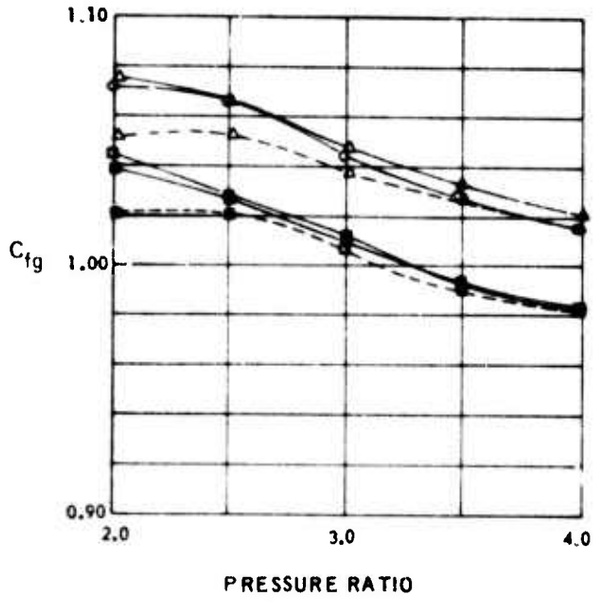


OPEN SYMBOLS = AMBIENT TEMPERATURE

SOLID SYMBOLS = 1150° F

$L_T/D_{eq}$

△ 1.0

○ .75

□ .50

◊ .25

SETBACK (S.B./Deq)

——— 0

- - - — .125

— — — .250

$L_E/D_{eq}$ = 2

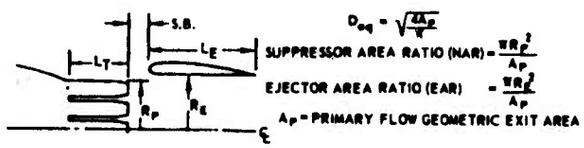


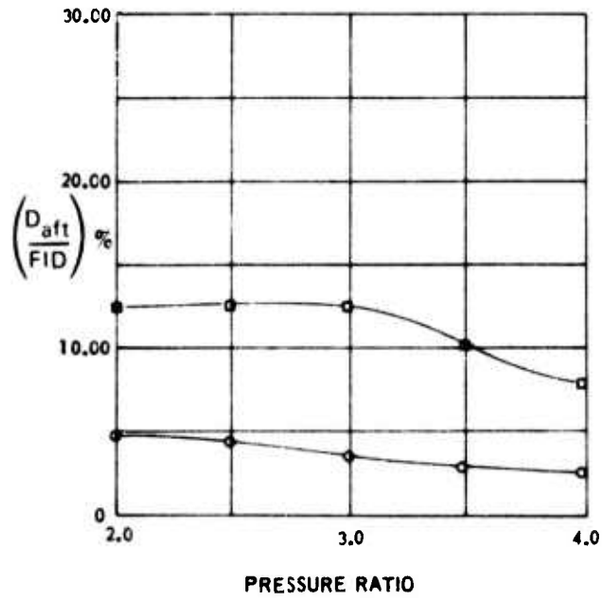


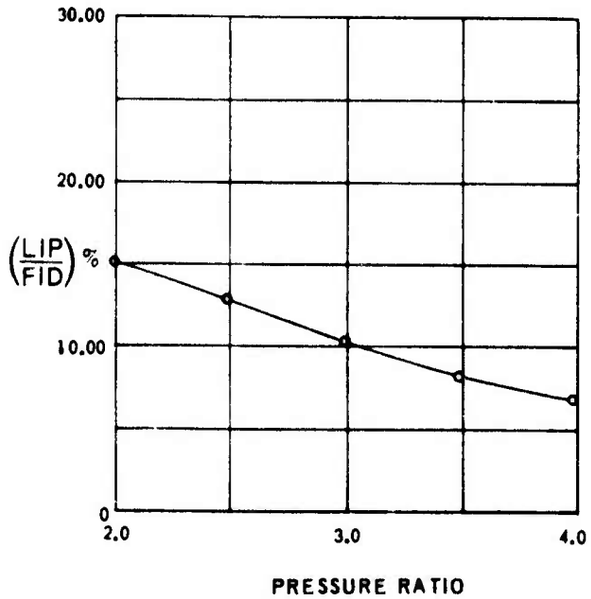


*Figure 69.—Gross Thrust Coefficient and Body Forces for 37-Tube, NAR = 3.3, EAR = 3.7, Close-Packed, Elliptical Ramp, Elliptical Convergent Tubes*

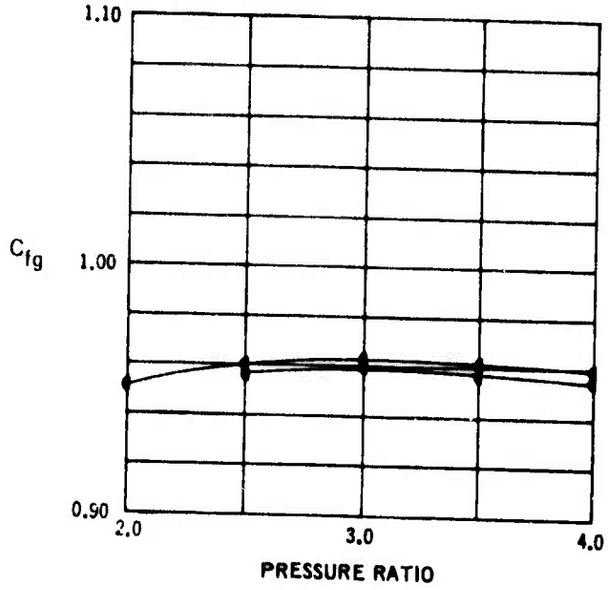


Open symbols = ambient temperature
Solid symbols = 1150° F

Accuracy: ± 0.25%

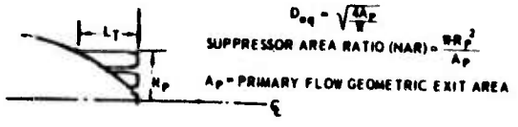


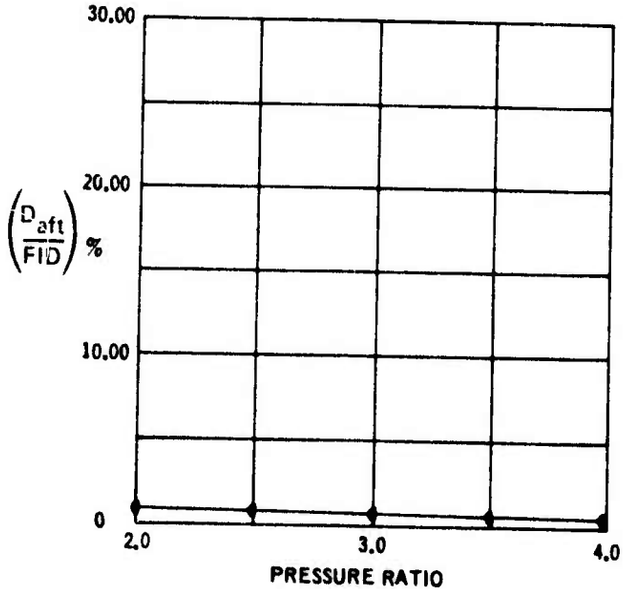


*Figure 70.—Gross Thrust Coefficient and Afterbody Drag for R/37*

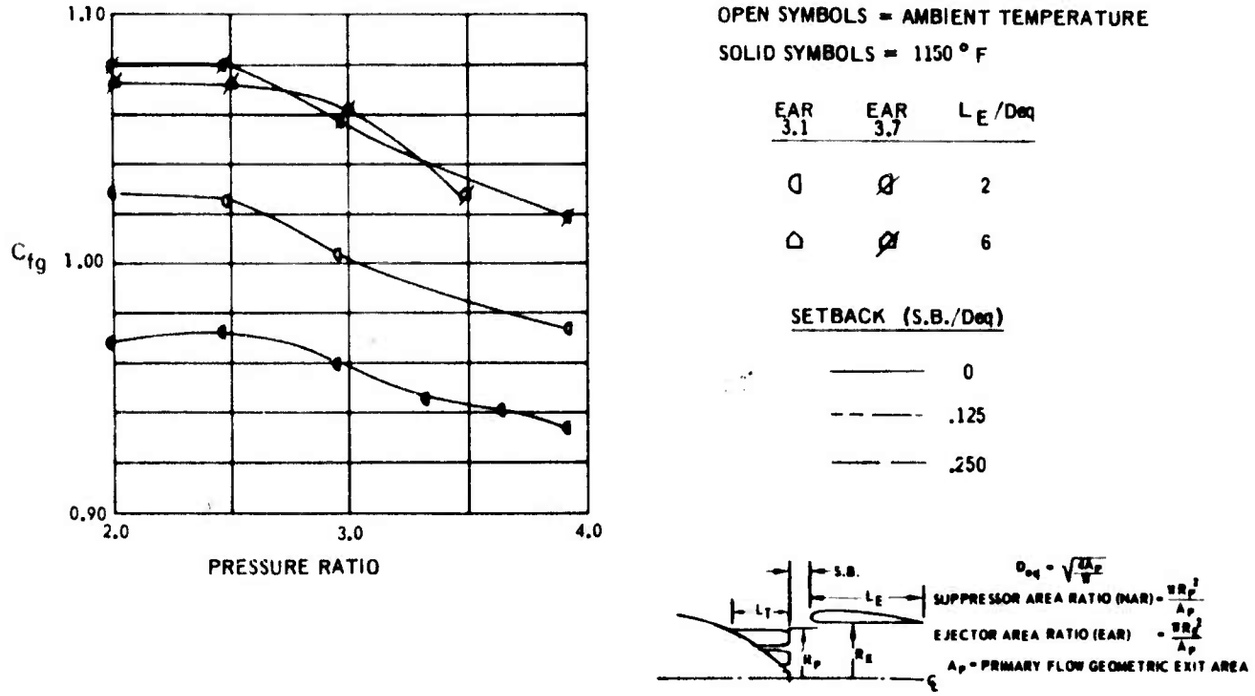


*Figure 71.—Gross Thrust Coefficient and Body Forces for R/37*

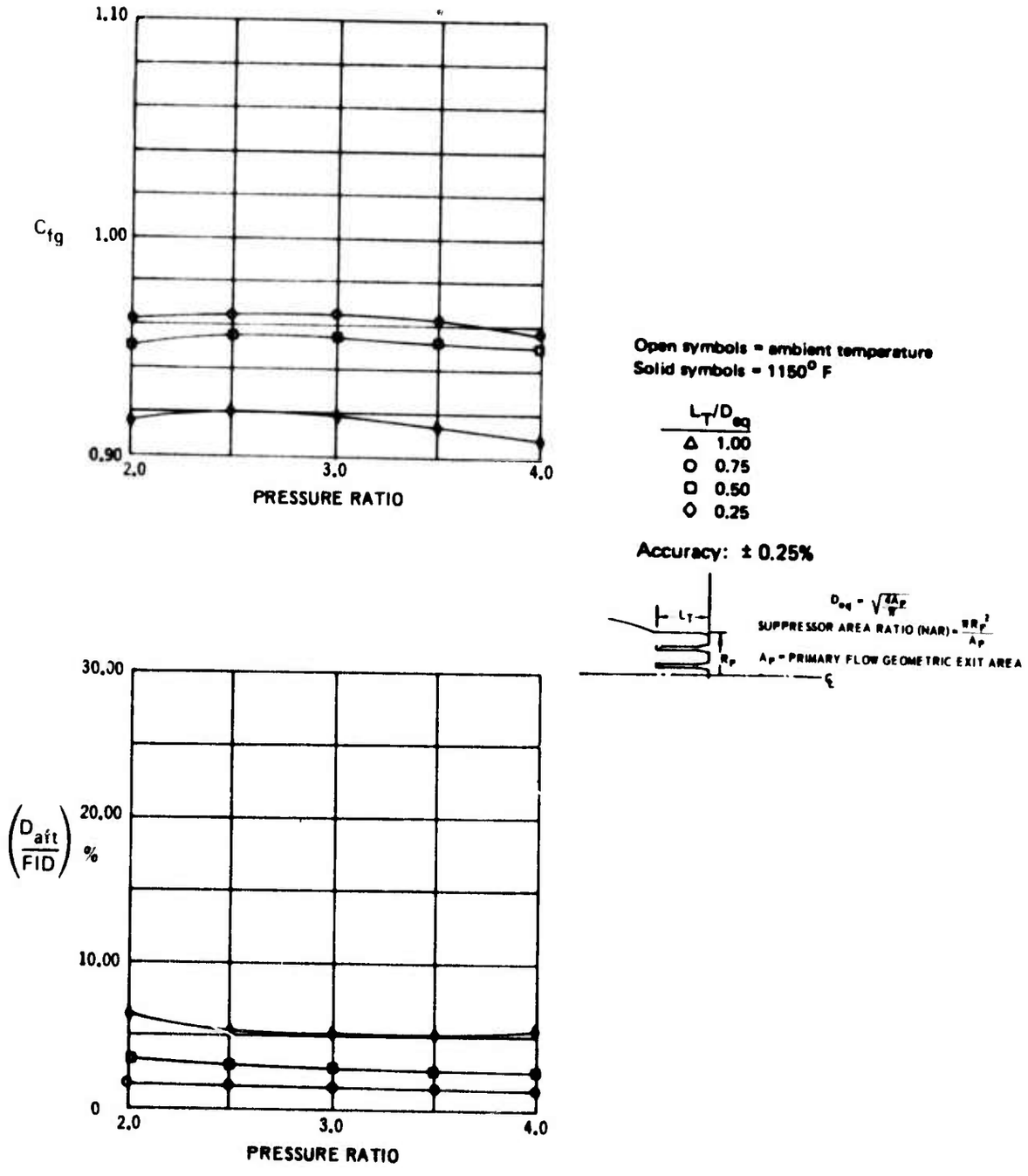


*Figure 72.—Gross Thrust Coefficient and Afterbody Drag for 61-Tube, NAR = 3.3, Close-Packed Array, Elliptical Ramp, Elliptical Convergent Tubes*

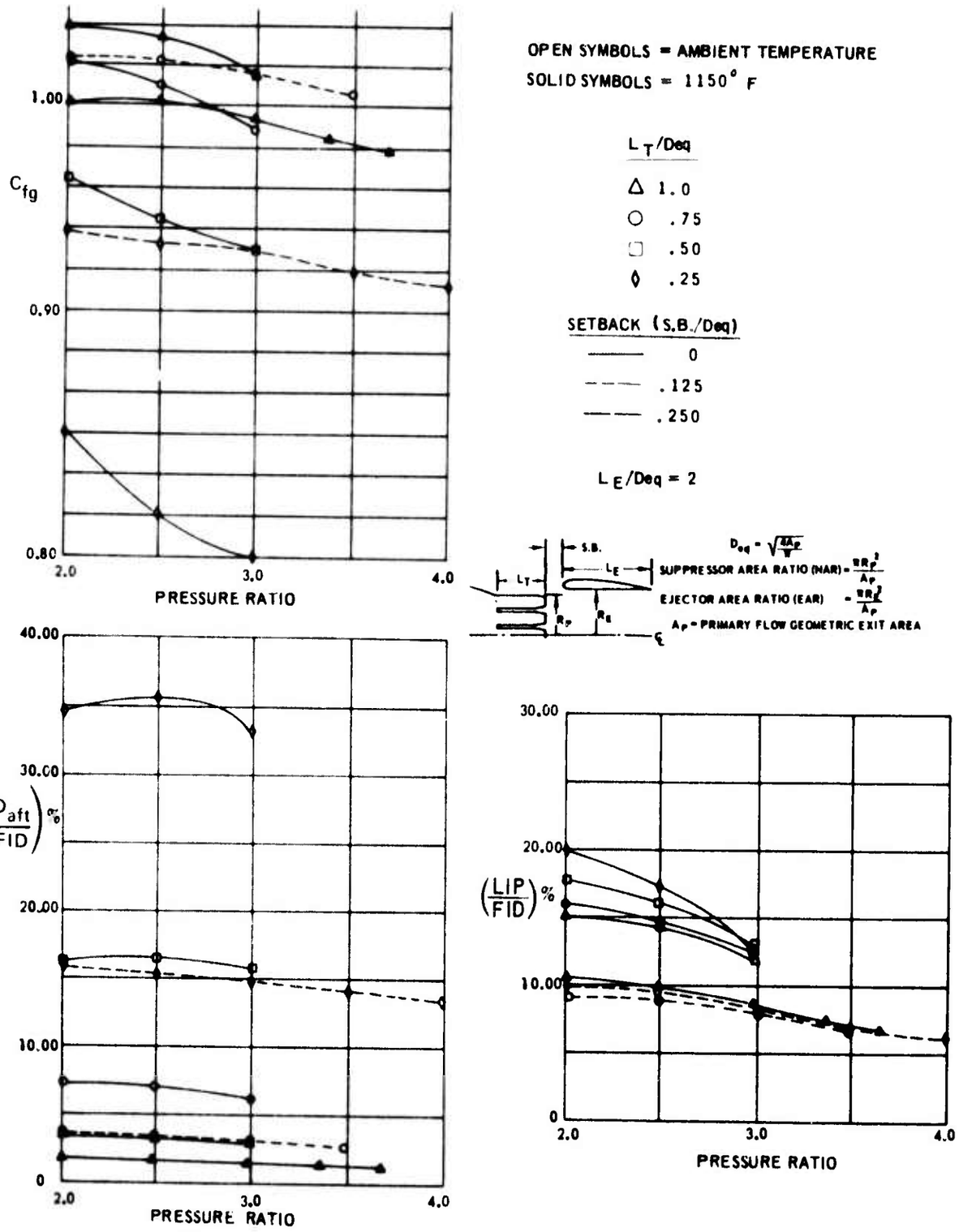


*Figure 73.–Gross Thrust Coefficient and Body Forces for 61-Tube, NAR = 3.3, EAR = 3.1, Close-Packed, Elliptical Ramp, Elliptical Convergent Tubes*

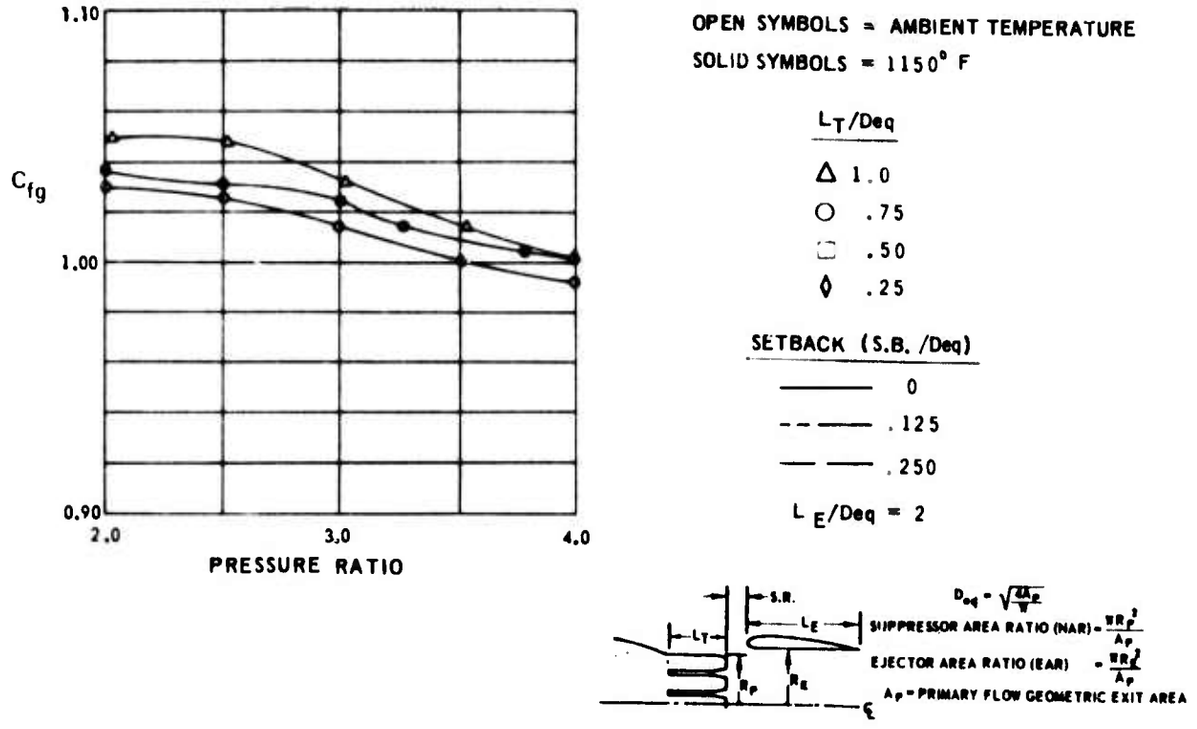


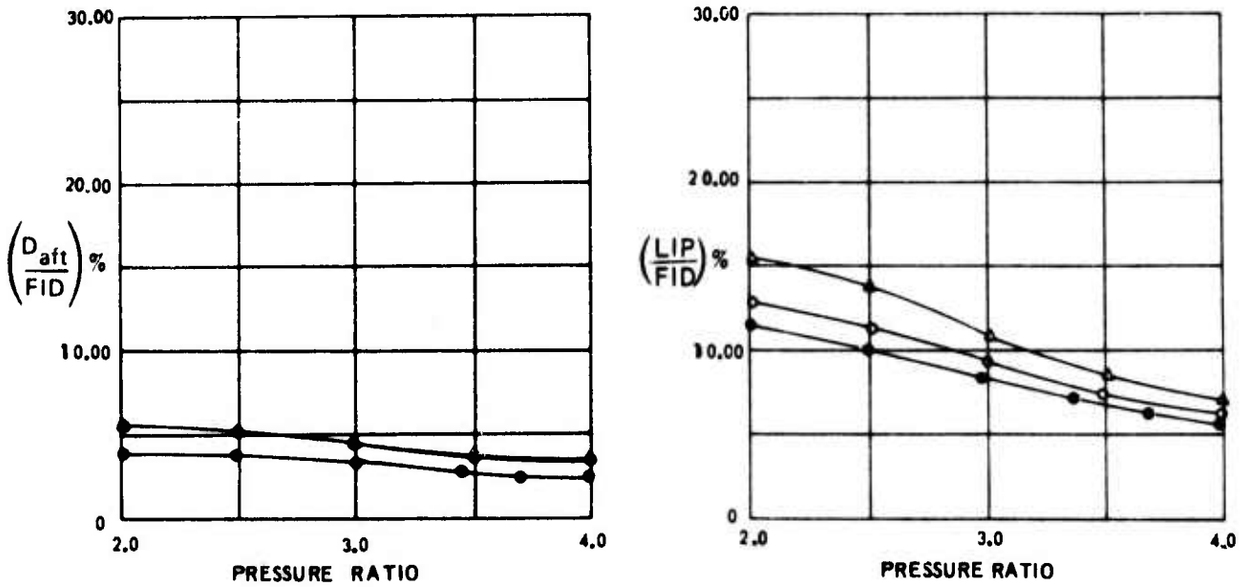


*Figure 74.—Gross Thrust Coefficient and Body Forces for 61-Tube, NAR = 3.3, EAR = 3.7, Close-Packed, Elliptical Ramp, Elliptical Convergent Tubes*

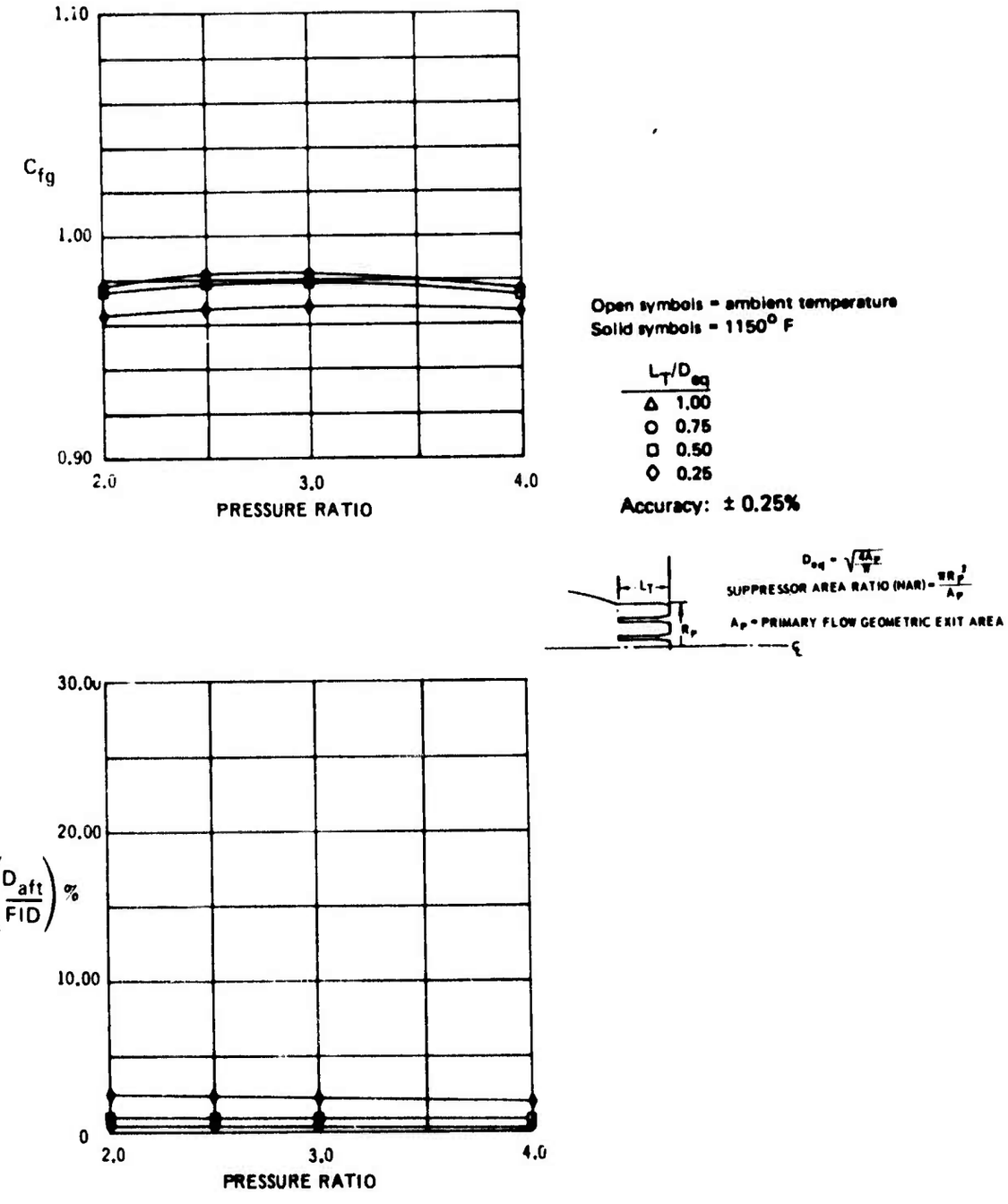


*Figure 75.—Gross Thrust Coefficient and Afterbody Drag for 31-Tube, NAR = 2.75, Radial Array, Elliptical Ramp, Elliptical Convergent Tubes*

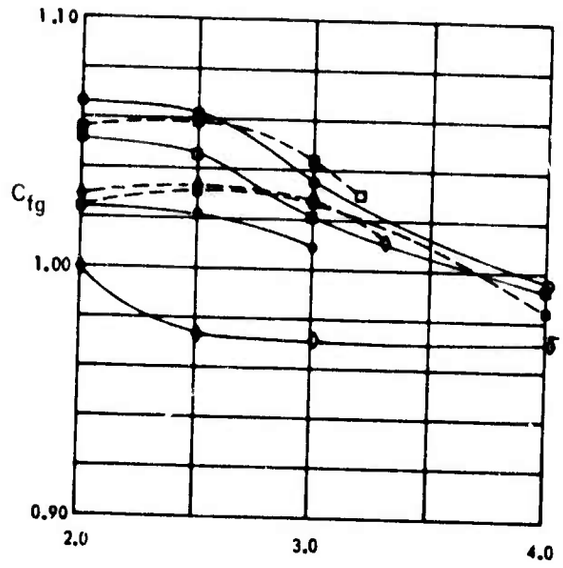


OPEN SYMBOLS = AMBIENT TEMPERATURE
SOLID SYMBOLS = 1150° F

$L_T/Deq$

△ 1.0
○ .75
□ .50
◊ .25

SETBACK ( S.B /Deq)

——— 0
– – – .125
— — — .250

$L_E/Deq$ = 2

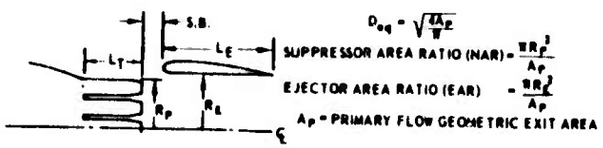


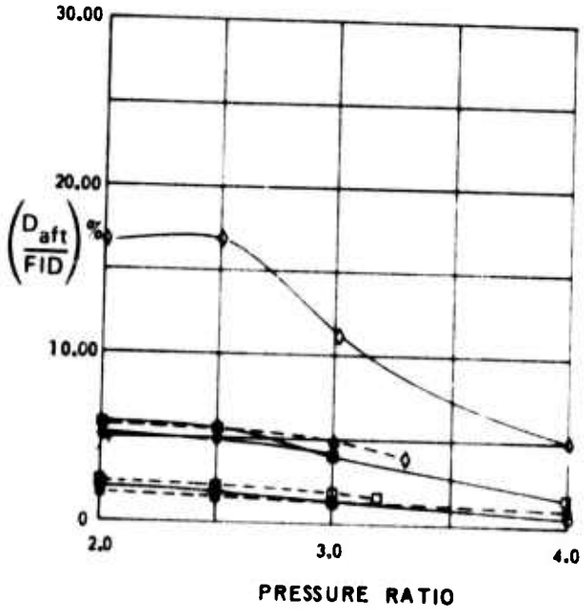


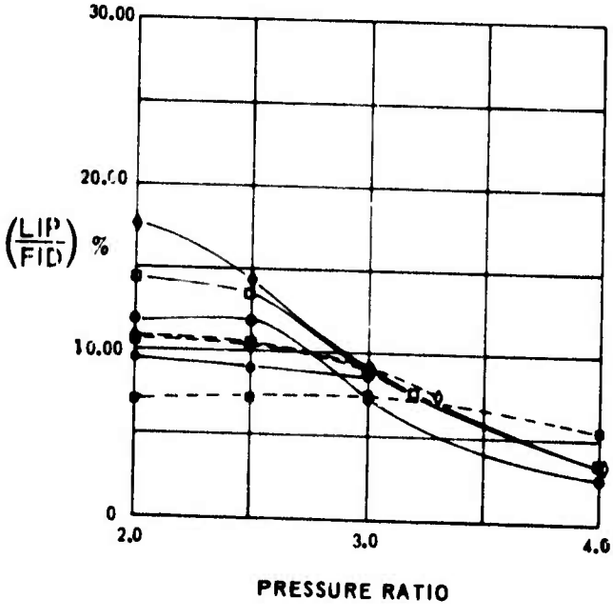


*Figure 76.—Gross Thrust Coefficient and Body Forces for 31-Tube, NAR = 2.75, EAR = 2.6, Radial Array, Elliptical Ramp, Elliptical Convergent Tubes*

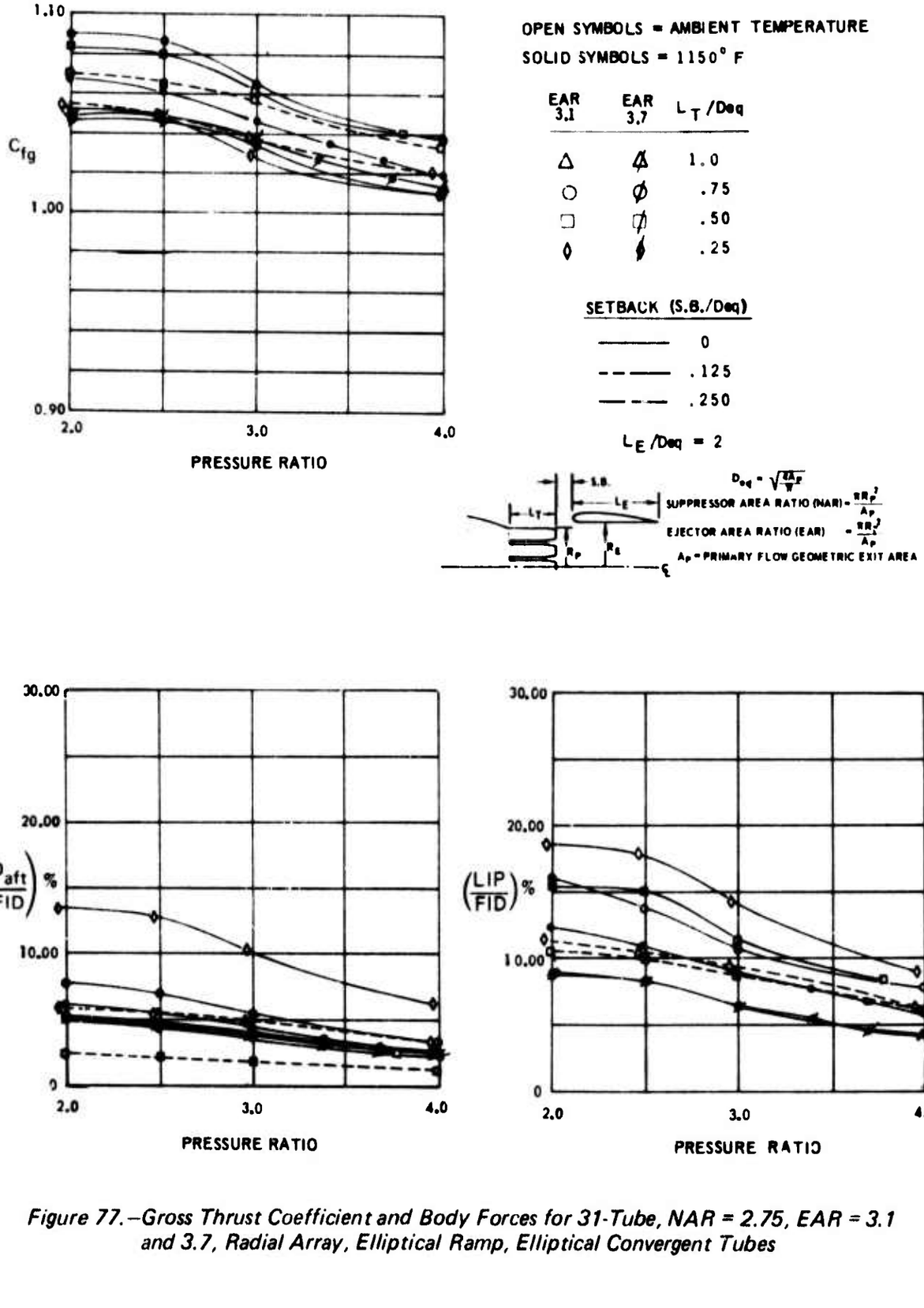


*Figure 77.–Gross Thrust Coefficient and Body Forces for 31-Tube, NAR = 2.75, EAR = 3.1 and 3.7, Radial Array, Elliptical Ramp, Elliptical Convergent Tubes*

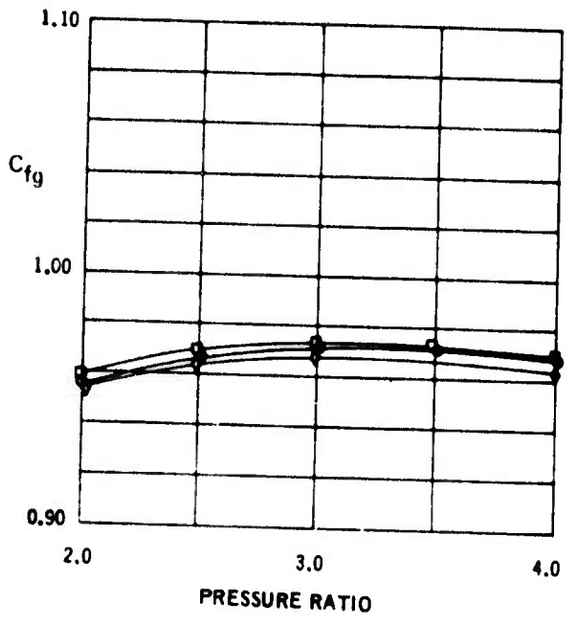


Open symbols = ambient temperature
Solid symbols = 1150° F

| $L_T/D_{eq}$ | |
|---|---|
| Δ | 1.00 |
| O | 0.75 |
| □ | 0.50 |
| ◇ | 0.25 |

Accuracy: ± 0.25%

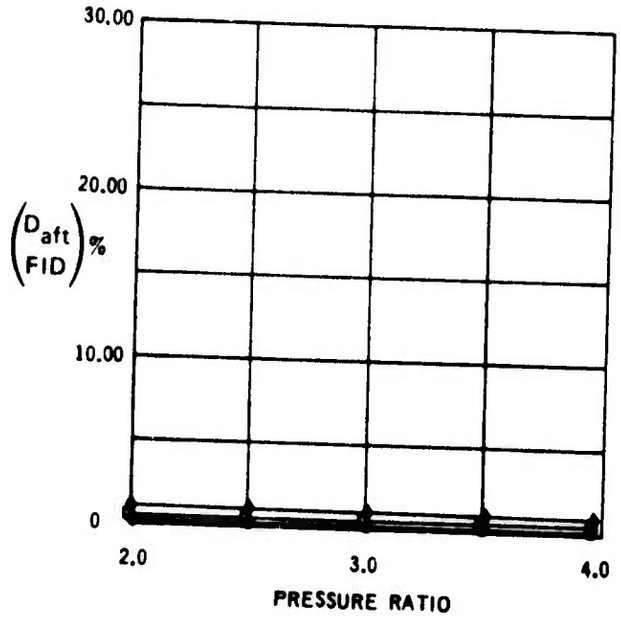


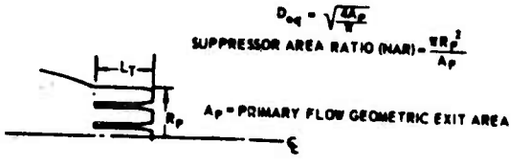


*Figure 78.—Gross Thrust Coefficient and Afterbody Drag for 37-Tube, NAR = 3.3, Radial Array, Elliptical Ramp, Round Nonconvergent Tubes*

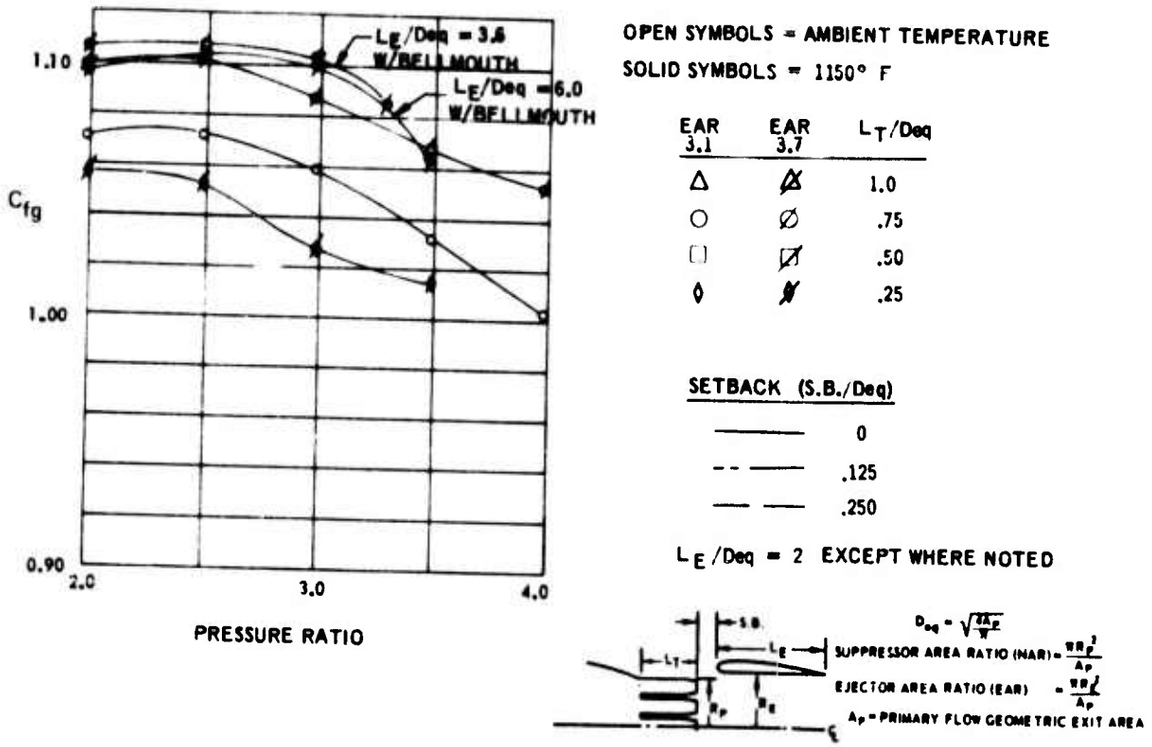


*Figure 79.—Gross Thrust Coefficient and Body Forces for 37-Tube, NAR = 3.3, EAR = 3.1 and 3.7, Radial Array, Elliptical Ramp, Round Nonconvergent Tubes*

# APPENDIX

This appendix presents detailed performance data for all test configurations discussed in the body of the report.

## EXPERIMENTAL RESULTS

For each combination of ejector area ratio and suppressor geometry, curves are presented for the gross thrust coefficient, suppressor afterbody drag, and ejector lip suction as percentages of ideal primary thrust. Each curve is presented as a function of pressure ratio, tube length, setback, and temperature. For convenience, the gross thrust coefficient and force curves are shown on the same page.

Whenever a data curve terminates at a pressure ratio less than four, the end point designates the onset of severe ejector vibrations presumably due to shock-induced flow instabilities. The ejector vibration is accompanied by supersonic flow at the ejector throat. This was indicated by static pressure measured inside the ejector at the ejector throat (i.e., tangent point between the ejector lip contour and the constant area section). The supersonic flow occurs around the entire circumference of the ejector (not just in line with the jets).

## LIST OF NOZZLE CONFIGURATIONS AND CORRESPONDING ILLUSTRATION–C.P. AND RADIAL ARRAYS

The following table provides the appropriate figure numbers for each configuration.

| Configurations | | | | | Figure Number |
|---|---|---|---|---|---|
| Round Convergent Nozzle | | | | | 61 |
| *Close-Packed Arrays* | | | | | |
| Tube No. | NAR | Tube Shape | Ramp Shape | EAR | |
| 19 | 3.3 | Ell.C. | Ell. | None* | 62 |
| | | | | 3.1, 3.7 | 63 |
| 37 | 2.75 | Ell.C. | Ell. | None | 64 |
| | | | | 2.6 | 65 |
| | | | | 3.1 | 66 |
| 37 | 3.3 | Ell.C. | Ell. | None | 67 |
| | | | | 3.1 | 68 |
| | | | | 3.7 | 69 |
| 37 | 3.3 | R/C | Contoured | None | 70 |
| | | | | 3.1, 3.7 | 71 |
| 61 | 3.3 | Ell.C. | Ell. | None | 72 |
| | | | | 3.1 | 73 |
| | | | | 3.7 | 74 |

*Radial Array*

| Tube No. | NAR | Tube Shape | Ramp Shape | EAR | |
|---|---|---|---|---|---|
| 31 | 2.75 | Ell.C. | Ell. | None | 75 |
| | | | | 2.6 | 76 |
| | | | | 3.1, 3.7 | 77 |
| 37 | 3.3 | R non-C. | Ell. | None | 78 |
| | | | | 3.1, 3.7 | 79 |

*Much of the no-ejector information comes from reference 1.

# REFERENCES


1. D. B. Morden, R. S. Armstrong, *SST Technology Follow-On Program – Phase II – Noise Suppressor/Nozzle Development – Volume VII – Performance Technology – A Guide to Multitube Suppressor Nozzle Static Performance – Trends and Trades*, FAA-SS-73-11-7, March 1975.

2. J. Atvars, et al, *SST Technology Follow-On Program – Phase II – Noise Suppressor Nozzle Development – Volume II – Noise Technology*, FAA-SS-73-11-2, March 1975.

3. D. B. Morden, R. S. Armstrong, *SST Technology Follow-On Program – Phase II – Noise Suppressor Nozzle Development – Volume IX – Analysis of the Lower Speed Performance of Multitube Suppressor/Ejector Nozzles (0-167 knots)*, FAA-SS-73-11-9, March 1975.

4. H. Lu, D. Morden, R. Benefiel, and C. Simcox, *SST Technology Follow-On Program – Phase I, Performance Evaluation of the NSC-119B Nozzle System; Volume I: Suppressed Mode*, AD-900-399L, February 1972.

5. C. D. McClung, *Test Data Report – Parametric Test of Conical Convergent Nozzles*, unpublished Boeing Document.

6. F. Pearlman, R. S. Armstrong, *SST Technology Follow-On Program – Phase II – Noise Suppressor/Nozzle Development – Volume VI – Thrust and Flow Characteristics of a Reference Multitube Nozzle With Ejector*, FAA-SS-73-11-6, March 1975.

7. J. Reid, *The Effects of Cylindrical Shroud on the Performance of a Stationary Convergent Nozzle*, Aeronautical Research Council Report and Memoranda no. 3320, Ministry of Aviation, London, England, 1963.

8. J. Atvars, et al, *SST Technology Follow-On Program – Phase II – Noise Suppression Nozzle Development – Volume III – Backup Data Report*, FAA-SS-73-11-3, March 1975.

9. M. P. Scofield, *One-Dimensional Ejector Mixing Program*, unpublished Boeing Document.